GOETHE UNIVERSITÄT FRANKFURT AM MAIN

GEORG SPEYER HAUS
INSTITUTE FOR TUMOR BIOLOGY AND EXPERIMENTAL THERAPY

The role of FUBP1 during differentiation of murine ESCs

Dissertation

zur Erlangung des Doktorgrades
der Naturwissenschaften

vorgelegt beim Fachbereich Biowissenschaften
der Johann Wolfgang Goethe-Universität
in Frankfurt am Main

von
Josephine Wesely
aus Zittau

Frankfurt am Main, 2016

(D30)

vom Fachbereich Biowissenschaften (FB 15) der
Johann Wolfgang Goethe-Universität als Dissertation angenommen.

Dekan:

Gutachter:

Datum der Disputation:

Erklärung

Ich erkläre hiermit, dass ich mich bisher keiner Doktorprüfung im Mathematisch-Naturwissenschaftlichen Bereich unterzogen habe.

Frankfurt am Main, den..... .....
(Unterschrift)

Eidesstattliche Versicherung

Ich erkläre hiermit an Eides statt, dass ich die vorgelegte Dissertation mit dem Titel

" The role of FUBP1 during differentiation of murine ESCs"

selbstständig angefertigt und mich anderer Hilfsmittel als der in ihr angegebenen nicht bedient habe, insbesondere, dass alle Entlehnungen aus anderen Schriften mit Angabe der betreffenden Schrift gekennzeichnet sind.

Ich versichere, die Grundsätze der guten wissenschaftlichen Praxis beachtet, und nicht die Hilfe einer kommerziellen Promotionsvermittlung in Anspruch genommen zu haben.

Frankfurt am Main, den..... .....
(Unterschrift)

Zusammenfassung 1
Summary 6
1 Introduction 9
1.1 The early stages of mouse embryonic development 9
1.2 Embryonic stem cells 12
1.2.1 ESC maintenance in cell culture 13
1.2.2 The transcriptional network of the main stem cell factors Oct4, Nanog and Sox2 14
1.2.3 Differentiation of ESCs into embryoid bodies (EBs) 15
1.3 Far upstream element binding protein 1 (FUBP1) 16
1.3.1 The transcriptional network controlled by FUBP1 17
1.3.2 The physiological role of FUBP1 in mice 19
2 Aim of this project 20
3 Materials and Methods 22
3.1 Materials for molecular biology experiments 22
3.1.1 Kits and Mastermix 24
3.1.2 Buffers 24
3.1.3 Antibodies 25
3.1.4 Cell lines, cell culture medium and supplements 25
3.1.5 Mouse lines 26
3.1.6 Laboratory equipment 27
3.1.7 Chemical reagents and solutions 28
3.2 Molecular biology methods 29
3.2.1 Transformation of DNA into competent DH5α bacteria by heat shock 29
3.2.2 Large scale plasmid purification 29
3.2.3 Small scale plasmid purification 30
3.2.4 Digestion of DNA by restriction enzymes 30
3.2.5 Agarose gel electrophoresis 30
3.2.6 DNA extraction from Agarose gel 31
3.2.7 Ligation of DNA 31
3.2.8 Protein quantification by Bradford assay 31
3.2.9 Sequencing of DNA 32
3.3 Biochemical methods 32
3.3.1 SDS-polyacrylamid gel electrophoresis (PAGE) 32
3.3.2 Protein transfer onto nitrocellulose membranes 33
3.3.3 Western Blot analysis 33
3.3.4 cDNA synthesis and quantitative real-time PCR 33

3.4 Flow Cytometry 35
3.5 Cell culture 35
3.5.1 Mammalian cell culture 36
3.5.2 Thawing and freezing of cells 36
3.5.3 Cell lysates 36
3.5.4 RNA preparation 36
3.5.5 Quantifying cell numbers with the Neubauer counting chamber 37
3.5.6 Production of lentiviral particles in HEK293T cells using polyethylenamine (PEI)-mediated transfection 37
3.5.7 Lentiviral transduction 37
3.6 Differentiation assays 38
3.6.1 ESC differentiation into embryoid bodies (EBs) 38
3.6.2 OP9 differentiation assay (hematopoietic progenitor) 38
3.6.2.1 Cultivation and passaging of OP9 cells 38
3.6.2.2 Preparation of OP9 cells for ES cell differentiation into hematopoietic progenitor cells ($CD45^+$) 38
3.6.2.3 Preparation of ES cells for the differentiation in co-culture with OP9 cells 39
3.6.2.4 Proliferation of erythroid lineage cells on OP9 39
3.7 Animal experiments and preparation 39
3.7.1 Genotyping 39
3.7.2 Tissue and organ preparation 40
3.7.3 Time matings and embryo preparation 40
3.8 Histology 40
3.8.1 Preparation of EBs for paraffin sections 40
3.8.2 Hematoxylin and Eosin staining 41
3.8.3 Immunhistochemichal staining 41
3.8.4 Cytospin and cytochemistry 41
4 Results 42
4.1 Characterization of mESCs and the differentiation to EBs 42
4.1.1 Stem cell and differentiation marker in ESCs 42
4.1.2 Differentiation of ESCs to EBs and analysis of germlayer development 42
4.1.3 Establishment and optimization of the OP9 assay to generate hematopoietic $CD45^+$ positive progenitor cells 44
4.1.4 Testing of different conditions for ESC differentiation into the erythroid lineage on OP9 cells 46
4.2 Establishment and characterization of *Fubp1* knockout ESC clones 47
4.2.1 FUBP1 is expressed in ESCs and during EB differentiation 47
4.2.2 Establishment of *Fubp1* knockout ESC lines with the CRISPR/Cas9 system 48

4.2.3 *Fubp1* KO ESC clones were not affected in their stem cell characteristic 50
4.2.4 Differentiation of *Fubp1* KO ESC clones to EBs showed a deficit in mesoderm differentiation 51
4.2.5 Differentiation of *Fubp1* KO ESC clones in co-culture with OP9 cells to hematopoietic progenitors 56
4.3 The role of FUBP1 in the early embryonic development 58
4.3.1 FUBP1 expression during murine embryonic development 58
4.3.2 Analysis of FUBP1 expression in young and adult WT mice 59
4.3.3 Proliferation and apoptosis analysis in the *Fubp1* GT mouse model 61
5 Discussion 63
5.1 Characterization and optimization of the ESC culture system and differentiation protocols 63
5.1.1 ESC cultivation, differentiation and analysis of stem cell marker, differentiation marker and FUBP1 expression 63
5.1.2 Optimization of the OP9 co-culture differentiation assay 64
5.2 Generation and characterization of *Fubp1* KO ESC clones 65
5.2.1 Generation of *Fubp1* KO clones using the CRISPR/Cas9 technology 65
5.2.2 The deletion of Fubp1 does not interfere with ESC growth and stemness 65
5.2.3 Deletion of FUBP1 in ESCs leads to a delay in mesoderm differentiation during EB formation 66
5.2.4 The absence of FUBP1 in ESCs does not affect the ability to differentiate into hematopoietic cells using the OP9 co-culture assay 68
5.3 FUBP1 during the development of mice and the analysis of the *Fubp1* GT mouse strain ... 70
5.3.1 FUBP1 is strongly expressed during embryogenesis and in almost every kind of tissue in adult mice 70
5.4 *Fubp1* KO ESC clones provide evidence for a broader phenotype in the *Fubp1* GT mice .. 71
6 Literature 73
7 List of Abbreviations 79

Zusammenfassung

Die wichtigsten Eigenschaften embryonaler Stammzellen (embryonic stem cells; ESCs), sind die Möglichkeit die Zellen in Langzeitkulturen zu halten und ihr Potenzial einen kompletten neuen Organismus zu generieren. Embryonale Stammzellen sind ein wichtiges Werkzeug um Untersuchungen der frühen embryonalen Entwicklung durchführen zu können. Die Ergebnisse erlauben ein besseres Verständnis zur Differenzierung der Stammzellen in alle unterschiedlichen Zelltypen. Da die Embryonalentwicklung von der Befruchtung bis zur Geburt einer Maus nur etwa 21 Tage dauert, ist es schwer, die ersten Phasen, der frühen Entwicklung wie die Blastozysten-entwicklung (Pre-Implantation), die Implantation der Eizelle, sowie die Zeit der Post-Implantation, zu untersuchen. Vor allem genetische Veränderungen, die man zum Verständnis der physiologischen Rolle bestimmter Moleküle genutzt werden sind schwer zu untersuchen, wenn sie in der Maus zu embryonaler Lethalität führen. Ersatzweise können ESCs genutzt werden, die mit Hilfe neuer Technologien zur Modifikation von Genen (z.B. mit dem CRISPR/Cas9 System) verändert werden können. Bei der Generierung sogenannter „knockout“ ES-Zelllinien kann schnell festgestellt werden, ob diese genetische Veränderung einen Einfluss auf den Erhalt der ESC-Stammzelleigenschaften hat oder nicht. Lassen sich ESC Klone mit der entsprechenden Mutation oder Deletion generieren, welche ihren Stammzellcharackter nicht verloren haben, ist dies ein Zeichen dafür, dass das Gen bzw. Protein nicht essentiell für die Stammzellen ist.

Um zu testen, ob die ESCs nach einer genetischen Veränderung noch in der Lage sind zu differenzieren, können Protokolle zur Generierung von „embryoid bodies“ (EBs) angewandt werden, was zur Differenzierung in die Zelltypen der drei Keimblätter führt. Essentiell für die Kultivierung von ESCs und der Erhalt ihres Stammzellcharackters ist der Faktor LIF (leukemia inhibitory factor). Wird dieser nicht zum Medium dazugegeben und werden die Zellen in einer Schale mit geringem Adhäsionspotenzial ausgesät, formen sich diese EBs und die ESCs beginnen zu differenzieren. Die Entwicklung der Zellen der drei Keimblätter kann mit Hilfe von Markern für die mesoderme, endoderme und ektoderme Differenzierung nachverfolgt werden. Gleichzeitig ist die Abnahme von Stammzellmarkern zu beobachten, die während dieses Prozesses immer geringer exprimiert werden.

Vor allem Transkrptionsfaktoren, die schnell und spezifisch Signalwege regulieren, spielen während der Embryonalentwicklung und während der Differenzierung von ESCs in vielen verschiedenen Zelltypen eine essentielle Rolle. Transkriptionsregulatoren sind Bestandteil

großer Signalnetzwerke und haben zu jedem bestimmten Zeitpunkt der Entwicklung eine sehr spezifische Rolle zu erfüllen, damit am Ende der Embryonalentwicklung ein kompletter und funktionsfähiger Organismus vorliegt. Der Transkriptionsregulator „Far Upstream Binding Protein 1“ (FUBP1) ist ein Protein, welches eine ganz bestimmte einzelsträngige DNA Sequenz, das „Far Upstream Sequenz Element“ erkennt und bindet. Anschließend interagiert die C-terminale Domäne mit dem Transkriptionsfaktor IIH und bildet einen „loop“ zur Promoterregion von *c-myc*, welches als erstes direktes Zielgen von FUBP1 beschrieben wurde. Diese „loop“ Bildung führt zum erneuten Binden der Polymerase an den Promotor und führt zu einer verstärkten Expression des Gens. Neben *c-myc* wurden auch *p21* und *USP29* als direkte Zielgene von FUBP1 identifiziert, wobei der molekulare Mechanismus der zu einer Repression bzw. Aktivierung der Zielgene führt noch nicht beschrieben ist. Zusätzlich sind eine Reihe weiterer indirekter Zielgene gefunden worden, aus denen sich schließen lässt, dass FUBP1 vor allem in der Regulation von Migration, Apoptose und Zellzyklus involviert ist. In den meisten Fällen wurden diese Zielgene in verschiedenen Krebsentitäten identifiziert, in denen FUBP1 überexprimiert vorliegt und damit Gene und Proteine aktiviert oder reprimiert werden, die die Entstehung und Progression eines Tumors unterstützen. Unsere Arbeitsgruppe konnte dies für das hepatozelluläre Karzinom (HCC) zeigen. Durch eine shRNA-vermittelte Inhibition von FUBP1 in HCC Zellen ließ sich das Tumorwachstum in Xenograft Maus Experimenten signifikant reduzieren. Zusätzlich wurden die Hochregulation von *p21* und *p15*, sowie die Herunterregulation von anti-apoptotischen Genen wie *Bik* und *Noxa* beobachtet. Mit der Entwicklung zweier *Fubp1* Genfallen Mausstämme (*Fubp1* GT) sollte die Frage nach der physiologischen Rolle von FUBP1 beantwortet werden. Die homozygoten *Fubp1* GT Mäuse sterben im Mutterleib am Tag E15.5 der Embryonalentwicklung, sind kleiner als Wildtypembryonen und ziegen ein anämisches Aussehen. Diese Mausmodelle wurden hinsichtlich der Hämatopoese untersucht, die zu diesem Zeitpunkt vor allem in der Leber stattfindet. Es konnte eine signifikante Reduktion der hämatopoietischen Stammzellen (HSCs) festgestellt werden sowie eine reduzierte Repopulation aller Blutzellen in Transplantationsexperimenten. Die Gruppe um Dave Levens entwickelte parallel eine *Fubp1* „knockout“ Maus und konnte einen sehr ähnlichen Phänotyp beschreiben. Zusätzlich konnte beobachtet werden, dass weitere FUBP1-defiziente Zelltypen bzw. Organe Auffälligkeiten zeigten z:B. war das Lymphgewebe unterentwickelt und der Thymus hypoplastisch.

In der vorliegenden Arbeit wurde die Rolle von FUBP1 in einem weiteren Stammzellsystem analysiert und gleichzeitig seine Bedeutung in anderen Zelltypen der frühen

Embryonalentwicklung untersucht. Um diese Fragen zu adressieren, wurden ESCs sowie Differenzierungsprotokolle genutzt und durch die Analyse früher *Fubp1* GT Embryonen (E9.5 bis E13.5) eine potenzielle Rolle von FUBP1 in der Entwicklung untersucht.

Zuerst wurden die ESCs auf die Expression der Stammzellmarker Oct4 und Nanog, sowie der 3 Differenzierungsmarker Brachyury (Mesoderm) Sox17 (Ektoderm) und Nestin (Entoderm) hin untersucht. Es zeigte sich in normalen ESCs eine starke Expression der Stammzellmarker, während die Differenzierungsmarker nicht detektiert wurden. Die Analysen der FUBP1-Expression zeigten eine starke Expression auf mRNA- und auf Proteinebene. Nach erfolgreicher Optimierung der Differenzierung von murinen ESCs zu sogenannten `*embryoid bodies*`(EBs), sowie der Etablierung des OP9 Ko-Kultur-Assays zur Differenzierung der ESCs in die hematopoietische Richtung, etablierte ich *Fubp1* knockout (KO) ESC Klone mit Hilfe der CRISPR/Cas9 Technologie. Nach Selektion und Überprüfung des *Fubp1* KOs durch Western Blot Analyse und cytohistologischer Färbungen wurden die ESCs einer detaillierten molekularen Analyse unterworfen. Hierbei zeigte sich keine offensichtliche Verschiebung der Zellzyklusverteilungun kein Anstieg an toten Zellen. Die mRNA Analyse zeigte für das FUBP1-Zielgen *p21* keine Veränderung des Expressionsniveaus, während *c-myc* signifikant erhöht vorlag. Publizierter Daten zufolge wird c-myc durch FUBP1 aktiviert, jedoch nicht reprimiert, sodass der beobachtete Anstieg des *c-myc* mRNA levels nicht auf den direkten Effekt der FUBP1-Deffizienz zurückzuführen ist. Zusätzlich zeigte sich auch eine signifikante Erhöhung der *Oct4* mRNA-Expression, während *Nanog* und die Differenzierungsmarker *Brachyury*, *Nestin* und *Sox17* unverändert und in vergleichbarer Menge zu den Kontrollen vorlagen. Während der Differenzierung der *Fubp1* KO Klone zu EBs zeigte sich eine signifikante Reduktion des mesodermalen Marker *Brachyury*. Die Analyse weiterer mesodermaler Marker wie *Flk-1*, *SnaiI*, *Snai2* sowie dem Zielgen von Brachyury, *Foxa2* bestätigte, dass in Abwesenheit von FUBP1 die ESCs zeitlich verzögert zu mesodermalen Zellen differenzieren. Mit Hilfe durchflusszytometrischer Analysen der EBs an den Tagen 3, 4 und 5 nach Beginn der Differenzierung wurde der prozentuale Anteil Brachyury- und Flk-1-exprimierender Zellen bestimmt. Hierbei bestätigte sich die verzögerte Bildung mesodermaler Zellen in den *Fubp1* KO Klonen während der Differenzierung. Die Analyse Flk-1 expremierender Zellen zeigte eine geringfügige Erhöhung der *Fubp1* mRNA-Expession. Auch ein möglicher kompensatorischer Effekt durch andere FUBP-Familienmitglieder wie z.B. FUBP3 kann ausgeschlossen werden. Während der ESC-Differenzierung verringert sich

die Expression von FUBP3 zwar, diese findet aber in den Kontroll- und in den *Fubp1* KO Klonen in vergleichbarem Ausmaß statt.

Die Anwendung einer OP9 Ko-Kultur zur Differenzierung der ESCs in hämatopoetische Linien sollte zeigen, ob mit den *Fubp1* KO ESCs ein Defekt in der frühen Entwicklung hämatopoetischer Stammzellen zu beobachten ist. Erneut konnte am Tag 5 der ESC-Differenzierung in der OP9 Ko-Kultur eine signifikante Reduktion der mesodermalen (Flk-1^+) Zellen und zusätzlich der Hämangioblasten festgestellt werden. Die weitere Differenzierung zu hämatopoetischen, $CD45^+$ Zellen zeigte jedoch keinen Unterschied im prozentualen Anteil $CD45^+$ Zellen am Tag 12 der Differenzierung. Auch die gezielte Differenzierung zu erythroiden Zellen durch Zugabe des Zytokins EPO (Erythropoietin) zum Medium zeigte keinen signifikanten Unterschied im Differenzierungsgrad der erythroiden Zellen zwischen Kontroll- und *Fubp1* KO Klonen. Die Rolle mesodermaler Marker, wie Brachyury und SnaiI sind essentiell für die Entwicklung eines gesunden Embryos. Publikationen zu KO-Mausmodellen dieser beiden Gene, zeigten, dass ihre Abwesenheit immer noch zur Bildung mesodermaler Zellen führt. Dennoch ist die Auswirkung der ineffizienten Differenzierung mesodermaler Zellen in Form vom Absterben des Embryos am Tag E10.5 für Brachyury-defiziente Mäuse bzw. im Blastozystenstadium für SnaiI-defiziente Mäuse zu beobachten.

In weiteren Experimenten wurden in dieser Arbeit die Expression von FUBP1 in WT-Embryos an den Tagen E9.5 und E13.5 der Embryonalentwicklung untersucht. Hierbei zeigte sich in beiden Entwicklungsstadien eine immunhistochemische Anfärbung von FUBP1 in den meisten Zellen des Embryos. Am Tag E9.5 war auffällig, dass das sich entwickelnde Herz und die Leber Zellen aufwiesen, die offensichtlich kein FUBP1 expremierten. Am Tag E13.5 hingegen waren nur noch wenige Zellen in der Leber FUBP1-negativ, während nun alle anderen Zellen FUBP1-gefärbt waren. Des Weiteren ergaben Analysen einer jungen (10 Tage nach Geburt) und einer ausgewachsenen Maus (12 Wochen alt), dass FUBP1 in allen Organen und Zelltypen exprimiert vorliegt. Lediglich in wenigen epidermalen Zellen angrenzend an das Darmgewebe und in roten Blutzellen, die keinen Zellkern mehr besitzen, war FUBP1 nicht expremiert.

Die Annahme, dass die Abwesenheit von FUBP1 in der Embryonalentwicklung zu verstärkten apoptotischen Vorgängen führen und gleichzeitig die massive Expansion von Zellen gestört sein könnte, wurde mit Hilfe immunhistochemischer Färbung von „*cleaved*

Caspase 3“ (Apoptosemarker) und „*Ki-67“* (Proliferationsmarker) in den homozygoten *Fubp1* GT Embryos an den Tagen E9.5 und E13.5 untersucht. Es zeigten sich hierbei weder eine erhöhte Anzahl apoptotischer Zellen noch eine Verringerung proliferierender Zellen allen untersuchten Organen der Embryos.

Die Ergebnisse dieser Arbeit lassen schließen, dass die hauptsächliche Regulation von Apoptose und Proliferation durch FUBP1 während der Embryonalentwicklung keine Rolle spielt. Es zeigte sich jedoch, dass FUBP1 als Transkriptionsregulator wichtig für die mesodermale Differenzierung von ESCs ist. Zu beobachten war, dass es in den FUBP1-defizienten ESCs zu einer Verzögerung der mesodermalen Differenzierung kommt. Es konnte bereits gezeigt werden, dass FUBP1 essenziell für die Selbsterneuerung von HSCs ist. Dies macht deutlich, dass FUBP1 neben der Proliferation und Apoptose ein breiteres Spektrum an Signalwegen reguliert, die für Stammzellen und deren Differenzierung von Bedeutung sind.

Summary

Transcriptional regulator proteins control the transcription of genes by acting as an enhancer or silencer. They are involved in a huge regulatory network to adjust intrinsic signal transduction in cells to their environment, e.g. retrieve a defined differentiation program due to extrinsic signals. The orchestrating network of a transcriptional regulator is complex and differs from cell type to cell type as well as between developmental stages. Moreover, the deregulation of a transcriptional regulator is often described to influence embryonic development and to support cell transformation towards a diseased state. Our group identified the transcriptional regulator FUBP1 in a screen for anti-apoptotic proteins and showed its cancer-supporting relevance in hepatocellular carcinoma (HCC). Additionally, a number of publications showed that FUBP1 is overexpressed in a range of solid cancer types such as prostate cancer, breast cancer or gastric cancer, while it is surprisingly inactivated in some oligodendroglioma. To identify the physiological role of FUBP1, two *Fubp1* gene trap mouse strains were established and displayed an embryonic lethal phenotype. A detailed analysis of homozygous mice showed that the embryonic lethality occurs around embryonic day E15.5 due to an impaired growth, an anemic phenotype and a reduced number of liver cells. The significant reduction of liver and hematopoietic stem cells was confirmed in further experiments and could be explained by a reduced self-renewal capacity and an increase of apoptosis in HSCs. The group of Dave Levens supported this role of FUBP1 in HSCs with the publication of their *Fubp1* knockout mouse model, in which they also showed a defect of the HSCs. Furthermore, it was discussed that other tissue than that of hematopoietic origin is affected. In detail, it was shown that the homozygous animals showed a smaller placenta, underdeveloped lymphoid tissue and increased parenchymal cellularity in the brain suggesting a broader spectrum of affected cells due to the loss of FUBP1.

To investigate the role of FUBP1 in the very beginning of embryogenesis, I established a FUBP1-deficient mouse ES cell line in our lab as well as cell culture protocols to allow differentiation into the three germ layers and specifically into the hematopoietic lineage. In particular, I generated *Fubp1* KO ESC clones using the CRISPR/Cas9 technology and could not observe an increase in apoptosis or changes in the cell cycle. There was no difference in the differentiation kinetics regarding the downregulation of the stem cell markers *Oct4* and *Nanog*. However, I could observe a prominent delay in the generation of the mesoderm germ layer cells as judged by analysis of *Brachyury*, *Flk-1*, *FoxA2*, *SnaiI* and *Snai2* expression

levels. Ectoderm and endoderm marker increased comparable to the control ESCs. Additionally, FACS analysis of Brachyury$^+$ and Flk-1$^+$ cells confirmed this observation by quantifying a significantly reduced number of Brachyury$^+$ cells at day 3 of EB formation and a significantly reduced number of Flk-1$^+$cells at day 5. However, sorting the Flk-1$^+$ cells from WT ESCS at day 5 of EB differentiation showed no difference in *Fubp1* mRNA expression levels, but a tendency towards a higher *Fubp1* mRNA expression level.

Because the hematopoietic cells origin from the mesoderm layer, I applied the OP9 co-culture assay to differentiate ESCs into hematopoietic progenitor cells. With the optimization of a two-step differentiation protocol, I could generate up to 30% Flk-1$^+$ cells after 5 days of cultivation and up to 6% CD45$^+$ cells after 12 days of differentiation. Using this assay, I observed a significant reduction of Flk-1$^+$ cells at day 5 but no differences in the amount of CD45$^+$ cells at day 12 of differentiation. The addition of the cytokine EPO at day 5 of ESC differentiation on OP9 cells forced the cells towards the erythroid lineage, but no difference became obvious between control and *Fubp1* KO clones.

My analysis of fetal and adult mouse tissues revealed that FUBP1 expression during embryogenesis and in adult tissues and organs is very prominent. I could not observe an increase or decrease in FUBP1 protein expression during embryogenesis from day E9.5 to E13.5. Surprisingly, one of the few examples of cells that do not express FUBP1 was observed in the liver between embryonic day E9.5 and 13.5, when a fast and huge expansion of hematopoietic cells occurs. Additionally, I analyzed the homozygous *Fubp1* GT mice at day E9.5 and E13.5 for an increase in apoptosis and a decrease in proliferation compared to the WT siblings. I observed a high rate of proliferating cells in both, WT and homozygous *Fubp1* GT mice and only a small number of apoptotic cells, supporting the assumption that FUBP1 is not necessary for the high proliferation rate during embryogenesis or the prevention of apoptosis, at least not under normal conditions.

Although I could not show that *Fubp1* KO ESCs fail to generate hematopoietic cells in the OP9 co-culture experiments, I observed a significant reduction and delay of mesoderm cells using two differentiation protocols. In a *Brachyury* knockout mouse model the failure of ESCs to differentiate into mesoderm cells resulted in an embryonic lethal phenotype at day E10.5. The absence of the mesoderm marker SnaiI in mice did not prevent mesoderm formation, but resulted in morphological abnormalities of mesoderm tissue in the embryo. This example shows that not even the complete absence of a mesoderm marker like SnaiI

does necessarily inhibit the transition from germ layer formation to later stages of development. However, this defect might lead at a later state to abnormalities and the death of the mouse embryo.

The role of FUBP1 during embryogenesis might rather involve the regulation of gene expression that is required for differentiation. To support this hypothesis and to obtain a more detailed picture of the regulatory network of FUBP1, ChIp assays of ESCs in the differentiation process to mesoderm cells can help to identify important mesoderm markers which are regulated by FUBP1. With a conditional mouse strain, it would be possible to identify potential lineage-specific roles of FUBP1, and this would also result in a better understanding of the oncogenic potential of FUBP1 in a variety of cancer entities.

1 Introduction

1.1 The early stages of mouse embryonic development

Mouse embryo development is mainly divided into three steps, the fertilization and the first cell division, followed by pre-implantation, when cell polarization and blastocyst formation take place, and finally the implantation. As shown in Figure 1 at the blastocyst state the embryos mature, escape from the *zona pellucidae* and gain implantation competency. The pre-implantated embryo at this day consists of the outer epithelial trophectoderm (TE), the primitive endoderm and the pluripotent inner cell mass (ICM), which can be isolated to generate embryonic stem cell (ESC) lines. In the next step, the TE attaches to the uterine to initialize the implantation (Wang and Dey 2006).

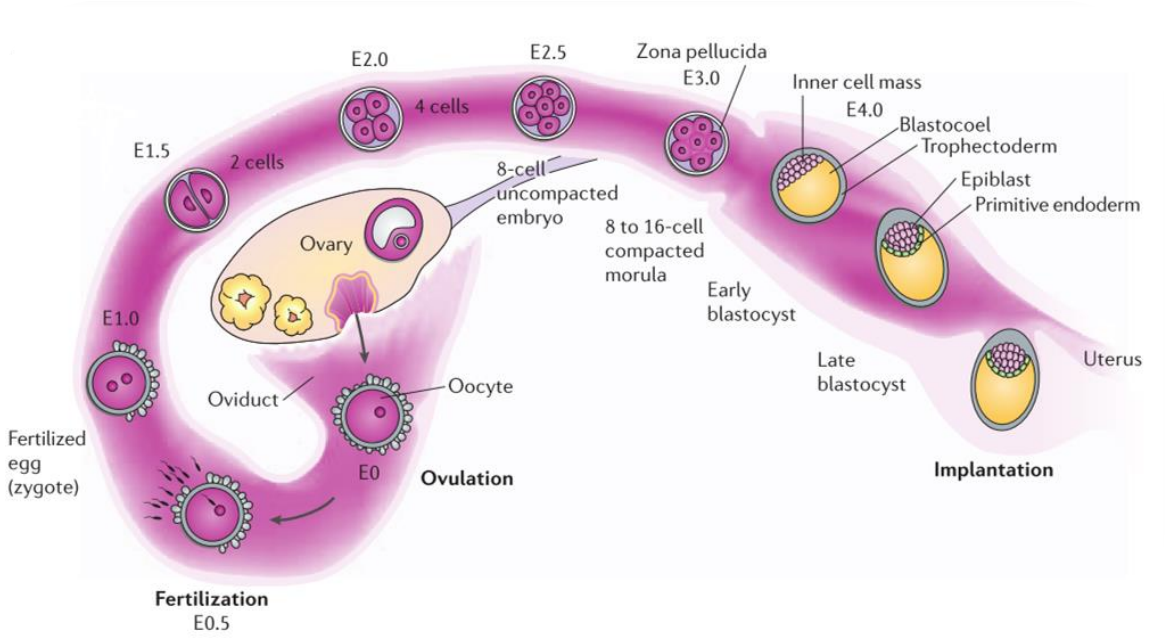

Figure 1: Steps of the early mouse embryonic development which starts with the first cell division and fertilization, reaching the post-implantation state (E2.5 to E4.5) and which ends with the implantation at E5 to E6 (Wang and Dey 2006).

Fertilization and the first cell divisions come with high dynamic changes in gene expression and epigenetic modifications, which could be analyzed in more detail with the development of new techniques, such as single cell analysis and high resolution imaging (Latham et al. 1991). Two waves of pre-implantation gene expression changes occur during this stage, and several genes were identified to lead to lethality when absent during pre-implantation state, e.g. *Smn* (survival motor neuron), whose absences drives massive cell death at the morula stage (Schrank et al. 1997) or *Mdm2* (mouse double minute 2 homologue), which resulted in

defective ICM growth and pre-implantation lethality (Montes de Oca Luna, Wagner, and Lozano 1995). Furthermore, absence of the two well described pluripotency genes *Nanog* and *Oct4* leads to the loss of pluripotency and start of spontaneous differentiation into endoderm-like cells or trophoblast-like cells, respectively (Mitsui et al. 2003; Nichols et al. 1998).

An important and very precisely regulated machinery is the appearance of cell polarity, and with this organization, the formation of the embryonic-abembryonic axis.

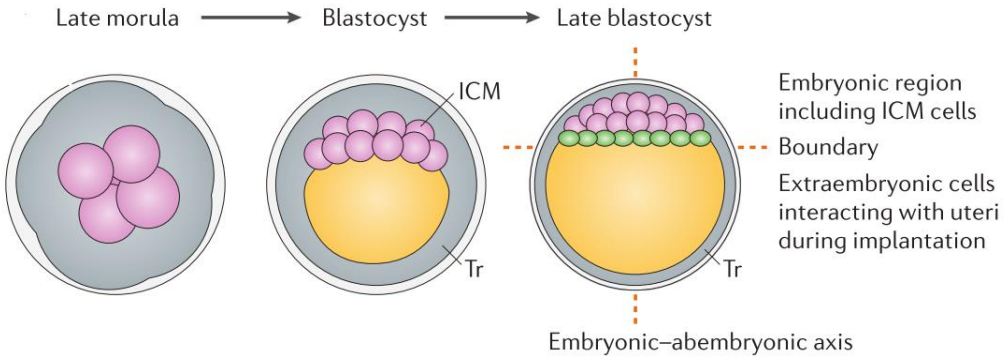

Figure 2: From the late morula state to the late blastocyst state a reorganization of different cell types takes place, which is tightly regulated by a network of signaling cascades, which are still not very well described and examined (Wang and Dey 2006).

It is still an ongoing debate how and when cells are receiving the signals for polarization. Several laboratories showed that 2-cell embryos divide asynchronously and that the daughter cells are differentially contributing to the ICM or TE (Surani and Barton 1984; Garbutt, Johnson, and George 1987). Others provided evidence that polarity with lineage differentiation comes with the onset of blastocyst formation, due to the mechanical pressure and space coming from the ellipsoidal *zona pellucida* (Motosugi et al. 2005).

The next phase is the competency of the blastocyst for implantation. A late implantation mouse model (Lopes, Desmarais, and Murphy 2004) was developed and used to analyze genes involved in implantation. Moreover, a global gene-expression study showed that the two states of blastocysts (blastocyst activation or dormancy) showed a distinct expression pattern of genes involved in cell cycle, cell signaling and energy metabolic pathways (Hamatani et al. 2004). Additionally, it was shown that catechol-estrogens produced from estrogens are involved in the activation of blastocysts (Paria et al. 1998). In five independent studies (Borthwick et al. 2003; Carson 2002; Kao 2002; Mirkin et al. 2005; Riesewijk et al. 2003) a number of signaling molecules such as cytokines hormones, lipid mediators and growth factors, which are locally produced and are involved in a signaling network for the

interaction between blastocyst and environment to induce implantation, could be identified. For example, complex changes in Wnt pathway regulators can be observed during transition from early blastocyst to implantation. While the Dickkopk1/DKK1, a Wnt pathway inhibitor increases, a decrease in LRP6, a Wnt co-receptor occurred (Semënov et al. 2001).

Finally, implantation takes place by apposition, attachment and penetration. The difficulties to connect one stage with the upregulation of one or two specific pathways are due to the overlap of all these processes (Wang and Dey 2006). Supporting this overlapping and very time-specific sequence, was the finding (Ye et al. 2005) that already a very short delay of blastocyst attachment can lead to early loss of the embryo by a feto-placental developmental failure.

Finally the post-implantation development takes place, where the embryo is embedded into the stromal surrounding (*deciduum*) which supplies the embryo with nutrition before forming the placenta. Angiogenesis seems to play a particularly important role. Angiogenesis is promoted by the vascular endothelial growth factor (VEGF), angiopoietin and progesterone (PG), but the link between these molecules is still unclear (Douglas et al. 2014) One can assume that a signaling crosstalk between the embryo and the surrounding environment as well as the hormonal changes of the pregnant female can lead to angiogenesis.

After the stages of fertilization, pre-implantation and finally implantation of the embryo, a specific organization and migration of cells takes place during gastrulation. It is described (Kraus et al. 2016) that a specific type of cells has the ability to induce the formation of the ectopic axis via the Wnt/ß-catenin signaling. A number of studies were performed to come up with a map of the different fates of the primitive streak in mice (Smith, Gesteland, and Schoenwolf 1994; Wilson and Beddington 1996), and it was shown that there has to be a different origin and signaling of mesoderm cells, which lead to migration towards the axial or the paraxial region. It is not exactly known which signaling pathways lead to the discrimination of the mesodermal cells in the different segments. However, studies with mice bearing mutations in the FGF receptor 1 (*fgfr1*) gene show a defect in the formation of paraxial mesoderm (Deng et al. 1994), while loss of bone morphogenetic protein-4 (*Bmp-4*) appears to effect the ventral mesoderm cells (Winnier, Blessing and Labosky 1995). Even Wingless-Type MMTV Integration Site Family, Member 3A (*Wnt3a*), which is known to be very important for the pluripotency of cells (Wray, Kalkan, and Smith 2010), seems to play a very restricted role for a specific mesoderm cell type coming from the primitive streak.

Therefore, mutations in Wnt3a resulted in a reduction of the width of the primitive streak, and no paraxial mesoderm marker expression at E8.5 to E9.5 was observed, but rather a shift to the neural tube formation and a broader expression of neural marker (Yoshikawa et al. 1997).

The identification of a defective phenotype during the very early state of embryonic development as a consequence of the specific deletion of a gene can be difficult to interpret. The usage of mouse embryonic stem cells and a variety of differentiation protocols are helpful tools to support a molecular hypothesis or to unravel the phenotype of death during early embryonic development.

1.2 Embryonic stem cells

Embryonic stem cells (ESCs) are pluripotent cells, *i.e.* they have an infinite self-renewal capacity and can differentiate into all lineages of the mature organism (Wray et al. 2010). Since the 1980s, mouse ESCs can be isolated from the inner cell mass of blastocysts (most suitable at day E3.5) and cultivated on feeder cells, which are usually inactivated fibroblasts, which are not able to divide anymore. It was shown that the leukemia inhibitory factor (LIF) can substitute the feeder cells, but a higher heterogeneity of ESCs and the appearance of spontaneously differentiated cells are more likely with this set up (Smith and Hooper 1987; Martello and Smith 2014). The development in the ESC research field holds high promise for biomedicine and transplantation medicine as well as for the pharmaceutic developmental research. Discovering novel genes important for specific differentiation decisions led to huge efforts to employ ESCs for cellular therapies to treat cardiovascular diseases, neurodegenerative diseases and diabetes (Soria, 2001; Talkhabi, Aghdami, & Baharvand, 2015; Tang et al. 2015; Bradley, Bolton, & Pedersen, 2002)

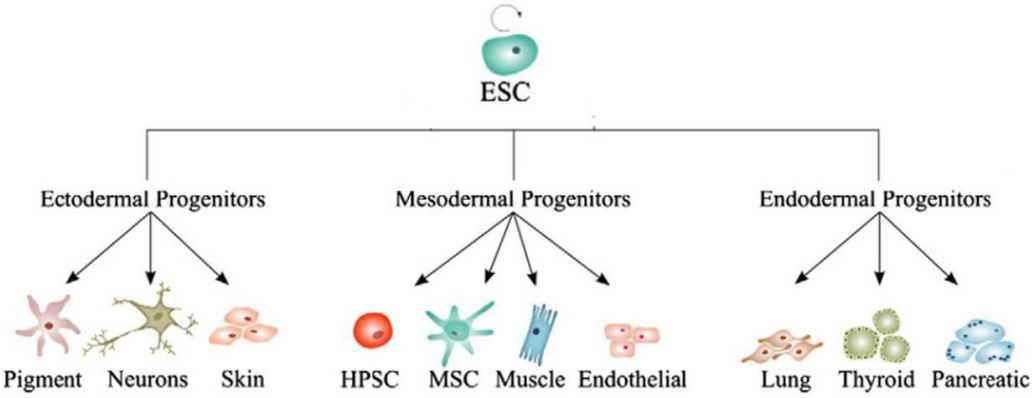

Figure 3: The generation of differentiated and functional cell types from embryonic stem cells is the promising prospective for therapeutic approaches. The first differentiation steps lead to the generation of

germ layer, endoderm, ectoderm and mesoderm. From then on tissue- and organ specific cell types can be developed (modified from Kaebisch et al. 2015).

Moreover, scientific questions about embryonic development and tissue-specific differentiation can be experimentally addressed by using ESC lines and differentiation protocols, while research with embryos or fetuses is inaccessible and ethically questionable. The molecular mechanisms governing tissue-specific differentiation as well as the discovery of genes involved in early embryo lethality can be studied in ESC lines.

1.2.1 ESC maintenance in cell culture

After more than 30 years of stem cell research, a number of protocols for the cultivation of these highly sensitive cells were published (Tamm, Pijuan Galitó, and Annerén 2013). The previously described soluble LIF factor acts through the LIFR receptor and activates the signal transducer and activator of transcription 3 (STAT3), an important regulator of mouse embryonic stem cell self-renewal (Tai, Schulze, and Ying 2014). STAT3 prevents the activation of lineage-specific differentiation programs. In more detail, LIF binds to the LIFR and leads to hetero-dimerization with gp130. The receptor-associated Janus kinases (JAKs) become activated and induce recruitment of Src homology-2 (SH2) domain-containing proteins such as STAT3. Subsequently, STAT3 molecules are phosphorylated on tyrosine 705 (Tyr705) residues and dimerize with another phosphorylated STAT3 (Huang et al. 2014). After translocation to the nucleus, they bind to promoter and enhancer regions of their target genes (Figure 4). The suppressor of cytokine signaling 3 (SOCS3) acts as an important negative regulator of the LIF/STAT3-pathway (Graf, Casanova, and Cinelli 2011).

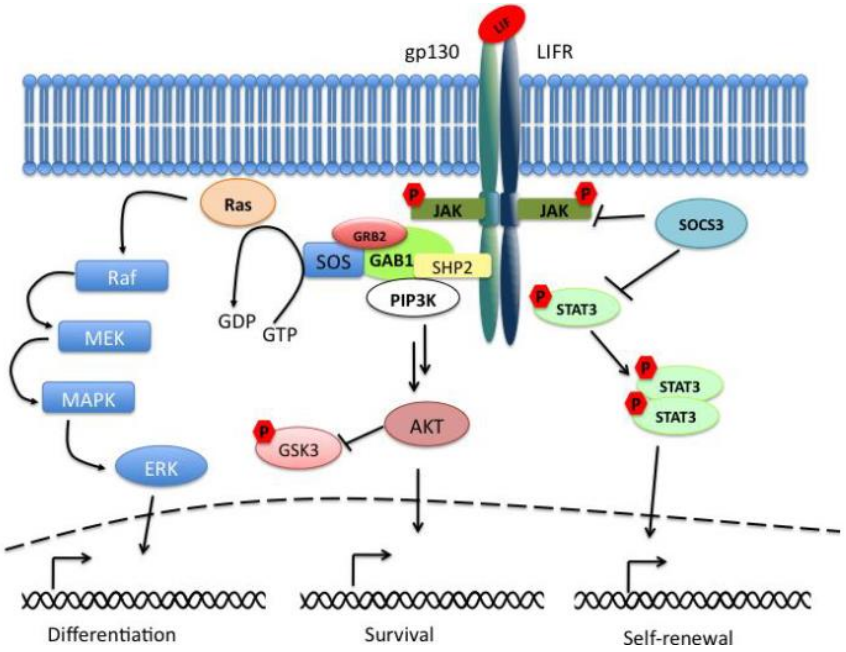

Figure 4: Schematic presentation of the LIF/STAT3 pathway (Graf et al. 2011). The LIF receptor is activated by LIF and activates afterwards STAT3, which is inhibiting several differentiation pathways. When Stat3 is phosphorylated it will be transferred into the nucleus and acts on promoter and enhancer regions.

1.2.2 The transcriptional network of the main stem cell factors Oct4, Nanog and Sox2

The first characterized key regulator to govern pluripotency was Oct4 (POU5F1), a member of the POU-family, also known as Oct3 (Okamoto et al. 1990; Schöler et al. 1989). Today, the transcriptional regulators (TRs) Oct4, Nanog and Sox2 are the most prominent and best characterized stem cell factors. These factors represent the central players of transcriptional hierarchy regulating the stemness network, as they are the most crucial factors in ESCs and during early development (Huang et al. 2015; Boyer et al. 2005). Furthermore, these proteins are tightly regulated and are able to control a huge network of other genes and factors. The expression level of Oct4 does not necessarily correlate with the stability of stemness, since an overexpression of Oct4 does not lead to an enhanced stem cell self-renewal. In other words, the changes induced by these factors and thereby the change of this huge transcriptional network make the difference between the decision of either remaining as stem cell or committing to a very defined differentiation process (van den Berg et al., 2010; Young, 2011). The analysis of promoter regions in multiple ES cell lines occupied by Oct4, Nanog and/or Sox2 resulted in the identification of 1,303 actively transcribed genes and 957 genes in an inactive state (Boyer et al. 2005). Further TRs have been implicated to play a role in ESC biology, including Stat3, Esrrb, Tbx3, Foxd3, LRH-1, Klf4, Myc, p53, and Sall4 (Hanna et al. 2002; Ivanova et al. 2006; Lin et al. 2005; Niwa et al. 1998; Sakaki-Yumoto et al. 2006).

Moreover, it was recently shown that TGF-ß and Wnt signaling play an important role in the maintenance of pluripotency, and that the three key players (Oct4, Nanog and Sox2) are regulating genes involved in these pathways. Add to this, half of the genes regulated by Oct4, Nanog and Sox2 are transcription factors important for the early differentiation into extra-embryonic, endodermal, mesodermal and ectodermal lineages (e.g., ESX1l, HOXB1, MEIS1, PAX6, LHX5, LBX1, MYF5, ONECUT1). A schematic picture of the Oct4, Nanog and Sox2 network shows an activating as well as a repressing network and further control of epigenetic factors (Boyer et al. 2005).

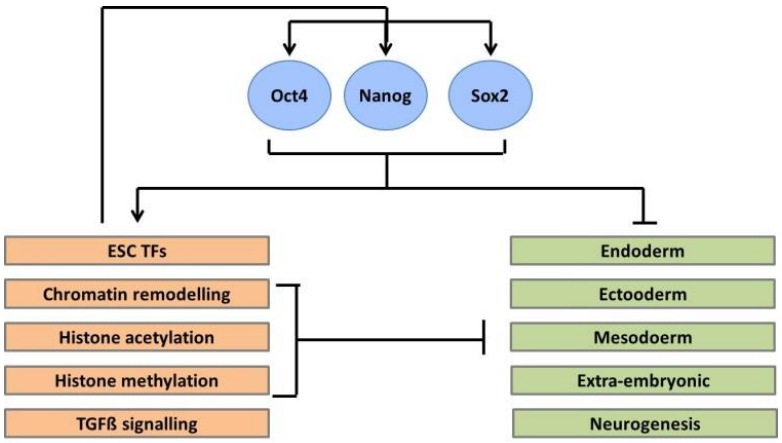

Figure 5: The signaling network of Oct4, Nanog and Sox2 is important for maintaining the ESC state. The three stem cell markers activate transcription factors, epigenetic factors and TGFß-signaling, and repressing genes that are important for the differentiation (adapted from Boyer et al., 2005).

1.2.3 Differentiation of ESCs into embryoid bodies (EBs)

Many protocols for the differentiation of ESCs into a variety of different cell types were established in the last two decades of stem cell research (Carotta et al. 2012; Fauzi, Panoskaltsis, & Mantalaris, 2012; Keller 2005; Soria 2001). However, the formation of embryoid bodies (EBs) which represents the early embryonic development, is a spontaneous germ layer differentiation induced by the absence of LIF and used in almost every differentiation protocol as a first step (Koike et al. 2007; Kurosawa 2007). The embryonic stem cells undergo a rapid differentiation process during the formation of EBs. Therefore, the stem cell markers such as Oct4 and Nanog are downregulated and in parallel, a rapid upregulation of markers for the three germ layers ectoderm, endoderm and mesoderm occurs (Poh et al. 2014). This process is completed around day 5 following LIF removal, and the EBs then represent the state of a mouse embryo at E7.5. Using ESCs and applying differentiation protocols can on one hand help to understand defects in the early embryogenesis and on the other hand reveal putative functions of proteins for specific cell types during differentiation.

1.3 Far upstream element binding protein 1 (FUBP1)

The far upstream element (FUSE) binding protein 1 (FUBP1) is one of the three known members of the FUBP family. The genes are located at different chromosomes in mice and humans. However, all members share the same protein architecture consisting of three distinct domains. The highest conservation can be found in the central DNA-binding domain (amino acids sequence homology of 81.5% (FUBP2) and 80.9% (FUBP3) compared to FUBP1) (Davis-Smyth et al., 1996; Duncan et al., 1994) .

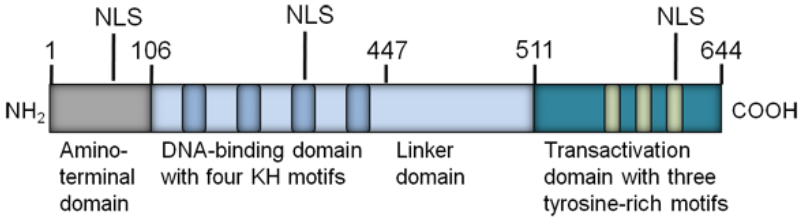

Figure 6: Schematic presentation of the FUBP1 domains. FUBP1 is composed of three distinct protein domains: An N-terminal repression domain, a central DNA-binding domain (containing 4 KH motifs which facilitate binding of FUBP1 to single-stranded DNA/RNA) and a C-terminal transactivation domain with three tyrosine-rich motifs. The central and the C-terminal domain are connected by a flexible linker domain. The amino acid positions of the respective domains are indicated above the diagram as well as the nuclear localization signals (NLS). Adapted from (Duncan et al., 1996)

Nevertheless, the family members were described to fulfill different functions, which can be explained by the reduced homology of the N-terminal repression and the C-terminal transactivation domain. FUBP3, for example, displays a less prominent nuclear localization compared to FUBP1 and 2, and it fails to bind the FUBP-interacting repressor (FIR) with its N-terminal domain. While FUBP1 and 2 are exclusively located in the nucleus, only 30% - 60% of FUBP3 can be found in this organelle, and the rest is seen in the cytoplasm (Chung et al. 2006). The weakest activating potential is described for FUBP2, and the role of FUBP2 might involve the regulation of splicing and the modulation and degradation of mRNA rather than the transcriptional regulation of genes (Gherzi et al. 2010). The best described family member, FUBP1, was initially identified as a transcriptional regulator that binds to the single stranded nucleic-acid sequence of the far upstream element (FUSE) DNA. FUBP1 consists of 644 amino acids with a molecular weight of 67.5 kDa. The N-terminal domain consists of amino acids 1-106, contains a stretch of eleven repeated glycine residues and a predicted amphipathic α-helix. The central domain (amino acids 107-447) consists of four units, each including a highly conserved K homology (KH) motif that mediates binding to single stranded DNA (Duncan et al., 1994) The KH motif was first identified in the human heterogeneous nuclear ribonucleoprotein K (hnRNP K). It consists of three α-helices packed

onto a three-stranded antiparallel β-sheet. The C-terminal transcription activation domain (amino acids 448-644), separated from the central domain by a flexible proline/glycine-rich linker, contains three tyrosine-rich motifs. Each of these motifs contributes to the transcriptional activation by FUBP1 (Duncan et al., 1996).

The first result about FUBP1 acting as a transcriptional regulator of *c-myc* was published by Avigan et al. in 1990. The authors could show that upon a basal expression of *c-myc* mRNA, the dsDNA is turned and melted upstream of the *c-myc* promoter region and the far upstream sequence element (*FUSE*) is presented as single stranded DNA. It was shown that this binding of FUBP1 to *FUSE* is required for maximal *c-myc* transcription upon interaction of FUBP1 with the TFIIH subunit of the transcriptional machinery (Figure 7) (Avigan, Strober, & Levens, 1990; Hsiao et al, 2010).

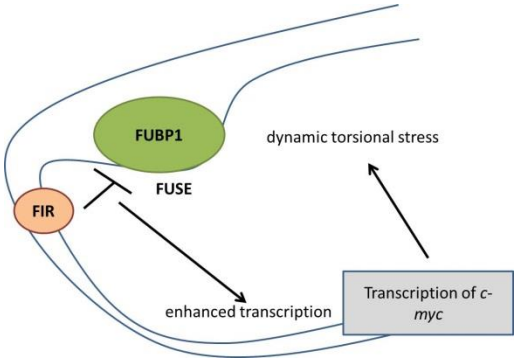

Figure 7: Model of dynamic *c-myc* peak expression mediated by FUBP1. Upon basal expression of *c-myc*, the *FUSE* element is accessible for FUBP1 because of relaxation of the DNA due to torsional stress. The antagonist FIR replaces the binding of FUBP1 to *FUSE* and downregulates the transcription again (Hsiao et al. 2010).

1.3.1 The transcriptional network controlled by FUBP1

A number of publications describe FUBP1 as a transcriptional regulator involved in apoptosis, cell cycle regulation and migration as well as in HCV replication. The data present a network of various partly unrelated FUBP1 target genes (Figure 8). One key explanation why FUBP1 is functioning in a variety of cancer entities is its direct regulation of the proto-oncogene *c-myc*, which is involved in the regulation of apoptosis, cell-cycle and replication (Meyer and Penn 2008). Both genes, *Fubp1* and *c-myc*, are described to regulate a huge number of genes by acting as a transcriptional activator and repressor.

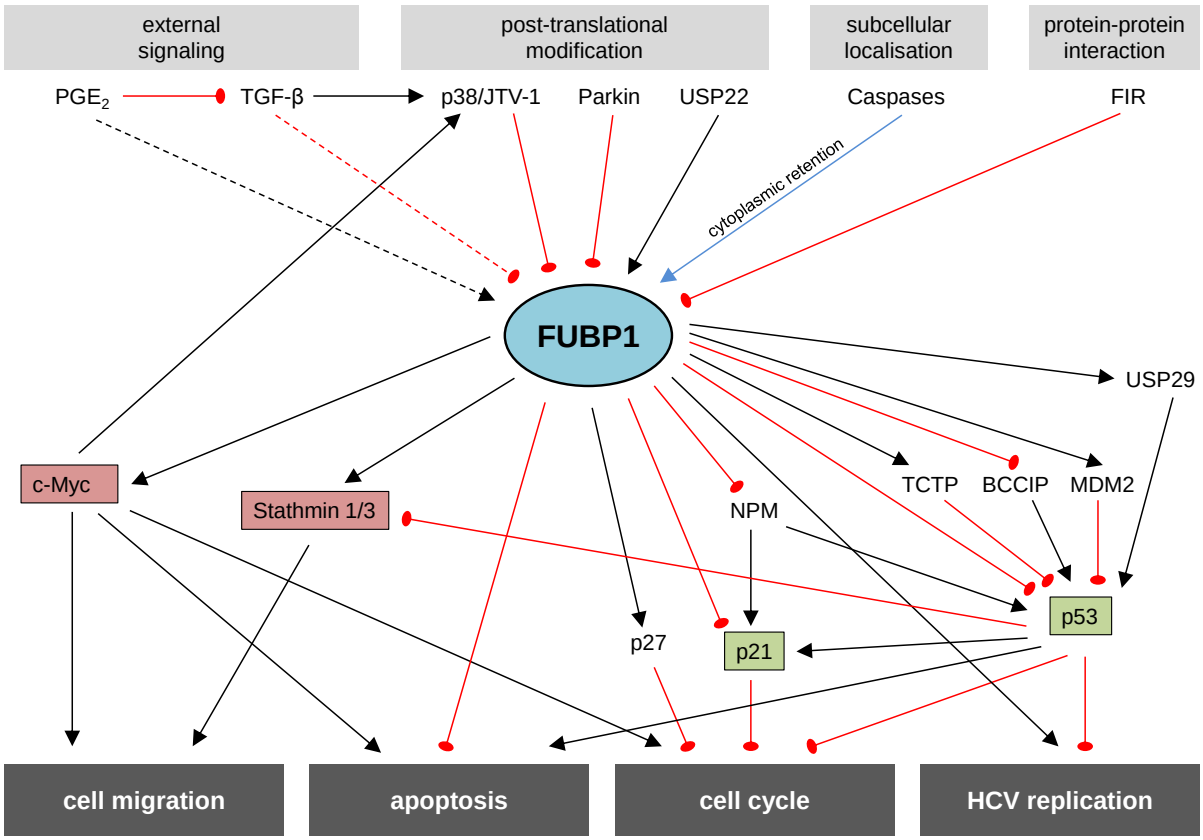

Figure 8: FUBP1 is involved in carcinogenesis by controlling cell migration, proliferation, apoptosis and HCV replication. The upstream regulation of FUBP1 is mediated by various mechanisms including cell extrinsic signaling post-transcriptional modifications (Liu et al. 2011), or activity control by its inhibitor FIR (Hsiao et al. 2010; Liu et al. 2006). Caspase-mediated cleavage results in cytoplasmic retention of FUBP1, where it functions as an RNA binding protein (Jang et al. 2009). Multiple downstream targets of FUBP1, which are involved in the regulation of cell migration, apoptosis, cell cycle and HCV replication (a major cause of HCC development), have been identified (Zubaidah et al. 2008), thereby linking FUBP1 to important hallmarks of tumorigenesis. The most prominent promoters (in red) and suppressors (in green) of carcinogenesis are displayed in rectangles. Black lines indicate activatory, red lines inhibitory influences (Gerlach 2015).

Our group identified FUBP1 as a highly expressed protein in more than 83% of 109 HCC samples (Rabenhorst et al. 2009). Additionally, high FUBP1 expression levels correlate with poor prognosis for HCC patients (Malz et al. 2009). Moreover, the stable knockdown of *FUBP1* in the human HCC cell line Hep3B led to an almost complete inhibition of tumor formation in a xenograft mouse model. The analysis of potential target genes involved in apoptosis and cell cycle demonstrated that FUBP1 induces the positive cell cycle regulator *Cyclin D2* and simultaneously represses the cell cycle inhibitors *p21* and *p15*. Furthermore, *p21* could be confirmed as a direct target of FUBP1. Additionally, the repression of the pro-apoptotic genes *BIK*, *NOXA*, *TRAIL* and *TNFα* in FUBP1-deficient HCC cells was demonstrated (Rabenhorst et al. 2009).

At the same time, Williams, Hamilton and Sarkar were able to identify FUBP1 as an interacting partner of the survival motor neuron protein (SMN) in a yeast two hybrid system, using a fetal brain cDNA library (Williams, Hamilton, and Sarkar 2000). The embryonic lethal phenotype of the SMN -deficient mice and the co-expression pattern of both proteins in the fetal brain led the authors to assume that SMN and FUBP1 might both be crucial for neuronal development.

Liu and others could show that JTV1 co-activates FUBP1 to induce *USP29* transcription and to stabilize *p53* upon DNA damage (Liu et al. 2011). Another publication from Kim et al. 2003 showed that the ubiquitination and thereby degradation of FUBP1 by tRNA synthetase cofactor p38 is required for lung cell differentiation. The cofactor p38 is associated with the multi-aminoacyl-tRNA synthetase (ARS) complex and plays an essential role for survival, since a genetic disruption of *p38* leads to neonatal lethality in mice. These mice show hyperplasia in lung, intestine and liver. Furthermore, interaction analyses showed that p38 binds to the C-terminal domain of FUBP1 and thereby ubiquitinates FUBP1, leading to a repression of FUBP1 activity (Kim et al. 2003; Han et al., 2006).

1.3.2 The physiological role of FUBP1 in mice

Three mouse models (one complete *Fubp1* knockout mouse strain published by Zhou et al., 2016, and two gene trap mouse models published by Rabenhorst et al., 2015) were developed to understand the physiological role of FUBP1. Both publications are describing an embryonic lethal phenotype and a significant reduction of HSCs in the fetal liver of FUBP1 deficient mice, thereby pointing towards the importance of FUBP1 during embryonic hematopoiesis. The overlapping results indicate the developmental delay of the embryos (smaller size and less weight compared to WT and heterozygous siblings) and the reduced number of HSCs in the fetal liver. In addition, the fetal liver HSCs were not able to engraft properly in transplantation experiments, while this effect was more drastic in the *Fubp1* KO mouse model. Adult LT-HSCs also showed an engraftment defect upon *Fubp1* shRNA-mediated knockdown (Rabenhorst et al. 2015). Moreover, Zhou et al., 2016 described additionally the defect of the mutant embryos to form healthy tissue like the placenta, lymphoid tissue and parts of the brain compared to the WT siblings. Analysis of the known target gene *c-myc* showed a dysregulation in FUBP1$^{-/-}$ MEFs. While the *c-myc* level in WT MEFs displays a very low variation in each analysis from different WT siblings, there was a big variation observed ranging from very low to a very high *c-myc* expression level in the homozygous *Fubp1* KO cells (Zhou et al. 2016).

Table 1: Comparison of the *Fubp1* KO mouse model and the *Fubp1* GT mose model.

	***Fubp1*$^{-/-}$** (Zhou et al. 2016)	***Fubp1*$^{null/null}$ (GT1 and GT2)** (Rabenhorst et al. 2015)
Method / Strain	Deletion of Ex8 to 13 (DNA binding domain) Strain: C57Bl/6J	GT1: gene trap integration into intron 18 GT2: gene trap integration into intron 1 Strain: C57Bl/6J
Living pups	no	no
Embryonic lethality	From E10.5 on decreasing	Dying around day E15.5
Morphology	Smaller and 20% less weight pale, runted, and hemorrhagic	Smaller, anemic
Histologic pathology (E19.5)	smaller stressed placenta, underdevelopment of lymphoid tissue, hypoplastic thymus increased parenchymal cellularity in brain	na
Fetal hematopoiesis	<u>E13.5 and 19.5</u> Reduced HSCs, no engraftment Reduced CFCs Disorders of erythroid, granulocyte/macrophage, and lymphoid lineages	<u>E15.5</u> Reduced HSCs and engraftment / self-renewal capacity Reduced number of erythroid and B-cells
Adult hematopoiesis	na	Increased apoptosis and prolonged generation time of *Fubp1* knockdown HSCs Production of all hematopoietic lineages
FUBP1 target gene analysis	<u>Fetal MEFs</u> Dysregulation of *c-myc* mRNA levels	<u>Adult HSCs</u> Upregulation of *p21* and *Noxa* Downregulation of *c-myc*

Apparently, FUBP1 plays a key role in the development of different organs and in the regulation of apoptosis by controlling important target genes such as *c-myc* or *p21*. On the contrary, the uncontrolled de-regulation of FUBP1 represents an oncogenic event in several cell types.

2 Aim of this project

Results obtained in the group of Prof. Dr. Martin Zörnig were demonstrating the importance of FUBP1 for embryonic development. The *Fubp1 GT* mouse model showed an embryonic lethal phenotype, and the embryos died around day E15.5. The analysis of the liver cells confirmed a reduced number of total liver as well as hematopoietic stem cells. Furthermore, it was shown that fetal and adult HSCs lacking FUBP1 poses a reduced engraftment potential in transplantation experiments (Rabenhorst et al. 2015). This observation reflects a diminished capacity of HSCs to self-renew in the absence of FUBP1. Moreover, the group of Dave Levens published the results of their *Fubp1* KO mouse model, supporting and confirming these results. They described a defect in hematopoiesis during embryogenesis. Additionally, they could show that beside the HSCs, other tissues were affected by the *Fubp1* knockout

(*e.g.* smaller placenta, underdevelopment of lymphoid tissue, hypoplastic thymus and increased parenchymal cellularity in brain) (Zhou et al. 2016).

The interesting fact that FUBP1 acts as a regulator of HSC self-renewal brought up the question for a potential role in other stem cell types like cancer stem cells but also in normal stem cells. Additionally, the finding that not only hematopoiesis is affected in FUBP1-deficient embryos, but that other tissue or cell types in the embryo are not properly developed represented a starting point for further analysis. Therefore, I decided to address the role of FUBP1 in mouse embryonic stem cells. The cultivation and the possibility to apply a number of differentiation protocols made these cells an obvious choice to study FUBP1 functionally during development.

By applying a number of differentiation protocols, I would close the gap between early embryonic development and hematopoiesis. With the use of modern gene editing techniques (e.g. CRISPR/Cas9 technology), we wanted to generate *Fubp1* knockout ESCs and compare their stem cell status to WT ESCs. Analysis of target genes such as *p21* and *c-myc* as well as the analysis of the cell cycle in these modified cells should give a hint for a deregulation of FUBP1 targets. As a non-disturbed behavior of the stem cells is necessary for proper embryonic development, ESCs could be used for general differentiation protocols (embryoid body formation) and for more specific protocols to differentiate the cells into the hematopoietic direction.

In parallel, we wanted to understand if there are further developmental defects in the *Fubp1* GT mouse model. Therefore, we were interested in the FUBP1 expression pattern in all the organs during early embryogenesis as well as possible changes in the adult mouse.

Overall, I wanted to combine the results of the WT embryo analysis for FUBP1 expression and the histological analysis of the *Fubp1* GT mouse model with the findings in the ESC and differentiation studies to draw a picture for FUBP1 functionality in the ESCs and the early embryonic development.

3 Materials and Methods

3.1 Materials for molecular biology experiments

Plasmids

pLCV2

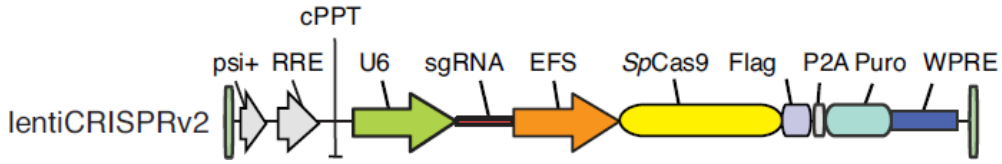

Figure 9: Scheme of the lentiviral *pLCRISPRV2* vector containing the *S. pyogenes Cas9* (*SpCas9*) and a single guide RNA (sgRNA). Psi+, Psi packaging signal; RRE, Rev response element; cPPT, central polypurine tract; EFS, elongation factor 1α short promoter; Flag, Flag octapeptide tag; P2A, 2A self-cleaving peptide; Puro, prumycin selection marker; WPRE, post--transcriptional regulartory element; Blast, blasticidin selection marker; Ef1a, elongation factor 1a promoter (Sanjana, Shalem, and Zhang 2014).

pMD2.G.VSV-G expression construct for the VSV-G virus envelope protein

p8.91 gag/pol - for matrix, core proteins, reverse transcriptase and integrin

The following gRNAs were cloned into the *pLCV2* vector for targeting the *Fubp1* locus.

Table 2: Guide RNA sequences

Plasmid name		Target mRNA sequence
pLCV.2 #1	caaaaattgggggtgatgc	Fubp1 aa 251 to 269
pLCV.2 #2	tcaaatgactatggttatg	Fubp1 aa 286 to 304
pLCV.2 #3	agatgccctgcagagagcg	Fubp1 aa 219 to 237
pLCV.2 NTC	ttccgggctaacaagtcct	Non target control

Preparation of large scale plasmid purification was performed using the DH5α bacteria strain.

Table 3: *E. coli* strains

Strain	Genotype	Manufacturer
DH5α	supE44 lacU169 (80lacZM15) hsdR17 recA1 endA1 gyrA96 thi-1 relA1	*Clontech Laboratories Inc.*, Mountain View, CA, USA

The following oligonucleotides were ordered at Biospring or Sigma for sequencing, genotyping and qPCR analysis.

Table 4: Oligonucelotides for sequencing, genotyping and qPCR analysis

Sequencing primer	Sequence 5´-3´
pLCV.2 #1 fw	cctgtcagtcccatacagtgc
pLCV.2 #1 rev	aaaagacccttagaagatggagg
pLCV.2 #3 fw	cgatggtcgtgcaagaatgtg
pLCV.2 #3 rev	tcgtgagaagacgccatctcc
Genotyping primer	
genSeq GT1 fw	ctgggttcaaatcc cactac
genSeq GT1 rev	acgggttcttctgttagtcc
genSeq GT2 fw	cctggcaggtctcttgagtt
genSeq GT2 rev	agtgattgactacccgtcagc

qPCR primer	Designed for use at T_m 60°C
mFUBP1 fw	agaagatggagatcagccagatgc
mFUBP1 rev	ctttgctgctgatgcattggaggt
mFUBP3 fw	aataattccacacctctggtggaccc
mFUBP3 rev	tactgccctttgatgtaccaaggc
mGAPDH fw	tgtgtccgtcgtggatctga
mGAPDH rev	ttgctgttgaagtcgcaggag
mc-myc fw	cctagtgctgcatgaggagac
mc-myc rev	cctcatcttcttgctcttcttca
mp21 fw	cctgacagatttctatcactcca
mp21 rev	caggcagcgtatatcaggag
mNanog fw	gaattctgggaacgcctcatc
mNanog rev	ccttgtcagcctcaggacttg
mOct3/4 fw	ggacatgaaagccctgcagaa
mOct3/4 rev	gacagatggtggtctggctgaa
mbrachyury fw	catcggaacagctctccaacctat
mbrachyury rev	gtgggctggcgttatgactca
mnestin fw	gggccagcactcttagctttgata
mnestin rev	tgagccttcagggtgatccag
mSox17 fw	ggacacgactgcggagtgaa
mSox17 rev	ggtcggcaaccgtcaaatg
mRunx1 fw	gcagaactgagaaatgctaccg
mRunx1 rev	gcaacttgtggcggatttgta
mRSPO3 fw	gtgaggccagtgaatggagt
mRSPO3 rev	ttacccttggctgaaggatg
mFLK1 fw	gggatggtccttgcatcagaa
mFLK1 rev	actggtagccactggtctggttg
mFoxa2 fw	tagcggaggcaagaagacc
mFoxa2 rev	cttaggccacctcgcttgt
mSnaiI fw	gccggaagcccaactatagcga
mSnaiI rev	ttcagagcgcccaggctgaggtact
mSnai2/slug fw	tggtcaagaaacatttcaacgcc
mSnai2/slug rev	ggtgaggatctctggttttggta
mWnt3a fw	caccaccgtcagcaacagcc
mWnt3a rev	aggagcgtgtcactgcgaaag
mFgfR1 fw	gcagagcatcaactggctg
mFgfR1 rev	ggagaagtaggtggtatcgctg
mBmp4 fw	ccgaatgctgatggtcgttt
mBmp4 rev	cctgaatctcggcgacttttt
m ß-catenin fw	tcttcaggacagagccaatgg
m ß-catenin rev	accagagtgaaaagaacggtagct
m GATA4 fw	caccccaatctcgatatgtttga
m GATA4 rev	gcacaggtagtgtcccgtc

For confirming the integrity of the viral packaging plasmids by restriction enzyme digestion, the following enzymes were used.

Table 5: Enzymes

Name	purpose	Manufacturer
*Bam*HI-HF	Test digest	*New England Biolabs* GmbH, Frankfurt
*Eco*RI-HF	Test digest	*New England Biolabs* GmbH, Frankfurt
*Spe*I	Test digest	*New England Biolabs* GmbH, Frankfurt

Table 6: Bacterial medium

Name	Ingredients/Concentration
LB medium	1% (w/v) Bacto-Trypton 0.5% (w/v) Yeast Extract 172mM NaCl

	pH 7.5
LB agar plates	LB medium 1% (w/v) Bacto-Agar
Ampicillin stock solution (1,000x)	50 mg/ml

3.1.1 Kits and Mastermix

Table 7: Kits and "ready-to-use" mix

Name	Manufacturer
Plasmid Maxi Kit	*Qiagen GmbH*, Hilden
QIAquick® Gel Extraction Kit	*Qiagen GmbH*, Hilden
DNeasy® Blood & Tissue Kit	*Qiagen GmbH*, Hilden
Omniscript RT Kit	*Qiagen GmbH*, Hilden
RNeasy mini Kit	*Qiagen GmbH*, Hilden
SYBR® Select Mastermix	*ThermoFisher Scientific*

Table 8: DNA and protein marker

Marker	Company
Gene Ruler™ 1kb Plus DNA ladder	*Invitrogen*, Darmstadt
Benchmark™ Prestainend Protein ladder	*Invitrogen*, Darmstadt

3.1.2 Buffers

Table 9: Agarose gel electrophoresis

Buffer	Ingredients/Concentration
Running buffer (0.5x TBE)	44.5mM Tris 44.5mM Boric acid 1mM EDTA pH 8.0
DNA loading buffer	100mM EDTA 1% SDS 0.25% (w/v) Bromophenol blue 0.25% (w/v) Xylenecyanol 20 % (v/v) Glycerol

Table 10: SDS polyacrylamide gel electrophoresis

Buffer	Ingredients/Concentration
SDS-sample buffer (5x)	62.5mM Tris-HCl, pH 6.8 2% (w/v) SDS 20% (v/v) Glycerol 0.1% (w/v) Bromophenol blue 50mM DTT
SDS-PAGE running buffer	50mM Tris 200mM Glycine 0.15% (w/v) SDS
Running gel buffer	1.5M Tris-HCl, pH 8.8
Stacking gel buffer	1M Tris-HCl, pH 6.8

Table 11: Cell lysis and blotting buffer

Buffer	Ingredients/Concentration
Cell lysis buffer	10mM Tris-HCl pH 7.4 20mM KCl 1.5mM $MgCl_2$ 0.5% SDS 1.3mM PMSF 1 Tablet *Complete Mini* Protease Inhibitor Cocktail (*Roche*, Mannheim) for 10 ml cell lysis buffer

Buffer	Ingredients/Concentration
Blotting buffer	48mM Tris 39mM Glycine 20% (v/v) Methanol
PBS	137mM NaCl 2.7mM KCl 8mM Na_2HPO_4 1.4mM KH_2PO_4
PBS-T	PBS 0.1% Tween-20
Blocking buffer	PBS 0.1% Tween-20 3% milk powder

3.1.3 Antibodies

Table 12: Antibodies

Name	Species	Dilution	Manufacturer
Anti-FBP1 (N-15)	Goat	1 : 1,000	*Santa Cruz Biotechnology*, Heidelberg
Anti-FUBP1 (ab181111)	Rabbit	1 : 4000	*Abcam plc*, Cambridge, UK
Anti-ß-Actin (C-11)	Goat	1 : 2,000	*Santa Cruz Biotechnology*, Heidelberg
Anti-Goat HRP	Rabbit	1 : 10000	*Invitrogen GmbH*, Darmstadt
Anti-Rabbit HRP	Donkey	1 : 10000	*Invitrogen GmbH*, Darmstadt
Human/Mouse Brachyury PE-conjugated Antibody	Goat	10 µL/10^6 cells	*R&D Systems*
Goat IgG PE-conjugated Antibody	Goat	10 µL/10^6 cells	*R&D Systems*
anti-mouse CD309 (VEGFR2, Flk-1) Antibody PE		1:50	*Biolegend*
anti-mouse CD144 (VE-Cadherin) Alexa Fluor® 647		1:50	*Biolegend*
Anti-Mouse CD45.2 PerCP-Cyanine5.5		1:50	*eBioscience*
Fixable Viability Dye eFluor® 506		1:50	*eBioscience*
CD71-APC		1:50	*eBioscience*
Ter119-PE		1:50	*Biolegend*
UltraComp eBeads			*eBioscinece*

3.1.4 Cell lines, cell culture medium and supplements

Table 13: Cell lines

Cell line	Description	Medium
HEK293T	human epithelial kidney cells derived from the HEK-293 cell line, which was transformed with the SV40 “large T”-antigen	DMEM, 10% FBS, 2mM L-Glu, 100 u/ml Pen, 100 µg/ml Strep
E14Tg2a	129/Ola mouse blastocyst, resistant to 6-thioguanine (10 µg/ml), extensive differentiation potential *in vitro* (Hooper et al. 1987)	1x GMEM, 2 mM glutamine, 1 mM sodium pyruvate, 1x nonessential amino acids, 10% (v/v), a 1:1000 dilution of ß-mercaptoethanol

Cell line	Description	Medium
		stock solution, and 500-1000 u/ml of leukocyte inhibitory factor
OP9	mouse, B6C3Fe-a/a, op, stromal like cells	α –MEM, 20% FCS, 100 u/ml Pen, 100 µg/ml Strep)

Table 14: Cell culture medium and supplements

Name	Manufacturer
DMEM	*GIBCO*, Eggenstein
GMEM medium	*Sigma*,
α –MEM	*GIBCO*, Eggenstein
DMSO	*Merck*, Darmstadt
DPBS	*PAA Laboratories*, Pasching
FBS	*PAA Laboratories*, Pasching
FBS for ESCs	*GIBCO*, Eggenstein
L-Glutamine	*PAA Laboratories*, Pasching
Antibiotics Penicillin/ Streptomycin	*PAA Laboratories*, Pasching
sodium pyruvate	*GIBCO*, Eggenstein
nonessential amino acids	*GIBCO*, Eggenstein
leukocyte inhibitory factor	*Chemicon*
Trypsin/EDTA 0.05%	*GIBCO*, Eggenstein
Trypsin/EDTA 0.25 %	*GIBCO*, Eggenstein

Table 15: Cytokines

Name	Description	Manufacturer
SCF	Stem cell factor	*Peprotech*
EPO	Human Erythropoietin	*Roche*

Table 16: Transfection reagents

Name	Description	Manufacturer
PEI	Poly(ethyleneimine) solution	*Sigma-Aldrich Chemie GmbH*, Steinheim

3.1.5 Mouse lines

General

Mice were bred and maintained under specific pathogen-free conditions in filter isolated, ventilated cages according to the german animal welfare law. For experimental use, mice were anaesthetized with isofluran and sacrificed by cervical dislocation.

Fubp1$^{null/+}$ GT1 and GT2

Two heterozygous *Fubp1*$^{null/+}$ gene trap mouse strains were used, which were established in the group of Dr. Martin Zörnig (Rabenhorst et al. 2015), via injection of the ES cell clones A033A08 (GT 1, gene trap integration into *Fubp1* intron 18; genotyping primer (Table 4) and 5SE293C09 (GT 2, gene trap integration into Fubp1 intron 1; genotyping primer (Table 4) obtained from the International Gene Trap Consortium (IGTC;

http://www.genetrap.org/index.html). The GT 1 strain expresses a non-functional fusion protein consisting of aa 1-589 of FUBP1, the ß-galactosidase (ß-Gal) and the aminoglycoside 30-phosphotransferase (APT) protein. The GT 2 strain expressed no FUBP1 protein sequence. The mutant animals were bred for at least 5 generations into the C57Bl/6J strain (Charles River) before analysis.

3.1.6 Laboratory equipment

Table 17: Centrifuges

Device	Manufacturer
Biocentrifuge, J2-21 M/E with JA-10 and JA-20 rotors	*Beckman*, Munich
Cold-Centrifuge Megafuge 1.0 R	*Heraeus*, Hanau
Cold-Centrifuge Mikro 220 R	*Hettich Lab Technology*, Tuttlingen
Desk-Centrifuge Biofuge pico	*Heraeus*, Hanau

Table 18: Electrophoresis

Device	Manufacturer
BioRad Power PAC 300	*BioRad Laboratories*, Munich
DNA Mini-Subcell for Agarose Gels	*BioRad Laboratories*, Munich
Electrophoresis Power Supply EPS 301	*Amersham Pharmacia Biotech Europe GmbH*, Nümbrecht
Gel-Chamber Model Hoefer HE 33 for Mini Gels	*Amersham Pharmacia Biotech Europe GmbH*, Nümbrecht

Table 19: Heat blocks and waterbath

Device	Manufacturer
Dri.Block DB-2D	*Techne Dexford*, Cambridge, England
Cooling-Thermomixer MKR 13	*HLC Biotech*, Bovenden
Thermomixer Compact for 1.5 ml Tubes	*Eppendorf AG*, Hamburg
Water-Bath	*GFL*, Burgwedel

Table 20: Incubators

Device	Manufacturer
Bacterial Incubator Function Line (37°C)	*Heraeus*, Hanau
Bacterial-Shaker-Incubator Multitron model (37°C)	*Infors AG*, Bottmingen, Switzerland
SANYO O_2/CO_2 Incubator (37°C, 5% CO_2)	*Panasonic*, USA
NuAire DHD autoflow (37°C, 5% CO_2)	*NuAire*, USA

Table 21: Devices

Device	Manufacturer
Autoclave Tuttnauer Systec 2540 EL	*Systec*, Wettenberg
Bioruptor® UCD 200 Sonicator	*Diagenode*, Liège, Belgium
Bunsen Burner Model 1230/1	*Carl Friedrich Usbeck KG*, Radevormwald
Cuvettes Polystyrol/Polystyrene	*Sarstedt AG&Co.*, Nümbrecht
Fluorescence Microscope Nikon Eclipse Te300	*Nikon*, Düsseldorf
Freezer (-20°C)	*Liebherr*, Ochsenhausen
Freezer CFC Free (-80°C)	*Sanyo*, Wiesbaden
Gene Amp® PCR System 9700	*PE Applied Biosystems*
Integra Pipetboy	*Integra Biosciences*, Fernwald
Laminar Air Flow (Biowizard KOJAIR)	*Kojair Tech Oy*, Vilppula

Device	Manufacturer
LightCycler®480	*Roche*, Mannheim
Microscope for Cell Culture	*Helmut Hund GmbH*, Wetzlar
Mircowave Sharp R-3V10	*Sharp Corp*.
NanoDrop™ 1000 Spectrophotometer	*Thermo Fischer Scientific*, Bonn
Neubauer Counting Chamber	*Marienfeld Superior*, Darmstadt
Odyssey® Infrared Imaging System	*LI-COR Biosciences GmbH*, Bad Homburg
pH-Meter Model PHM 83 autocal	*Radiometer*, Copenhagen, Denmark
Pipettes Model Pipetman®	*Gilson*, Limburg-Offheim
Pipettes Model Transferpette® S	*Brand GmbH&Co.KG*, Wertheim
Pipetus® with Storage Battery	*Hirschmann*, Neckartenzlingen
Refrigerator (4°C)	*Bosch*
Roller RM5 Assistant 348	*Karl Hechst GmbH&Co.KG*, Sondheim
Rotate roller	*Gerlinde Kister*, Mühlhausen
SmartSpecTM3000 Spectrophotometer	*BioRad Laboratories*, Munich
vacuum pump	*KNF Neuberger LABOPORT*, Freiburg
Vortex Genie 2	*Bender & Hobein AG*, Zürich, Switzerland

3.1.7 Chemical reagents and solutions

Table 22: Reagents and solutions

Object	Manufacturer
Acrylamide Solution (Rotiphorese Gel 30)	*Carl Roth GmbH&Co.KG*, Karlsruhe
AG490	*Calbiochem®*, *Merck*, Darmstadt
Agarose UltraPureTM Agarose	*Invitrogen GmbH*, Darmstadt
Ampicillin	*AppliChem GmbH*, Darmstadt
APS (Ammonium Persulfate) 10% in H_2O	*Sigma-Aldrich Chemie GmbH*, Steinheim
Boric Acid	*Carl Roth GmbH&Co.KG*, Karlsruhe
Bradford Reagent (Roti®-Quant)	*Carl Roth GmbH&Co.KG*, Karlsruhe
Bromophenol Blue	*Carl Roth GmbH&Co.KG*, Karlsruhe
BSA (Bovine Serum Albumin)	*PAA Laboratories*, Pasching
Chloroform	*Carl Roth GmbH&Co.KG*, Karlsruhe
Complete Mini Protease Inhibitor Cocktail	*Roche*, Mannheim
DTT (Dithiothreitol)	*Sigma-Aldrich Chemie GmbH*, Steinheim
ECLTM Western Blotting Substrate SuperSignal West Femto and Pico	*Thermo Fischer Scientific*, Bonn
EDTA (Ethylene Diamine Tetra Acetate)	*Sigma-Aldrich Chemie GmbH*, Steinheim
EGTA (Ethylene Glycol Tetraacetic Acid)	*Sigma-Aldrich Chemie GmbH*, Steinheim
Ethanol	*Carl Roth GmbH&Co.KG*, Karlsruhe
Ethidium Bromide	*Carl Roth GmbH&Co.KG*, Karlsruhe
Etoposide	*Sigma-Aldrich Chemie GmbH*, Steinheim
Formaldehyde	*Carl Roth GmbH&Co.KG*, Karlsruhe
Glucose	*Carl Roth GmbH&Co.KG*, Karlsruhe
Glycerol	*Carl Roth GmbH&Co.KG*, Karlsruhe
IllustraTM dNTP Set	*GE Healthcare Europe GmbH*, München
Isopropanol (2-Propanol)	*Carl Roth GmbH&Co.KG*, Karlsruhe
KCl (Potassium Chloride)	*Carl Roth GmbH&Co.KG*, Karlsruhe
KH_2PO_4 (Potassium-Dihydrogenphosphate)	*Carl Roth GmbH&Co.KG*, Karlsruhe
KoAc	*Carl Roth GmbH&Co.KG*, Karlsruhe
LiCl	*Carl Roth GmbH&Co.KG*, Karlsruhe
Methanol	*Carl Roth GmbH&Co.KG*, Karlsruhe
$MgCl_2$	*Sigma-Aldrich Chemie GmbH*, Steinheim

Object	Manufacturer
Na_2HPO_4	*Carl Roth GmbH&Co.KG*, Karlsruhe
NaAc	*Carl Roth GmbH&Co.KG*, Karlsruhe
NaCl	*Carl Roth GmbH&Co.KG*, Karlsruhe
NaOH	*AppliChem GmbH*, Darmstadt
Odyssey Blocking Buffer	*LI-COR Biosciences GmbH*, Bad Homburg
Phenol	*Sigma-Aldrich Chemie GmbH*, Steinheim
Phosphatase Inhibitor Cocktail 1, 2 and 3	*Sigma-Aldrich Chemie GmbH*, Steinheim
PMSF (Phenylmethylsulfonylfluoride)	*Carl Roth GmbH&Co.KG*, Karlsruhe
RNA Stabilization Reagent RNA Later	*Qiagen GmbH*, Hilden
RNase Inhibitor RiboLockTM	*Fermentas GmbH*, St. Leon-Rot
Roti®-Quant	*Carl Roth GmbH&Co.KG*, Karlsruhe
SDS (Sodium Dodecyl Sulfate)	*Carl Roth GmbH&Co.KG*, Karlsruhe
Sodium Deoxycholate	*Sigma-Aldrich Chemie GmbH*, Steinheim
TEMED (N,N,N',N'-Tetramethylethane-1,2-Diamine)	*Carl Roth GmbH&Co.KG*, Karlsruhe
TPA (12-O-tetradecanoylphorbol-13-acetate)	*Sigma-Aldrich Chemie GmbH*, Steinheim
Tris	*Carl Roth GmbH&Co.KG*, Karlsruhe
Triton X-100	*Fluka, Buchs*, Switzerland
Tween-20	*Carl Roth GmbH&Co.KG*, Karlsruhe

3.2 Molecular biology methods

3.2.1 Transformation of DNA into competent DH5α bacteria by heat shock

Foreign DNA can be introduced into competent bacteria by "transformation". For this purpose, chemo-competent *E. coli* bacteria (DH5α) were thawed on ice, and 50 µl of cells were mixed with 10-20 µl of plasmid DNA. After incubation on ice for 30 minutes, cells and DNA were exposed to a heat shock at 42°C for 90 seconds. After a second incubation on ice for 2 minutes, 600 µl of LB medium were added, and the bacterial culture was incubated at 37°C for 30 minutes. Afterwards, the suspension was centrifuged at 4,000 x g for 1 minute, 620 µl of supernatant was discarded and the pellet was resuspended in the remaining LB medium. The bacteria were streaked on LB-ampicillin agar plates and incubated overnight at 37°C.

3.2.2 Large scale plasmid purification

For large scale purification of the plasmid of interest, *E. coli* DH5α were transformed with the plasmid, and one clone was picked to inoculate a starter culture of 4 ml LB medium containing a final concentration of 50 µg/ml ampicillin. After 10-18 hours of incubation, the main culture of 250 ml LB medium was inoculated with 300-500 µl of the starter culture and incubated for 18 hours at 37°C and 160 rpm. Isolation of the plasmid was performed with either the Plasmid Maxi Kit (*Qiagen GmbH*, Hilden) or the NucleoBond® EF Xtra Maxi Kit (*Macherey-Nagel GmbH & Co.KG*, Düren) according to the manufacturer's instructions.

3.2.3 Small scale plasmid purification

The small scale plasmid DNA isolation and purification was performed by alkaline lysis of the bacteria with subsequent alcohol precipitation of the DNA (Birnboim, 1983).

1.5 ml of a 2-4 ml overnight culture of transformed bacteria were transferred into 2 ml tubes and centrifuged for 1 minute. The supernatant was discarded and the cells were resuspended in 100 µl GTE buffer. 200 µl of lysis buffer were added and the tube was inverted 4-6 times. The solution was incubated on ice for 5 minutes. The denatured proteins, chromosomal DNA and cellular debris were precipitated by the addition of 150 µl KOAc. The tube was inverted 4-6 times and incubated on ice for another 5 minutes. After centrifugation for 5 minutes, the plasmid-containing supernatant was transferred into a new 1.5 ml tube. The plasmid DNA was precipitated during a two-step procedure: First, 1 ml of 100% ethanol was added, the solution was gently mixed by vortexing, incubated for 2 minutes at room temperature and centrifuged for 10 minutes. Then, the supernatant was discarded and 500 µl of 70% ethanol were added to wash the DNA pellet and remove remaining salts. The solution was gently mixed by vortexing and centrifuged for 10 minutes. The supernatant was aspirated and the plasmid DNA pellet was air-dried. The pellet was resolved in 30 µl sterile deionized H_2O containing 60 µg/ml RNase A (*Roche*, Mannheim). The plasmid DNA was resuspended at 4°C over night, alternatively, it was shaken at 37°C for 20 minutes. An aliquot of the isolated plasmid DNA was analytically digested using the relevant enzymes, and the rest was stored at -20°C.

3.2.4 Digestion of DNA by restriction enzymes

The digestion of plasmid DNA was performed by restriction enzymes in a reaction mix consisting of 10x reaction buffer, 1/10 of the volume of required restriction enzymes and, if necessary, 10% BSA. For analytical restriction digestion, 0.5-1 µg DNA was diluted in a reaction volume of 10 µl. Preparative digestion was performed by using up to 10 µg DNA in a 50 µl reaction volume. DNA was digested at optimal enzyme activity temperature either for 1-2 hours or 6-8 hours. The digestion was stopped by heat inactivation. Before the DNA fragments were separated by gel electrophoresis 6 x DNA loading buffer was added.

3.2.5 Agarose gel electrophoresis

For the detection of DNA fragments and to quantify their length, agarose gel electrophoresis was used. Agarose forms an inert matrix, and by applying an electric field, the negatively

charged DNA can migrate through the matrix to the anode. DNA fragments move with different speed through the agarose gel inversely correlated with their size. The addition of ethidium bromide, which intercalates into the DNA double helix, allows to visualize the DNA under UV-light. Plasmid DNA or PCR products were separated in 1% agarose/0.5 x TBE gels with 0.5 µg/ml ethidium bromide. Electrophoresis was performed in 0.5 x TBE buffer and at 10 V/cm gel length. Before loading, the DNA samples were mixed with 6 x DNA loading buffer. As a size marker, the GeneRuler™ 1 kb Plus DNA Ladder or the GeneRuler™ 100 bp Plus DNA Ladder (*Fermentas GmbH*, St. Leon-Rot) was used.

3.2.6 DNA extraction from Agarose gel

Fragments containing the DNA of interest were excised and extracted from the gel using the QIAquick® Gel Extraction Kit (*Qiagen GmbH*, Hilden) according to the manufacturer's instructions.

3.2.7 Ligation of DNA

For the ligation of DNA fragments with complementary nucleotide overhangs, the enzyme DNA ligase was used. It catalyzes the formation of phosphodiester bonds between 5´phosphates and 3´hydroxyl groups of DNA strands. Vector and insert DNA fragments were mixed at a vector-to-insert-ratio of 1:3 or 1:1 that was calculated with the following formula:

$$\text{Insert [ng]} = 3\text{x}\frac{Vector\ [ng]x\ Insert[bp]}{Vector\ [bp]}$$

In general, an excess of the insert DNA and the addition of CIP (alkaline phosphatase calf intestinal) during the digestion of the vector reduces the probability of vector self-ligation. The total reaction volume was 10 µl, including 1 µl T4 DNA ligase (*New England Biolabs*: 40 u/ml) and 1 µl 10 x ligase buffer. The ligation was performed at 16°C overnight or at room temperature for 2-6 hours. For transformation of competent *E. coli* cells, 5 µl of the reaction sample was used.

3.2.8 Protein quantification by Bradford assay

The Bradford protein assay was used to determine the protein concentration. The dye *Coomassie Brilliant Blue G-250* interacts with proteins, resulting in a shift of the absorption from 465 nm to 595 nm. The change in the absorption is proportional to the protein

concentration of the sample. For the calculation of unknown protein concentrations, a calibration curve obtained with eight different BSA concentration standards was used. The assay was performed as described in the manufacturer's instructions (Roti®-Quant, *Carl Roth GmbH & Co .KG*¸ Karlsruhe). 5 µl of cell lysate (or BSA-standard) were diluted in 800 µl H_2O and then 200 µl of 5 x Roti®-Quant were added 5 minutes before measuring absorption at 595 nm with a spectrophotometer (SmartSpecTM3000 Spectrophotometer, *BioRad Laboratories*, Munich).

3.2.9 Sequencing of DNA

Sequencing of DNA was performed by *GATC Biotech AG*. Samples were prepared according to the GATC sample requirements, and the sequences were analyzed with NCBI-BLAST (http://blast.ncbi.nlm.nih.gov/ → nucleotide BLAST).

3.3 Biochemical methods

3.3.1 SDS-polyacrylamid gel electrophoresis (PAGE)

SDS polyacrylamide gels were used for the separation of protein mixtures based on their molecular weight. Upon polymerization of the acrylamide solution, it forms a netlike structure. The size of the pores in the gel depends on the percentage of acrylamide. Proteins were denatured by the negatively charged detergent sodium dodecyl sulfate (SDS) and reduced by ß-mercaptoethanol, which induces hydrolysis of S-S linkages. After application of an electric field, the proteins migrate towards the anode. Proteins migrate first through the stacking gel, which contains a low percentage of SDS. At the border to the running gel, protein movement is decelerated. Proteins with lower molecular weight move faster through the pores of the running gel than proteins with higher molecular weight.

Table 23: Composition of gels for the SDS-PAGE.

Component	2.5% stacking gel	10% running gel	12% running gel
H_2O	5.25 ml	6.25 ml	5.25 ml
Acrylamid/Bisacrylamid (37.5:1)	1.25 ml	5 ml	6 ml
SDS 20% (w/v)	37.5 µl	75 µl	75 µl
1.5M Tris-HCl pH 8.8	-	3.75 ml	3.75 ml
1M Tris-HCl pH 6.8	925 µl	-	-
APS 10% (w/v)	100 µl	100 µl	100 µl
TEMED	5 µl	10 µl	10 µl
total	7.5 ml	15 ml	15 ml

Protein samples were mixed with 5 x SDS sample buffer and denatured at 95°C for 5 minutes. The separation by SDS-PAGE was performed in 1 x SDS-PAGE buffer using the Mini Protean II System (*BioRad*, Munich). Electrophoresis was performed at 80 V for the stacking gel and 120 V for the running gel. The BenchMark™ Prestained Protein Ladder (*Invitrogen*, Karlsruhe) was used as a size standard. Subsequently, proteins were detected by immunoblotting (Western Blot analysis).

3.3.2 Protein transfer onto nitrocellulose membranes

To detect proteins with a specific antibody, protein transfer from the SDS-PAGE gel to a nitrocellulose membrane was performed. Three Whatman papers were soaked with 1 x blotting buffer and placed on top of the anode of a semi-dry blotting chamber (*Keutz*, Reiskirchen). The membrane was incubated with blotting buffer and then placed on the Whatman papers. Subsequently, the SDS gel was added on top, followed again by three layers of Whatman paper. The cover of the chamber, containing the cathode, was closed, and the proteins were blotted at 0.8 mA/cm^2.

3.3.3 Western Blot analysis

Incubation of the membrane with blocking buffer (TBS-T, 3% milk powder) for 1 hour at room temperature prevents unspecific protein binding. For specific protein detection, the membrane was incubated with the respective first antibody (diluted in blocking buffer) at 4°C overnight. The membrane was washed 3 x 10 minutes with TBS-T to remove unbound antibody. Finally, the membrane was incubated with the corresponding secondary antibody (coupled with HRP) for one hour. HRP catalyzes the conversion of the enhanced chemiluminescence (ECL) substrate into its product which also results in the emission of light. The emitted light was detected with X-ray films (Super RX Fuji Medical X-Ray Film; FUJIFILM Corporation, Tokyo, Japan), and development of these films was performed with a X-Ray Film Processor XR 24 Pro (Dürr Dental AG, Bietigheim-Bissingen).

3.3.4 cDNA synthesis and quantitative real-time PCR

First, RNA concentration was determined on a NanoDrop 1000 Spectrophotometer (Thermo Scientific) by measurement of absorption at a wavelength of 260 nm. To analyze RNA purity, the 260/280 and 260/230 ratios were calculated (280 nm: absorption by contaminating proteins, 230 nm: absorption by different contaminating organic compounds). The 260/280

ratio should be in the range of 1.8- 2.0, the 260/230 value should be between 2.0 and 2.2 for clean RNA preparations.

Afterwards, RNA was converted into cDNA using the Omniscript RT kit (Qiagen) according to the manufacturer´s instructions. 1 µg of RNA was transcribed in a 20 µl reaction mix containing RT reaction buffer, oligo(dT) and random hexamer primer, dNTPs, RNAse inhibitor (RiboLock, Fermentas) and Reverse Transcriptase. Separate control reactions where performed without Reverse Transcriptase (RT control).

In principle, qPCR is a method based on a conventional PCR reaction. It is performed in the presence of a fluorescent agent that is measured during the course of the reaction as an indicator of the amount of the amplified target sequence. Quantification of the fluorescent signal allows monitoring target amplification, not only at the end of the reaction as in conventional PCR, but throughout all PCR cycles. Specificity of qPCR assays based on dyes can be ensured by the combination of melting curve and agarose gel analysis, together with sequencing of the reaction product. The qPCR was performed with the SYBR select mastermix in technical duplicates using the following protocol.

Table 24: Pipetting scheme for qPCR analysis

Component	1x
SYBR select mm	10 µl
Primer fw	0.6 µl
Primer rev	0.6 µl
H_20	6.8 µl
cDNA (1:10 dilution)	2 µl
total	20 µl

The samples were amplified using the following program

Table 25: qPCR program

PCR program	Time	Temperature	Cycle
Initialization	2 minutes	95°C	1
Amplification	30 seconds	95°C	40
	30 seconds	60°C	
	30 seconds	72°C	
Melting curve	10 seconds	50°C	1
	10 seconds	+2.2°C	
	…	95°C	

Ct values were used for the calculation of the relative mRNA expression compared to the housekeeping gene *Gapdh*.

3.4 Flow Cytometry

Analysis of transduction and transfection efficacy

For the quantification of cells producing the reporter/fluorescence protein after transduction or transfection, the FACS Calibur (*Becton Dickinson Biosciences*, Heidelberg) was used. Cells were harvested and transferred to FACS tubes. After centrifugation (5 minutes, 1,000 rpm, 4°C), they were washed with PBS, again pelleted by centrifugation, resuspended in 200 µl PBS plus 3% FBS and stored on ice. After measurement, data sets were analyzed using the Cell Quest-Pro software (*Becton Dickinson Biosciences*, Heidelberg). At least 10,000 events were acquired for each sample.

Surface marker

For flow cytometry analysis, cells were washed twice with cold PBS and centrifuged at 1,000 rpm. The pellet was then re-suspended in FACS buffer (3-5% FCS in PBS) and incubated with cell surface antigens and a fixable viability dye. The cells were stained for 30 minutes on ice, washed and re-suspended in 200 µl FACS buffer. Flow cytometry was performed using BD FACSCanto II Flow cytometer, and analysis was done using Diva software.

Intracellular staining

For cell fixation, cells were suspended in 1x PBS buffer and washed twice with 1x PBS buffer by centrifugation at 1,000 rpm for 5 min each time. The supernatant was discarded and cells were fixed in a final concentration of 4% formaldehyde for 20 min at room temperature. Afterwards, cells were washed twice with 1x PBS buffer by centrifugation at 1,000 rpm for 5 min each time. They were then permeabilized by adding 0.1% Triton X-100 in 1x PBS buffer for 15 min at room temperature. Cells were washed twice with 1x PBS buffer by centrifugation at 1,000 rpm for 5 min each time. Blocking was performed by incubation with 3 ml blocking buffer (0.5g BSA in 100 ml PBS) for 1 hr at room temperature. The antibody was added to each sample and incubated for 1 hr at room temperature, following another washing step. Finally, cells were resuspended in 0.3 – 0.5 ml 1x PBS buffer and analyzed.

3.5 Cell culture

Cell culture experiments were performed in a cell culture lab in a sterile bench. Before freezing or after thawing cells, 1 µl of medium was collected for a mycoplasma test. Only mycoplasma-free cells were used for experiments.

3.5.1 Mammalian cell culture

Cells were cultured in a cell incubator at 37°C with 5% CO_2 in a humidified atmosphere. If not mentioned otherwise, the growth medium (DMEM or Advanced MEM) contained 10% v/v fetal bovine serum (FBS), 1% v/v L-glutamine (100mM) and 2% v/v penicillin/streptomycin (10,000 u/10,000 µg/ml). For inactivation of the complement system, FBS was incubated at 56°C for 30 minutes, before it was added to the medium.

Cells were passaged twice a week. Culture medium was removed, cells were washed with PBS and treated with 0.05% Trypsin-EDTA solution for 3 - 10 minutes at 37°C. The detached cells were collected in fresh medium, and a suitable amount of cells was transferred to a new culture dish.

3.5.2 Thawing and freezing of cells

For long term storage, cells were frozen at -80°C in FBS containing 10% v/v dimethyl sulfoxide (DMSO) to reduce the formation of ice crystals. Cells were treated as if being prepared for passaging and transferred to a 50 ml reaction tube. The harvested cells (centrifugation at 400 x g, 4°C for 5 minutes) were resuspended in freezing medium, transferred into cryo tubes and slowly frozen in a "freezing modul" at -80°C.

For thawing, cells were warmed and transferred to a 15 ml reaction tube with 10 ml fresh medium. Cells were harvested by centrifugation (5 minutes, 400 x g, and 4°C). Medium was aspirated to remove residual DMSO; cells were resuspended in fresh medium and transferred into cell culture dishes.

3.5.3 Cell lysates

To extract proteins from cultivated cells, a confluent 10 cm dish was washed with PBS, 100 µl freshly prepared lysis buffer was pipetted onto the dish, and the cells were scratched off with a cell scraper. The lysate was collected in a 1.5 ml tube and incubated on ice for 20 minutes. Sonication was performed with a Bioruptor® UCD 200 (*Diagenode*, Liège, Belgium; settings: Duty Cycle 30%, Output 3, 2x10 Pulses). The lysates were stored at -20°C.

3.5.4 RNA preparation

Cells were harvested and RNA isolation was proceeded as described in the manufacturers handbook (RNeasy mini kit, *Qiagen*).

3.5.5 Quantifying cell numbers with the Neubauer counting chamber

Cells were trypsinized for counting, collected in a reaction tube with fresh medium, and 10 µl cell suspension were pipetted between the Neubauer counting chamber and the cover glass. The Neubauer counting chamber consists of 4 big squares, which are subdivided into 16 smaller squares. All cells in 4 of the big squares were counted (x), and a mean of cells per big square was calculated. The volume (v) of the cell suspension in one big square is 0.1 µl. The multiplication of the cell number in 0.1 µl with the factor 10^4 leads to the cell number (n) per ml.

$$n\ \frac{cells}{ml} = \frac{x}{4} cells * v * 10^4\ \frac{\mu l}{ml}$$

3.5.6 Production of lentiviral particles in HEK293T cells using polyethylenamine (PEI)-mediated transfection

The day before transfection, $5x10^6$ HEK293T cells were seeded in a 10 cm dish. For every expression vector, 5 dishes were needed. 2 µg *pMDG2* (vsv - for the capsid protein), 6.5 µg *p8.91* (gag/pol - for matrix, core proteins, reverse transcriptase and integrin) and 10 µg of the expression vector were mixed per dish. In addition, 500 µl PBS was mixed with 35 µl 10mM PEI-Max. To start the complex formation, the PEI solution was added to the DNA solution and carefully mixed. After incubation for 15 minutes at room temperature, the mixture was added to the cells, together with 6.5 ml DMEM.

48 or 72 hours after transfection, virus supernatant was collected and filtered through a 0.45 µg syringe filter unit. The virus was concentrated by ultracentrifugation at 20,500 x g at 4°C for 2 hours, and aliquots were frozen at -80°C.

3.5.7 Lentiviral transduction

$1x10^6$ cells were seeded in 6 well plates 24 hours before transduction. 5 ml original lentivirus supernatant was mixed with 1 ml fresh medium. 3 ml/well were given to the cells. Spininfection was performed by centrifugation at 1,000 rpm and 32°C for 60-90 minutes, and the medium was exchanged after 6 hours. Alternatively, 10-30 µl of the concentrated virus were given to the cells, and the medium was changed after 48 hours.

3.6 Differentiation assays

3.6.1 ESC differentiation into embryoid bodies (EBs)

ESCs were washed twice with PBS, trypsinized and centrifuged at 1,000 rpm for 5 min and resuspended in PBS. The cell number was calculated, and $2x10^4$cells/ml were plated on bacterial plates with differentiation medium (in total 5 ml). Bacterial plates were placed in a 25 degree angle so that the possibility for the cells to adhere on the plate was minimized. After 24-48 hours, small EBs were formed and plates were placed horizontally again. During the first days, the plates should be moved (slowly shaken) once a day. EBs were collected at day 3, day 5, day 7 and day 10.

3.6.2 OP9 differentiation assay (hematopoietic progenitor)

3.6.2.1 Cultivation and passaging of OP9 cells

The OP9 cells were washed with PBS before adding trypsin for 2 min and incubation at 37°C. The cells were pipetted up and down several times to dissolve aggregates and filtered through a 100 µm filter before being centrifuged at 1,200 rpm for 5 minutes. The cells were split in a 1:4 ratio every 4^{th} day. The quality of OP9 cells is dependent upon the particular FCS batch used, and cells should be maintained carefully, as they are easily losing their supportive activity. If cultivated too densely, OP9 stroma cells will differentiate into adipocytes. If cultivated too thin, OP9 cells are change properties towards fibroblast-like cells that do not support ES cell differentiation or hematopoietic cells very well. Although OP9 cells do not change their morphology significantly if cultivated under suboptimal conditions their support function will become worse. The cell number should remain at 1-1.5 x 10^6 cells / 25 cm^2 flask when confluent, and the cells should not be used after passage 30.

3.6.2.2 Preparation of OP9 cells for ES cell differentiation into hematopoietic progenitor cells ($CD45^+$)

The efficient OP9 co-culture system to induce differentiation of mouse embryonic stem (ES) cell to hematopoietic progenitor cells was developed by Nakano, Kodama, & Honjo, 1994. Stromal OP9 cells do not produce functional macrophage colony-stimulating factor (M-CSF) which leads to a preferential differentiation of ES cells into hematopoietic cells (which differ from the monocyte-macrophage lineage). The usage of the OP9 system helps to elucidate the molecular mechanisms of hematopoietic system development and hematopoietic cell differentiation.

OP9 cells were prepared 4 days before starting the ES differentiation culture. It is important that OP9 cells are already confluent and can form a niche for the ES cells before seeding because cell-cell contact between the stroma cells supports the ES cell differentiation critically. OP9 cells are contact-inhibited, so no additional treatment or irradiation is needed before seeding of ES cells onto the stroma cells. At the day of seeding the ES cells, another plate of OP9 cells were prepared for re-seeding at day 5.

3.6.2.3 Preparation of ES cells for the differentiation in co-culture with OP9 cells

Day 0: ESCs were washed twice with PBS, trypsinized and centrifuged at 1,000 rpm for 5 min and resuspended in PBS. The cell number was calculated, and 10,000, 30,000 20,000 or 50,000 cells were plated in duplicates on confluent OP9 cells using differentiation medium.

Day 5: Microscopic analysis of GFP negative islands in between the OP9 (GFP^+) cell layer. Optimal plates are showing an even deviation of islands which do not touch each other. Cells were replated on OP9 cells in dilutions of 1:10, 1:25, 1:50, 1:100, 1:200. Differentiation medium was supplemented with SCF (100 ng/µl) [3 µl into 3 ml], and the cells were additionally analyzed by flow cytometry for mesoderm marker.

Day 12: Plates were analyzed for floating cells in the medium produced by endothelial crypts. Cells in the supernatant as well as trypsinized cells were collected and stained for hematopoietic progenitor marker and analyzed by flow cytometry.

3.6.2.4 Proliferation of erythroid lineage cells on OP9

OP9 cells were prepared as described before, and 10,000 ES cells were seeded for mesoderm differentiation. At day 5, ESCs were re-plated on new OP9 cells, and 2 U/ml human recombinant erythro-poietin (EPO) was added. Between day 6 to 8 erythroid progenitor (EryP) cells were developing, and at day 10-12 definite erythroid (EryD) cells could be analyzed (described in Zheng et al., 2008) by FACS analysis using a CD71 and Ter119 marker.

3.7 Animal experiments and preparation

3.7.1 Genotyping

For DNA extraction, mouse tail-biopsies were lysed in a buffer containing 5% Proteinase K (QIAGEN) at 60°C. The enzymatic digestion was stopped by heat inactivation of the samples

for 10 minutes. The solution was then centrifuged, and the DNA in the supernatant was used for PCR reactions.

3.7.2 Tissue and organ preparation

The organs were removed and fixed overnight in 4% paraformaldehyde/PBS at 4°C. Before fixation, intestines were flushed clean with PBS, opened longitudinally and rolled into 'Swiss rolls'. The fixed tissues were dehydrated and embedded in paraffin; 4 µm sections were prepared on slides. Before staining, the sections were deparaffinized in xylene and rehydrated in alcohols of decreasing strengths and finally into PBS.

3.7.3 Time matings and embryo preparation

Two female mice were put together with one male mouse in the evening and were separated the next morning. Vaginal plugs were noted and the weight of the female mice was recorded. This day was counted as day E0.5, and after 9 days, the weight of the mice was again analyzed. Females that had gained 2 g or more were sacrificed to prepare E9.5 embryos After 13 days only animals with additional 3 g were selected for the analysis of E13.5 embryos. The yolk sac of the single embryos was taken for genotyping; the embryo itself was fixed in 4% paraformaldehyde/PBS at 4°C. Afterwards, it was preceded as described in 3.7.2.

3.8 Histology

3.8.1 Preparation of EBs for paraffin sections

Embryoid bodies were collected in a 15 ml Falcon at different time points (2x10 cm plates per time point and sample). After 30 min, EBs were set on the bottom of the falcon and supernatant was carefully removed with a pipet. All following steps required a time of 30 min to let the EBs settle, because they were not centrifuged to prevent dissection of the EBs into single cells. 5 ml of PBS was added to wash the EBs. The supernatant was removed after 30 min, and 4 % PFA was added (3 ml) and incubated for 30 min at RT. The EB aggregates were prepared by performing a stepwise sucrose gradient starting with 10% sucrose in PBs, 20% sucrose and finally 30% sucrose, each step with 2 ml sucrose for 30 min. Afterwards, the supernatant was removed and 100 µl warmed HistoGel™ (ThermoScientific) was added carefully. After solidification, the HistoGel™ containing EBs were embedded in paraffin and processed for IHC.

3.8.2 Hematoxylin and Eosin staining

The de-paraffinized and rehydrated tissue sections were stained for one minute in Hematoxylin QS (vector labs) to stain the nuclei of the cells. They were then rinsed in running tap water until the water was colorless. The cytoplasm was subsequently stained with 3% Eosin (Sigma) containing 0.5% acetic acid. The residual eosin was washed away with running water, and the sections dehydrated with alcohols of increasing percentage (50%-100%). The sections were incubated in xylene for 5 minutes and air-dried, covered with mounting medium, and a coverslip was placed on top to protect the tissue.

3.8.3 Immunhistochemichal staining

The immunhistochemichal staining for FUBP1, cleaved Caspase3 and Ki-67 were performed on 4 µm paraffin sections using the BOND-MAX Automated IHC/ISH Stainer (Leica) by applying the following protocol:

Bond^{TM} Dewax solution		72°C
EtOH solution	10 min	100°C
Bond^{TM} Wash	3 min	RT
Peroxid	10 min	RT
Anti-FUBP1 (ab181111)	30 min	RT
Polymer	8 min	RT
Bond^{TM} Wash	4 min	RT
DAB (3, 3'-diaminobenzidine)	8 min	RT
Hämatoxylin	10 min	RT
Dest. H_2O	1 min	RT

After removing the paraffin from the section and several incubation steps with EtOH, the sample is incubated with the according antibody. DAB is oxidized in the presence of peroxidase and hydrogen peroxide resulting in the deposition of a brown precipitate in the cells or the cell nucleus. A counterstain afterwards visualizes the negative cells in blue.

3.8.4 Cytospin and cytochemistry

ESCs were trypsinized, washed with PBS and 20,000 to 100,000 cells were resuspend in 70 µl PBS, Cells were centrifuged onto a polysine adhesion slide (ThermoFisher) using the Cellspin II centrifuge (Tharmac). Cells were stained as described in 3.8.3.

4 Results

4.1 Characterization of mESCs and the differentiation to EBs

4.1.1 Stem cell and differentiation marker in ESCs

ESCs are characterized by their self-renewal capacity and the ability to differentiate into all cell types of the organism. We genetically manipulated the already established murine ESC line E14TG2a in our laboratory and used differentiation protocols to induce germ layer formation in EBs. The E14TG2a cell line was originally generated from the E14 cell line (mouse ES cells isolated from the inner cell mass of a blastocyst).The cells are able to differentiate *in vitro*, but show a resistance to 6-thioguanine (10 µg/ml) while E14 cells are successfully killed with this this drug concentration (Hooper et al. 1987; Kuehn et al. 1987). First, we analyzed the expression level of the stem cell markers Oct4 and Nanog, as well as the expression of three selected germ layer marker for mesoderm, endoderm and ectoderm cells. The results are shown in Figure 10 (Brachyury, Nestin, and Sox17).

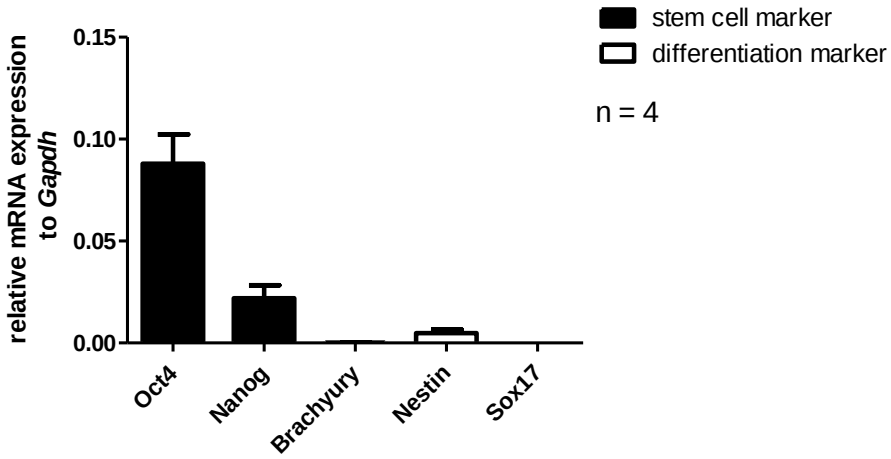

Figure 10: Analysis of stem cell- and differentiation markers in ESCs. *Oct4* and *Nanog* are highly expressed in ESCs, while *Brachyury*, *Nestin* and *Sox17* are expressed at a very low level. The data are presented as mean ± SD, 4 independent differentiation experiments in technical duplicates with ES cells were performed.

4.1.2 Differentiation of ESCs to EBs and analysis of germlayer development

For the differentiation of ESCs to EBs, the medium was changed to a differentiation medium (chapter 3.6.1) and the cells were seeded on bacterial dishes, which are not surface-treated, to minimize the cells´ ability to attach. After 24 hours small cell bodies were observable as

shown in Figure 11. After 3 to 5 days, the EBs were differentiated and consisted of the cell types of the three germ layers.

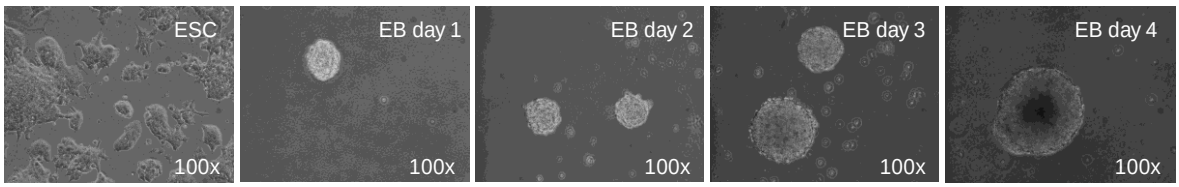

Figure 11: Differentiation of ESCs to EBs. From left to right: ESCs on gelatin-coated plates showing a flat morphology, growing in colonies. EB formation shown at day 1 until day 4 in differentiation medium, EBs were formed that contain cell types of the three germ layers mesoderm, endoderm, and ectoderm.

It is well described that the stem cell markers *Oct4* and *Nanog* are significantly expressed in ESCs, and that their mRNA expression level rapidly decrease during differentiation (Wang et al. 2012). To confirm that the ESCS used in this study showed this typical change in ESC stem cell marker expression, the ESCs were differentiated and analyzed by qPCR for the pluripotency factors *Oct4* and *Nanog*. The cells were harvested at day 0, day 5, day 10 and day 15.

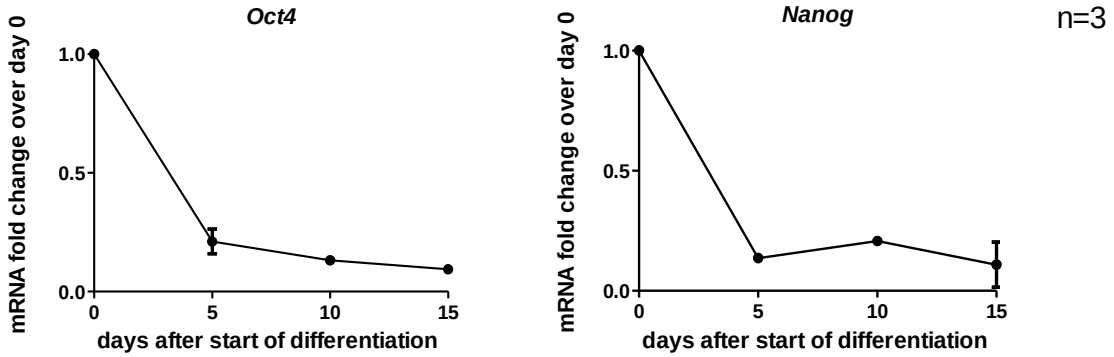

Figure 12: mRNA expression of stem cell markers *Oct4* and *Nanog* during differentiation. Oct4 and Nanog were rapidly downregulated during the first 5 days of differentiation into EBS. The data are presented as mean ± SD, 3 independent differentiation experiments in technical duplicates with WT ES cells were performed.

Together with the decreased expression of stem cell markers during EB differentiation, which is shown in Figure 12, an increase in the expression of differentiation markers was observed. The first step during differentiation of ESCs and embryos is the formation of an embryoid body or blastocyst, respectively, containing the three germ layers (Poh et al. 2014). The expression analysis of *Brachyury* (mesoderm marker), *Nestin* (marker for the ectoderm layer),

and *Sox17* (marker for endoderm initialization) showed a significant upregulation at day 5 Figure 13).

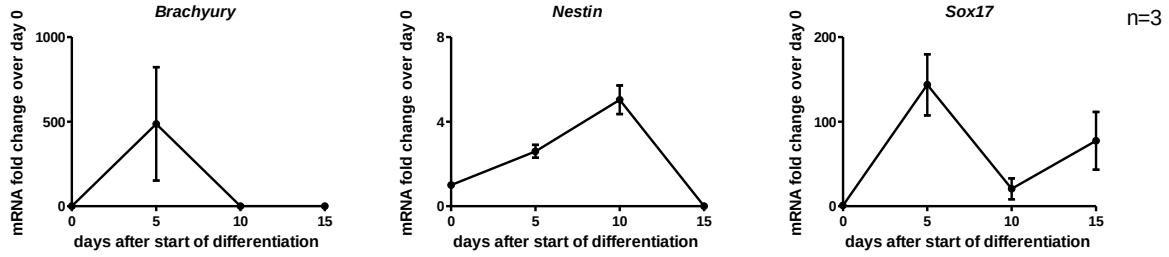

Figure 13: mRNA expression of germ layer markers *Brachyury* (mesoderm), *Nestin* (ectoderm) and *Sox17* (endoderm) during differentiation of ESCs to EBs. *Brachyury* showed a peak expression at day 5 and decreased afterwards to a very low level. *Nestin* showed its peak expression at day 7 and *Sox 17* at day 5, both decreased afterwards to a low expression level. The data are presented as mean ± SD, 3 independent differentiation experiments in technical duplicates with WT ES cells were performed.

4.1.3 Establishment and optimization of the OP9 assay to generate hematopoietic CD45$^+$ positive progenitor cells

For the validation of the optimal cell number of ESCs on OP9 cells for their differentiation to mesoderm and hemangioblast cells and, in the second step, to hematopoietic progenitor cells (CD45$^+$), we started with 4 different cell numbers (10^4, 20^4, 30^4 and 50^4) that were seeded on OP9 cells in the differentiation medium. At day 5 of differentiation, cells were trypsinized and replated with a dilution of 1:10, 1:100 and 1:200. The remaining cells were analyzed by flow cytometry for Flk-1$^+$/VE-Cad$^-$ (mesoderm) and Flk-1$^+$/VE-Cad$^+$ (hemangioblast) cells. It was first described by Nishikawa et al., 1998 that this combination of marker can be used to follow the differentiation steps from ESCs to mesoderm and hemangioblasts and further towards the hematopoietic direction without using an differentiation method. After 7 days of further differentiation into hematopoietic progenitor cells, the analysis was performed by flow cytometry using in addition the CD45 marker**.**

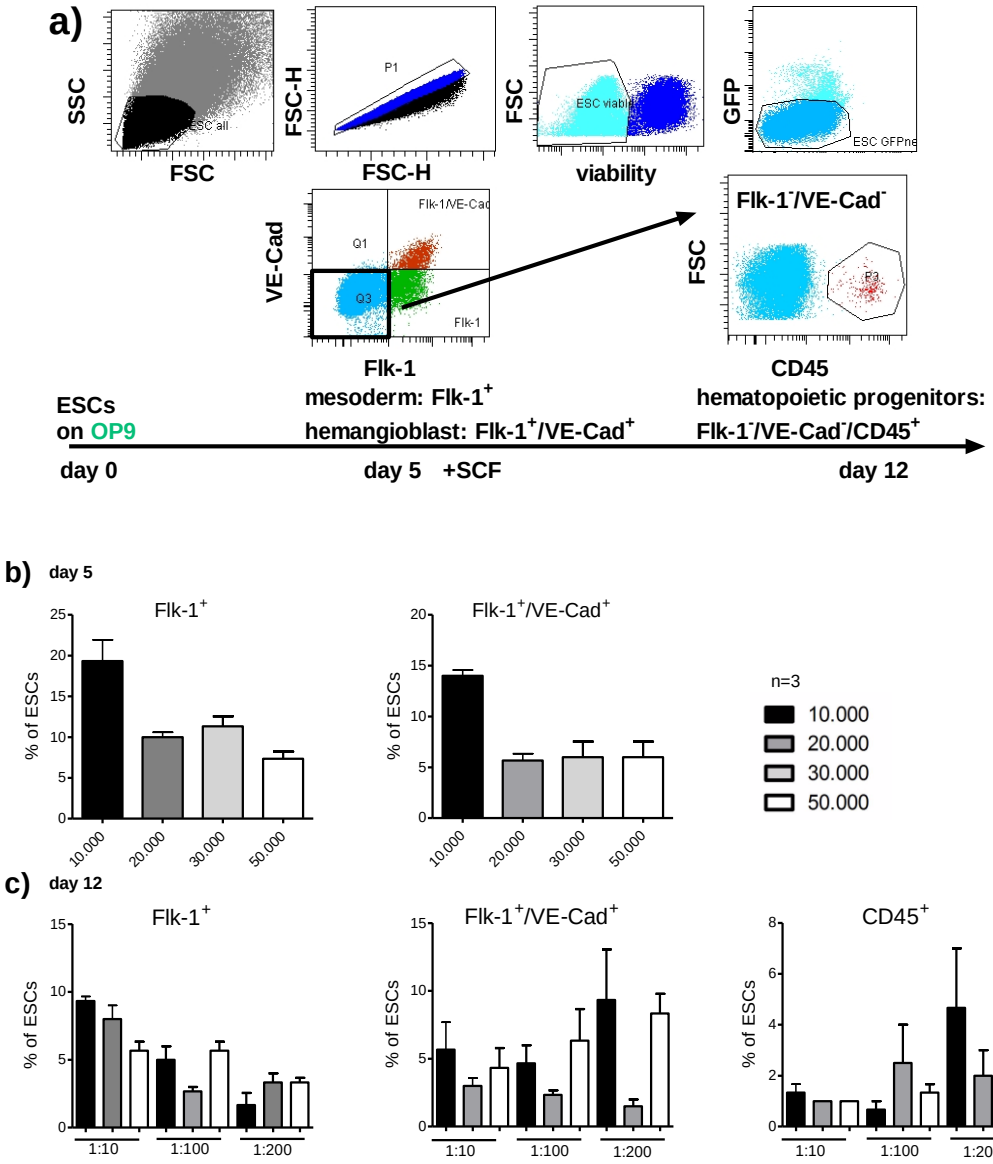

Figure 14: Test with different cell numbers and dilutions for the optimization of mesoderm, hemangioblast and hematopoietic differentiation. a) The gating strategy shows the discrimination between life and dead cells, and the gating for the surface markers shows only ESCs (GFP$^-$). b) At day 5 of ESC/OP9 co-culture the sample with a starting cell number of 10.000 cells showed the highest proportion of cells expressing Flk-1$^+$ and Flk-1$^+$/VE-Cad$^+$. c) At day 12 of differentiation, Flk-1$^+$ cells were less present in the 1:200 diluted cells than in the 1:10 and 1:100 diluted cells. Flk-1$^+$/VE-Cad$^+$ cells were appearing with the highest amount in the 1:200 dilution, the same was observed for CD45$^+$ cells. The data are presented as mean ± SD, the experiment shows one differentiation experiments in technical triplicates.

We could generate Flk-1$^+$ as well as Flk-1$^+$/VE-Cad$^+$ cells at day 5 of differentiation in the co-culture system with the OP9 cells and showed that 10.000 ESCs was the best amount of cells for generating mesoderm and hemangioblast cells (Figure 14b). After re-plating the cells in different dilutions, the analysis at day 12 of co-culture showed the highest amount of CD45$^+$ cells within the highest dilution (1:200). Further, the analysis showed a reduction of Flk-1$^+$

and Flk-1$^+$/VE-Cad$^+$ double positive cells, which was expected as these cells are differentiating from day 5 to day 12 towards the more differentiated hematopoietic progenitor cells (Figure 14c). Therefore, we decided that the best conditions for this assay would be to start with 10.000 ESCs and to re-plate these cells at day 5 in a 1:200 dilution.

4.1.4 Testing of different conditions for ESC differentiation into the erythroid lineage on OP9 cells

As we could observe a reduced number of mature erythroid cells in the *Fubp1* GT mouse model (Rabenhorst et al. 2015), we wanted to use the OP9 co-culture system to differentiate the ESCs into the erythroid lineage by applying the cytokine EPO as it was described before (Zheng et al. 2008). Therefore, we tested different medium conditions to enrich erythroid progenitors and definitive erythroid cells. 10.000 ESCs were plated on OP9 cells and differentiated for 5 days, and afterwards, the medium was changed to either fresh medium, medium containing SCF or medium containing SCF and EPO. The erythroid cells in the supernatant were analyzed for CD71 and Ter119 expression at day 12 of differentiation. The gating strategy to define early and late erythroblasts and reticulocytes using these markers was adapted from Fraser, Isern, & Baron, 2007 (Figure 15a).

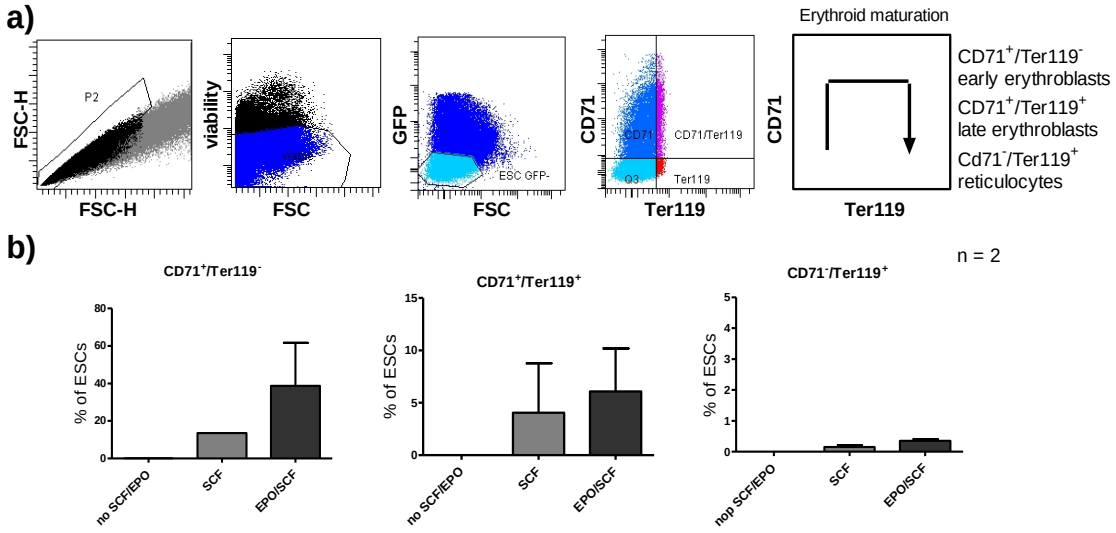

Figure 15: ESC differentiation into erythroid cells using different conditions in the OP9 co-culture system. A) The gating strategy was adapted from Fraser, Isern, & Baron, 2007. CD71 expression starts in the early erythroblasts and with the maturation towards the late erythroblasts the cells which express both, CD71 and Ter119. With the further maturation into reticulocytes the CD71 marker is downregulated again. B) After the addition of fresh medium without cytokines, medium with SCF or medium with both SCF and EPO, the cells were analyzed at day 12 for the expression of CD71 and Ter119. There was no production of erythroid cells in the absence of SCF and/or EPO. The addition of SCF alone was sufficient for erythroid cell differentiation. The addition of SCF and EPO led to an enrichment of erythroid cells

compared to SCF alone. The highest proportion of cells was measured with CD71^{+}/Ter119$^{-\ cells}$. We could generate 5% late erythroblasts and a small number of reticulocytes (0.5 -1%). The data are presented as mean ± SD of 2 biological replicates.

We could show that in the absence of SCF and EPO, no differentiation of erythroid cell took place, while the addition of SCF alone is sufficient to differentiate the ESCs into the erythroid lineage. This effect can be increased by the addition of EPO. In more detail (Figure 15Figure 14b), we could generate 40% of early erythroid cells and 5% of late erythroid cells with the addition of SCF and EPO into the medium, although the amount of reticulocytes was low (0.5-1%).

4.2 Establishment and characterization of *Fubp1* knockout ESC clones

4.2.1 FUBP1 is expressed in ESCs and during EB differentiation

We could previously show that FUBP1 is important for the hematopoiesis during embryogenesis and in adult HSCs (Rabenhorst et al. 2015). Furthermore, the embryogenic lethality of the *Fubp1* GT mouse model points towards the question of the role of Fubp1 in the early embryogenic development and in embryonic stem cells. To obtain a better insight into the biological importance of FUBP1 in embryogenesis and ESCs, we analyzed FUBP1 and its direct target gene *p21* to see if FUBP1 is significantly expressed and/or if it is differentially regulated during EB formation. The analysis of FUBP1 expression in ESCs and during differentiation showed a significant expression level (protein and RNA). However, no change of the *Fubp1* mRNA level during differentiation was detectable. We also observed that the *p21* mRNA slightly increased during differentiation (Figure 16).

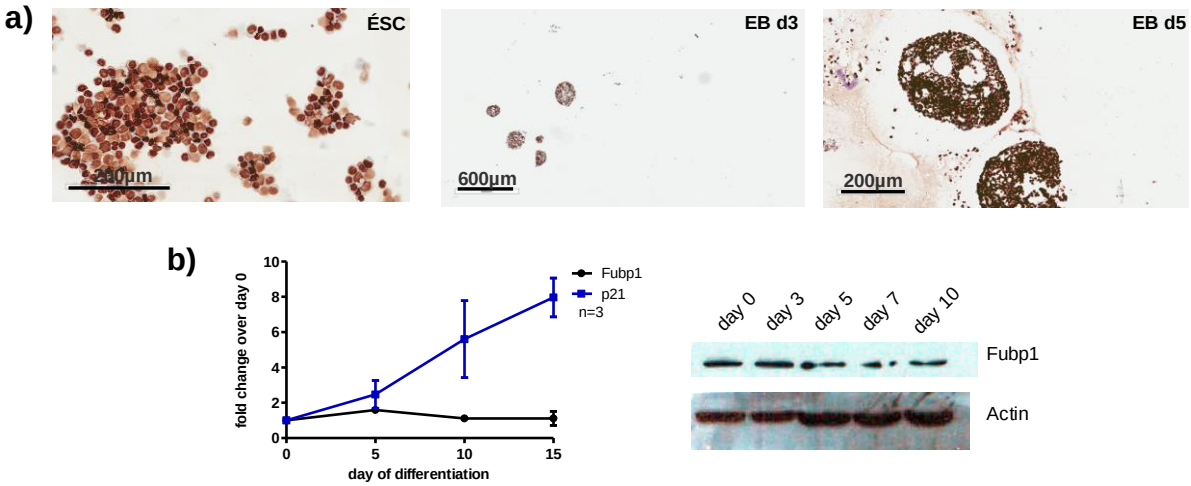

Figure 16: FUBP1 is expressed in ESCs and during differentiation into EBs. A) ESCs and EBs at day 3 and 5 of differentiation were positively stained for FUBP1 protein (Abcam 181111). b) *Fubp1* mRNA expression was not altered during EB differentiation, while *p21* increased. The mRNA analyses are presented as mean ± SD of 3 biological replicates

Interestingly, the histochemical analysis of ESCs showed a mixture of cells with strong and weak FUBP1 expression, while EBs were evenly strong stained for FUBP1.

4.2.2 Establishment of *Fubp1* knockout ESC lines with the CRISPR/Cas9 system

To understand and analyze the potential role of FUBP1 in ESCs and early development we used the CRISPR/Cas9 gene editing system, kindly provided from F. Schnütgen (University Frankfurt). We used a lentiviral plasmid, consisting of the *S. pyogenes* Cas9 (*Sp*Cas9), the guide RNA (gRNA) under the U6 promoter and both linked with an elongation factor 1 "short promoter" (EF) as shown in Figure 17. Three different gRNAs targeting the first (gRNA1) or second exon (gRNA2 and 3) of the *Fubp1* sequence and additionally a non-target control guide RNA (NTC) were used.

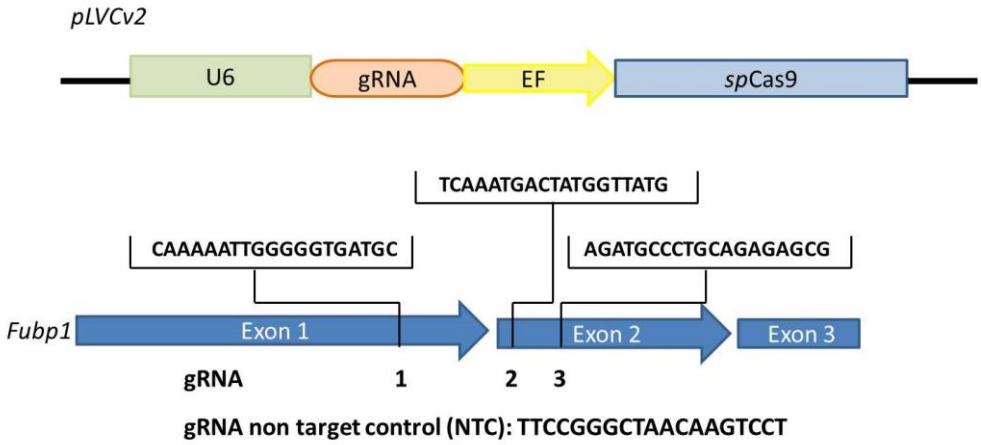

Figure 17: Generation of lentiviral CRISPR/Cas plasmids for targeting *Fubp1*. Three different gRNAs to target exon 1 or exon 2 of the *Fubp1* gene were designed and cloned into the *pLVCv2* vector. Additionally, a non-target control was generated.

ESCs were transduced as described before (chapter 3.5.7) and selected with 2 µg/ml puromycin. Single clones were picked, and western blot analysis was performed to screen for FUBP1 knockout clones. In parallel, a non-target control gRNA was used to produce non-target control clones.

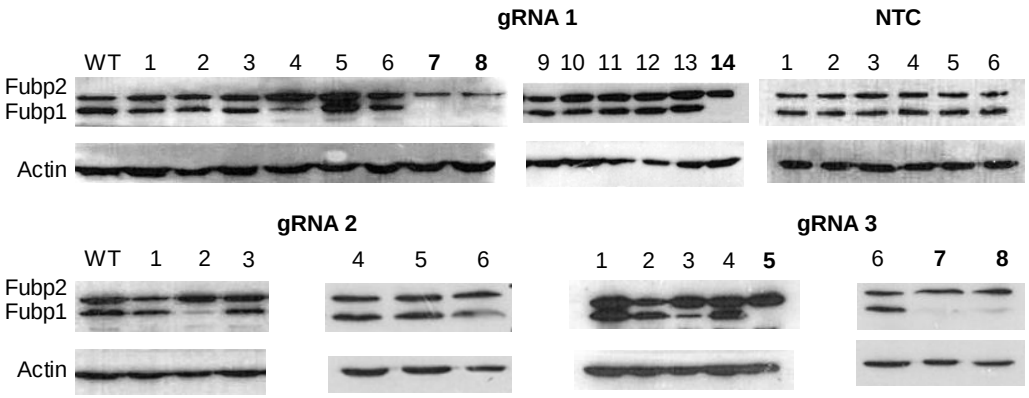

Figure 18: Three rounds of CRISPR/Cas9 lentiviral transduction and selection were performed and single clones were isolated. FUBP1 protein expression was analyzed and clones not expressing FUBP1 (bold numbers) were selected for sequencing. Non-target clones (NTC) showed no alteration of FUBP1 expression levels.

Additionally, genomic DNA was isolated, and target loci were sequenced to ensure that gene editing was successful on both chromosomes.

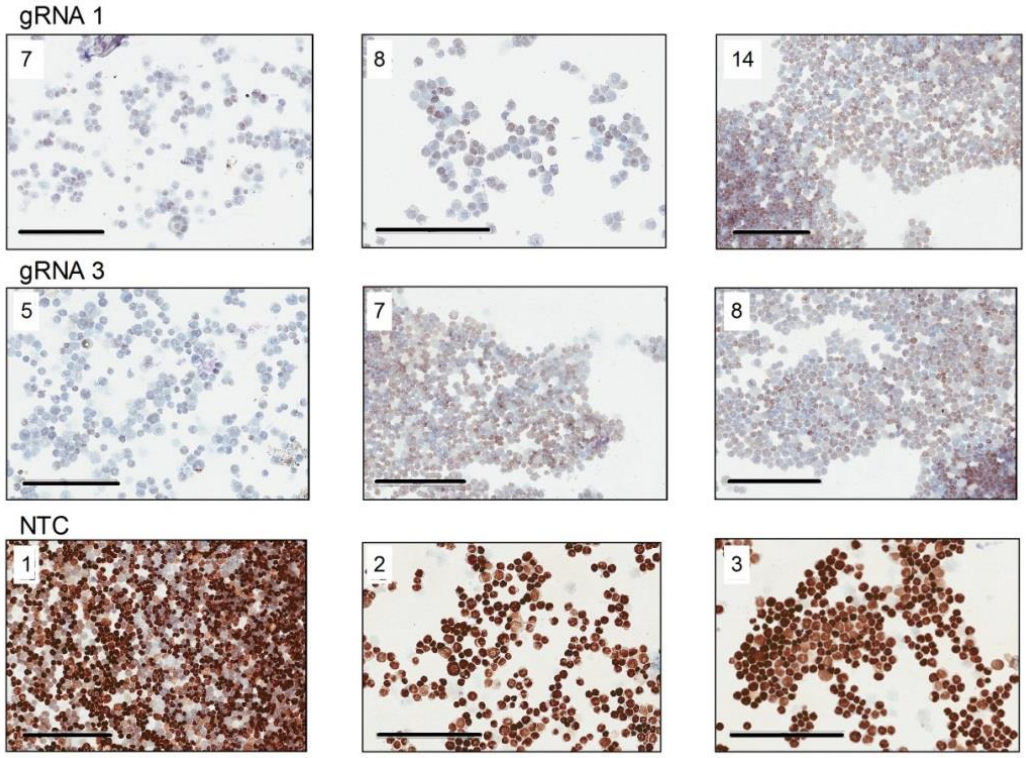

Figure 19: Cytochemichal staining for FUBP1 in the knockout clones and NTC clones. Cells were centrifuged onto a slide and stained for FUBP1. Clones 7, 8 and 14 (originated from a transduction with gRNA1) and clones 5, 7 and 8 (originated from cells transduced with gRNA3) were all negative for FUBP1 staining, while the NTC transduced cells (clones 1, 2 and 3) are showing a positive FUBP1 staining. Scale bar presents the size of 200 µm.

6 *Fubp1* KO clones without FUBP1 (short name: 1_7, 1_8, 1_14 and 3_5, 3_7, 3_8) and 5 NTC clones (short name: NTC1, NTC2, NTC3 NTC4 and, NTC5) were used for the further experiments and analysis.

4.2.3 *Fubp1* KO ESC clones were not affected in their stem cell characteristic

Following the identification of 6 *Fubp1* KO clones, I looked for changes in the cell cycle distribution as well as for the expression level of the FUBP1 target genes *p21* and *c-myc*. The absence of FUBP1 did not affect the cell cycle of the ESCs, but I could observe a significantly higher level of *c-myc* mRNA, while the *p21* mRNA expression level was not altered. Further analysis of the stem cell markers *Oct4* and *Nanog* showed that *Oct4* levels were higher in the KO clones compared to the NTC clones. The differentiation markers *Brachyury*, *Nestin* and *Sox17* were expressed and at a very low level comparable between KO and NTC clones (Figure 20).

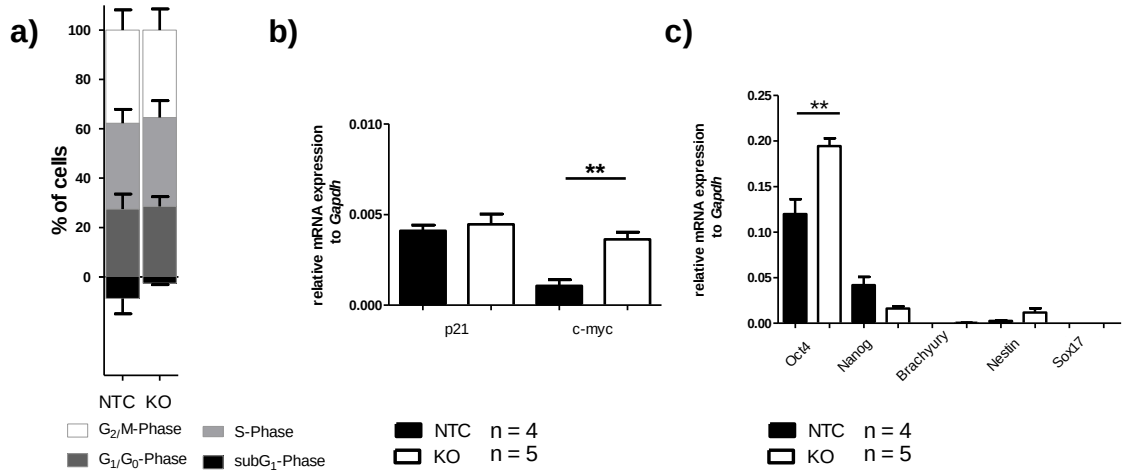

Figure 20: Analysis of *Fubp1* KO ESCs. a) The analysis of the cell cycle distribution revealed no changes in the absence of FUBP1. b) The target gene of FUBP1, *c-myc*, showed a significantly higher expression in the KO clones, but no change of the *p21* mRNA level was observed. c) *Oct4* was significantly upregulated in the *Fubp1* KO clones, while neither *Nanog* nor the differentiation markers (*Brachyury*, *Nestin*, *Sox17*) were altered in their expression. The mRNA analyses are presented as mean ± SD of one experiment in technical duplicates, using 4 NTC clones (1, 2, 3, and 4) and 5 different KO clones (KO1_7, KO 1_8, KO,3_5, KO3_7, and KO3_8) as biological replicates. Test for statistical significance: student's t-test (* P < 0.05, ** P < 0.01).

4.2.4 Differentiation of *Fubp1* KO ESC clones to EBs showed a deficit in mesoderm differentiation

Next, I was interested if the KO of *Fubp1* in the ESCs affects their differentiation capacity into EBs which were composed of the three germ layers. EBs were generated and analyzed for stem cell marker as well as for germ layer marker.

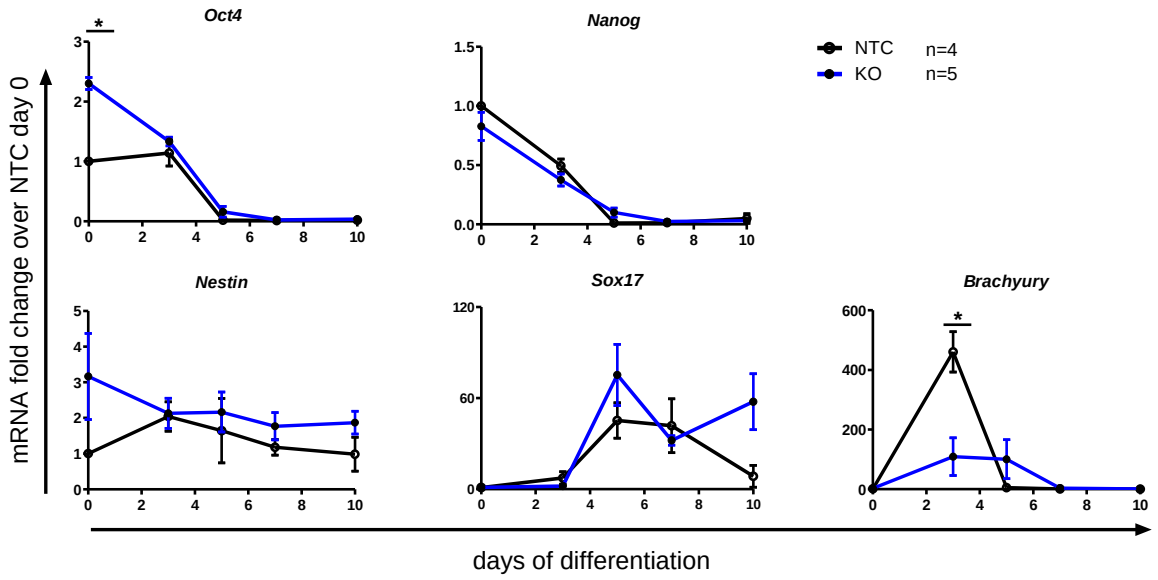

Figure 21: Differentiation of *Fubp1* KO ESCs into EBs. The differentiating *Fubp1* KO ESCs showed a decrease of the stem cell markers *Oct4* and *Nanog* similar to the NTC clones. The mRNA analysis of the germ layer markers *Nestin* and *Sox17* was comparable to the NTC cells, while the mesoderm marker *Brachyury* was significantly reduced at day 3 of differentiation. The mRNA analyses are presented as mean ± SD of one experiment in technical duplicates, using 4 NTC clones (1, 2, 3, and 4) and 5 different KO clones (KO1_7, KO 1_8, KO,3_5, KO3_7, and KO3_8) as biological replicates. Test for statistical significance: student's t-test (* P < 0.05).

The differentiation of ESCs can be followed by the analysis of stem cell marker expression such as *Oct4* and *Nanog.* The *Fubp1* KO clones differentiated and decreased the expression of the stem cell markers decreased to the same extent as in the NTC cells. In parallel, the upregulation of differentiation marker occurred. This was comparable between NTC and KO ESCs in the case of ectoderm and endoderm differentiation, while the mesoderm marker *Brachyury* was significantly reduced in *Fubp1* KO ESCs. To confirm an abnormality during mesoderm differentiation of FUBP1-deficient EBs, several genes were analyzed that had been linked to mesoderm differentiation. Besides *Brachyury*, *Flk-1* and *SnaiI* were reported to become upregulated during mesoderm differentiation (Nishikawa et al. 1998; Carver et al. 2001). Additionally, *Wnt3a*, *FgfR1* and *Bmp4* were shown to be very important for the different mesoderm compartments in the very early embryonic development. Mutations in these genes are affecting the paraxial or intermediate mesoderm plates in the embryo. I analyzed one more endoderm and ectoderm marker, *ß-catenin* and *Gata4* (Engert et al. 2013; Poh et al. 2014)

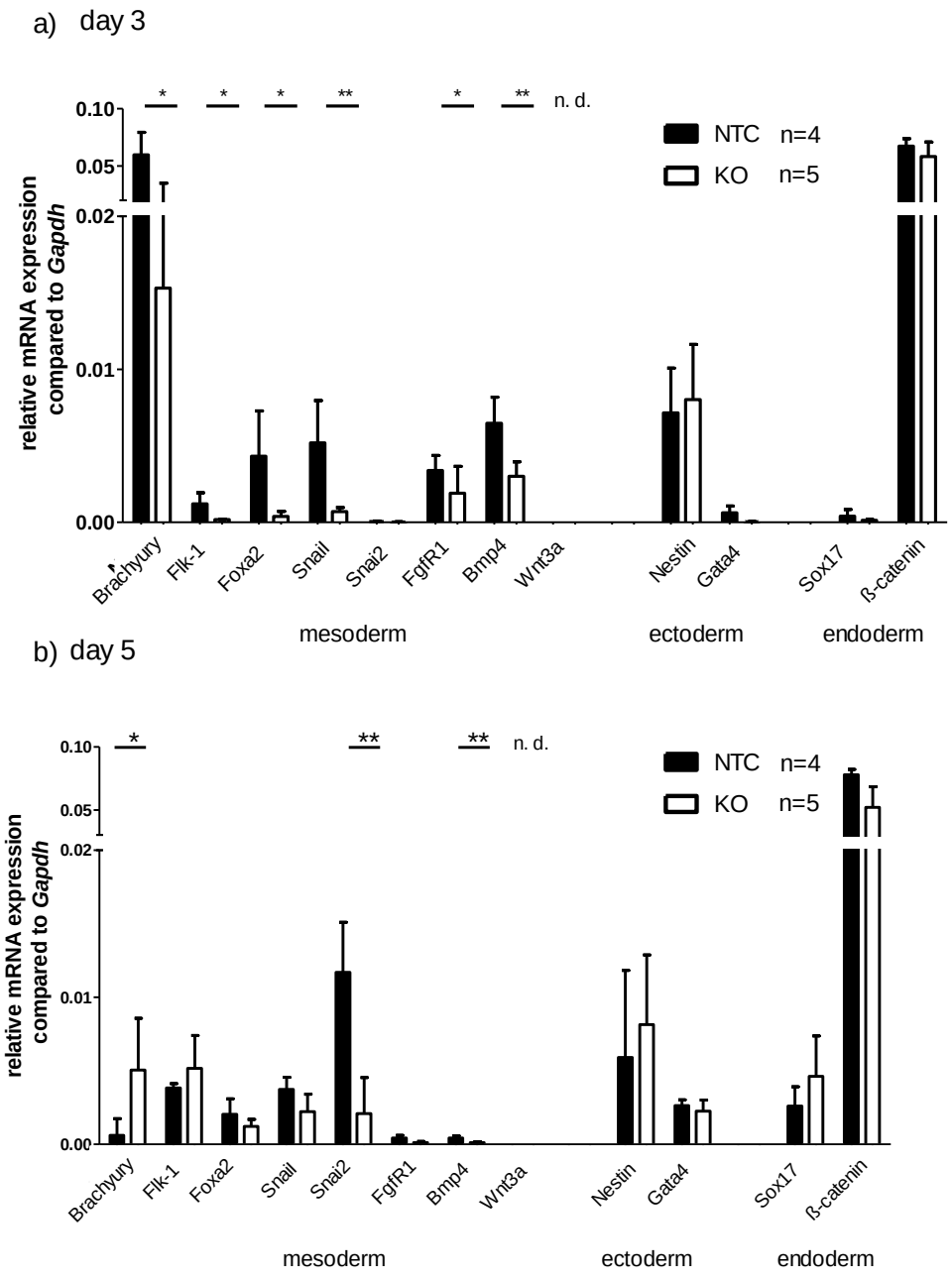

Figure 22: Analysis of mesoderm, endoderm, and ectoderm marker expression at day 3 and 5 of EB differentiation. a) The mesoderm marker *Brachyury*, *Flk-1*, *Foxa2*, *SnaiI* as well as *FgfR1* and *Bmp4* are significantly lower expressed in the KO clones at day 3 of differentiation compared to NTC clones. *Snai2* and *Wnt3a* are not significantly expressed at this time point. An upregulation of the ectoderm as well as the endoderm marker was observed without a difference between NTC and *Fubp1* KO clones. b) Day 5 of differentiation shows a comparable expression level of ectoderm and endoderm marker as well as for *Flk-1*, *Foxa2*, *SnaiI* and *FgfR1*. *Bmp4* and *Snai2* are significantly lower expressed in the *Fubp1* KO clones, while *Brachyury* shows a higher expression in the *Fubp1* KO clones compared to NTC clones. The mRNA analyses are presented as mean ± SD of one experiment in technical duplicates, using 4 NTC clones (1, 2, 3, and 4) and 5 different KO clones (KO1_7, KO 1_8, KO,3_5, KO3_7, and KO3_8) as biological replicates. Test for statistical significance: student's t-test (* P < 0.05 ** P< 0.01).

The analysis of a range of different mesoderm markers as well as further ectoderm and endoderm marker revealed that at day 3 and day 5 of EB differentiation the expression of

ectoderm and endoderm cell markers was comparable between NTC and *Fubp1* KO clones, indicating that endoderm and ectoderm differentiation is not affected in the absence of FUBP1. However, for 7 out of 9 mesoderm markers analyzed I observed a significant reduction of their expression levels in the *Fubp1* KO clones, which was balanced at day 5 of differentiation for most of the markers except *Snai2* and *Bmp4* which remained at a lower level in the *Fubp1* KO clones. Interestingly, *Brachyury* was highest in the NTC clones at day 3 of differentiation while it showed a peak expression in the *Fubp1* KO clones at day 5 that was still lower than in the NTC clones at day 3. However, to support this mRNA data, we decided to analyze the development of Brachyury- and also of Flk-1-expressing cells via flow cytometry. We applied an intracellular staining at day 3, 4 and 5 of EB differentiation to compare the actual Brachyury positive cells between NTC clones *Fubp1* KO clones. In a second set up, we analyzed the number of Flk-1 positive cells during differentiation (Figure 23).

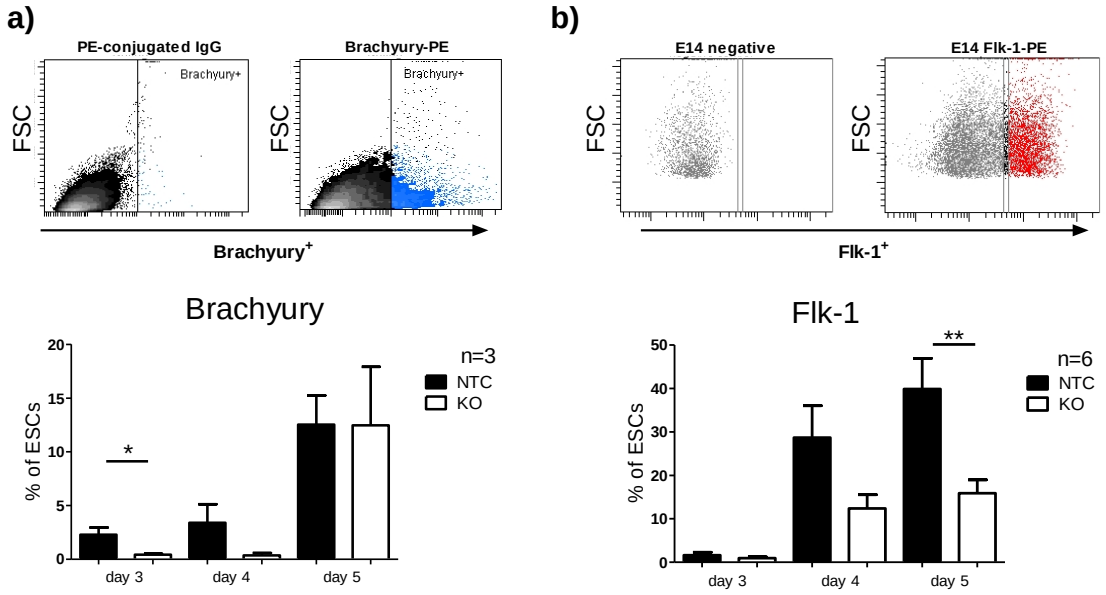

Figure 23: Expression analysis of the mesoderm markers Brachyury and Flk-1 at day 3, 4 and 5 of EB differentiation by flow cytometry. a) The number of Brachyury$^+$ cells is significantly reduced at day 3 and 4 of EB differentiation in *Fubp1* KO clones. At day 5 of differentiation, 15% of NTC and *Fubp1* KO clones were Brachyury$^+$. b) None of the cells were expressing Flk-1 at day 3 of EB formation. The percentage of Flk-1$^+$ cells increased at day 4 to 20% and at day 5 to 50% in the NTC clones, while less than 20% of *Fubp1* KO clones expressing Flk-1 at day 4 and 5 of differentiation. The analysis is presented as mean ± SD of one experiment using 3 NTC (1, 2 and 3) clones and 3 different *Fubp1* KO clones (KO1_7, KO 1_8, and KO3_8) as biological replicates. Test for statistical significance: student's t-test (* P < 0.05 ** P< 0.01).

In summary, I collected evidences that FUBP1 might be important for the generation of the mesoderm germ layer, although FUBP expression levels were not upregulated or changed

during EB differentiation. As EBs consists of a mixed cell population containing partly ESCs, and mainly a mixture of all three germ layers, I was wondering whether the mesoderm cell population showed a change FUBP1 levels. For this purpose, I sorted Flk-1 positive and negative cells at day 4 of differentiation and analyzed the *Fubp1* mRNA expression (Figure 24).

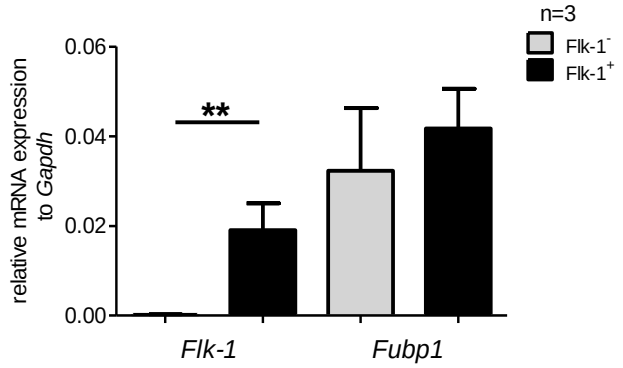

Figure 24: *Fubp1* mRNA expression level in Flk-1$^+$ and Flk-1$^-$ EB cells showed no significant difference. *Flk-1* mRNA was analyzed to confirm the positive and negative population. The analysis is presented as mean ± SD of three independent WT differentiation experiments, and cells were sorted at day 4 of differentiation. Test for statistical significance: student's t-test (P< 0.01).**

The *Flk-1* mRNA expression in Flk-1 positive (and no expression in negative cells) supports the specificity of the cell sort, however, there was no significant difference in the *Fubp1* mRNA expression levels in these two populations, but a tendency that *Fubp1* might be higher expressed in Flk-1$^+$ cells (Figure 24). Additionally, a possible compensation or even deregulation of *Fubp*3 could be another reason for the delayed upregulation of the mesoderm marker. As it was shown by Weber et al. 2008, FUBP3 initially binds to the *FUSE* element of *c-myc*, and is replaced by FUBP1, which then lead to the activation of *c-myc* transcription. Therefore, we added *Fubp3* in our panel of genes at day 0, day 3, and day 5 of EB formation (Figure 25)

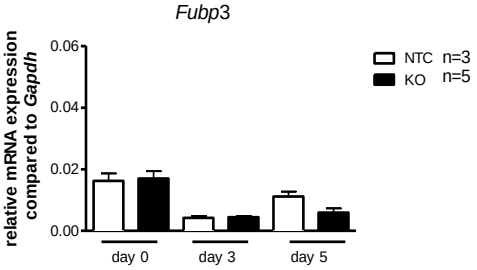

Figure 25: Analysis of possible compensatory effects due to a deregulation of *Fubp*3. The *Fubp*3 mRNA expression levels decreased during differentiation to EBs in *Fubp*1 KO clones in a comparable grade to

NTC clones. The analysis is presented as mean ± SD of one experiment using 3 NTC clones (1, 2, and 3)and 5 different *Fubp1* KO clones (KO1_7, KO 1_8, KO,3_5, KO3_7, and KO3_8) as biological replicates.

Finally, we were looking at markers for the development of early hematopoietic progenitors in this EB differentiation experiment due to the observed influence of FUBP1in hematopoietic stem cells and in erythroid differentiation (Rabenhorst et al. 2015).

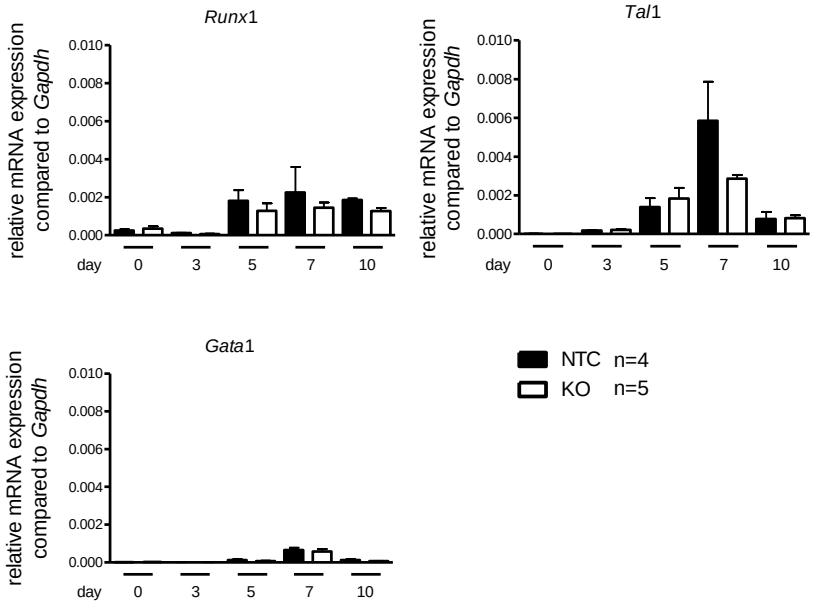

Figure 26: mRNA analysis of *Runx*1, *Tal*1 and *Gata*1 during EB differentiation. There was no difference observed between NTC clones and *Fubp*1 KO clones in the expression levels of these early hematopoietic progenitor markers. However, there was a tendency towards a lower *Tal1* expression in the *Fubp1* KO clones. The analysis is presented as mean ± SD of the relative mRNA expression compared to the housekeeping gene *Gapdh*, using 4 NTC clones (1, 2, 3, and 4) and 5 different *Fubp1* KO clones (KO1_7, KO 1_8, KO,3_5, KO3_7, and KO3_8) as biological replicates.

4.2.5 Differentiation of *Fubp1* KO ESC clones in co-culture with OP9 cells to hematopoietic progenitors

After confirming that the absence of FUBP1 led to a delay of mesoderm differentiation, we performed a co-culture differentiation assay to better describe the role of FUBP1 during the differentiation from ESCs towards the hematopoietic system. Because of the importance of FUBP1 for HSCs in the fetal liver as well as in adult HSCs (Rabenhorst et al. 2015), we wanted to apply the previously established and optimized OP9 assay (described in chapter 4.1.3) for the *Fubp1* KO ESCs. 10,000 cells per well were plated in technical duplicates for WT, three NTC clones and five *Fubp1* KO clones and were analyzed at day 5 for mesoderm differentiation (Flk-1 expression) and for hemangioblasts (Flk-1 and VE-Cadherin expression). After re-plating and upon the addition of SCF, the next analysis was performed at

day 12 with the same settings and using in addition the CD45 marker for hematopoietic progenitors.

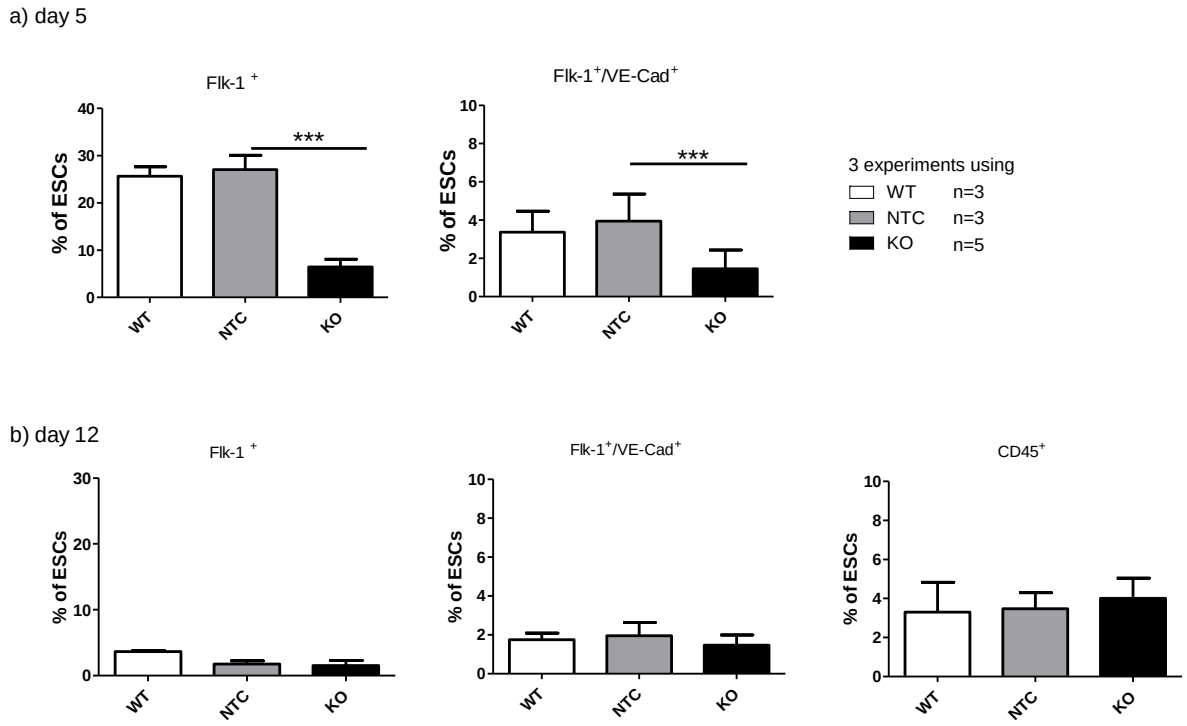

Figure 27: Analysis of *Fubp1* KO clones for their potential to differentiate into hematopoietc progenitor cells. a) The mRNA analysis at day 5 showed a significant reduction of mesoderm (Flk-1^{+}) and hemangioblast (Flk-1^{+}/VE-Cad$^{+)}$ cells in the *Fubp1* KO clones. Further differentiation towards the hematopoietic progenitors at day 12 (b) showed a reduction of mesoderm and hemangioblast marker expression in all samples to a comparable manner. Hematopoietic progenitor cells (CD45^{+}) were generated in WT, NTC and Fubp1 KO clones. The analysis is presented as mean ± SD of two experiments using 3 WT (technical replicates only), 3 NTC clones (1, 2, 3, and 4) and 5 different *Fubp1* KO clones (KO1_7, KO 1_8, KO1_14, KO3_7, and KO3_8) as biological replicates. Test for statistical significance: student's t-test (* P< 0.001).**

The data obtained from this assay support the results from the EB differentiation, as we can see a delay or reduction of mesoderm marker expression in the *Fubp1* KO clones (Figure 27). Nevertheless, there was no difference at the later time point of differentiation analyzing the hematopoietic progenitors with the CD45 marker.

The OP9 stromal cells are carrying a mutation in the *M-CSF* gene, leading to the absence of M-CSF production, which was shown to push ESCs in a co-culture towards the hematopoietic direction, especially for erythroid, lymphoid and B-cell differentiation (Nakano et al. 1994). Because of the evidences that FUBP1 might play a role for the erythroid lineage differentiation in the *Fubp1* GT mouse model during embryogenesis (Rabenhorst et al. 2015),

we decided to support the cells with EPO to push them into the erythroid lineage in the OP9 co-culture assay (optimization described in chapter 4.1.4).

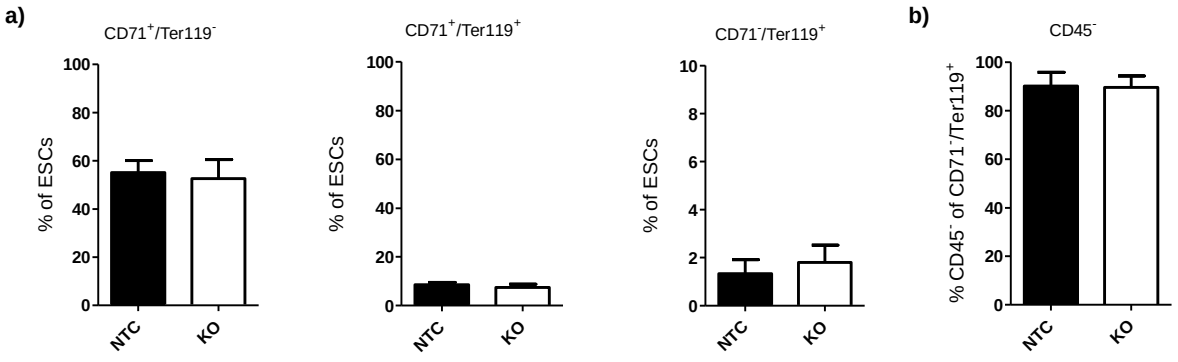

Figure 28: Erythroid differentiation of *Fubp1* KO clones. a) *Fubp1* KO clones differentiate into the erythroid lineage significantly slower compared to NTC clones. The percentage of CD71$^+$/Ter119$^-$ cells was significantly reduced in the *Fubp1* KO clones. b) Analysis of Cd71$^-$/Ter119$^+$ cells for their CD45 expression showed that more than 90% of these cells are not expressing Cd45, and that there was no difference between *Fubp1* KO and NTC clones. The analysis is presented as mean ± SD of one experiment using 3 NTC clones (1, 2, and 3) and 5 different *Fubp1* KO clones (KO1_7, KO 1_8, KO,1_14, KO3_7, and KO3_8) as biological replicates. Test for statistical significance: student's t-test (* P< 0.05).

The differentiation of ESCs in the OP9 co-culture assay with the addition of SCF and EPO leads to the generation of erythroid cells at different maturation stages. I could observe no difference between NTC and *Fubp1* KO clones during this erythroid maturation, starting with the early erythroid progenitors (CD71$^+$/Ter119$^-$) cells. The further differentiation and maturation to the late erythroid progenitors (CD71$^+$/Ter119$^+$) cells and finally to the definitive erythroid cells (CD71$^-$Ter119$^+$/CD45$^-$) cells, shown in Figure 28, were also not affected.

4.3 The role of FUBP1 in the early embryonic development

4.3.1 FUBP1 expression during murine embryonic development

For the better understanding of the role of FUBP1 during embryogenesis and to explain the early death of FUBP1-deficient embryos we wanted to analyze the expression of FUBP1 in the mouse embryo. For this purpose, we set up time-matings and sacrificed animals at E9.5 and E13.5 days *post coitum* (dpc) for FUBP1 expression in WT embryos.

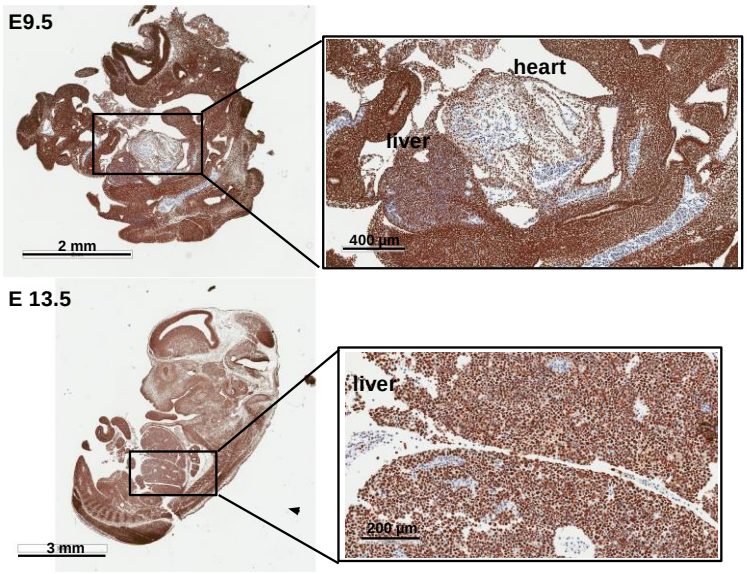

Figure 29: Analysis of FUBP1 expression in embryos at 9.5 *dpc* and 13.5 *dpc*. We observed a strong staining in the somites of the embryo at E9.5 and some negative cells in the heart and liver. At day 13.5, the tail and head region was highly positive for FUBP1, and only some cells in the liver appeared negative. Staining was performed on 4 µm paraffin sections with the FUBP1 antibody ab181111.

Embryos at the early time point E9.5 of development showed a very strong FUBP1 staining in the whole embryo. Only some cells in the heart and in the liver appeared to lack FUBP1 expression. From day E8.5 to 9.5, the folding of the embryo takes place, which means that the somites are moving from one side of the head region to the other side to form the typical embryonal position, which is better seen in the embryos at day E13.5. There was no big change of the pattern of FUBP1 positive cells in the E13.5 embryo. Only the cells in the liver showed a pattern of FUBP1-positive and negative cells (Figure 29).

4.3.2 Analysis of FUBP1 expression in young and adult WT mice

After we could not observe an exclusive staining for FUBP1 in the embryo or a change in expression from day E9.5 to E13.5 (Figure 29), I wanted to find out if FUBP1 is expressed in embryogenesis and not in adult mice, and therefore plays a specific role during embryonic development. The analysis of the kidney, spleen, liver and lung of a young versus adult mouse showed that there a regions in the spleen of the young mice which were not positive for FUBP1, while in the adult mice, every cell type in the spleen was positively stained. However, there were no differences in the staining for FUBP1 between young and old mice when comparing the kidney, lung and liver (Figure 30). Additionally I analyzed the colon, heart, and bone of adult mice. In the connective tissue of the colon, some cells were negative for FUBP1 staining.

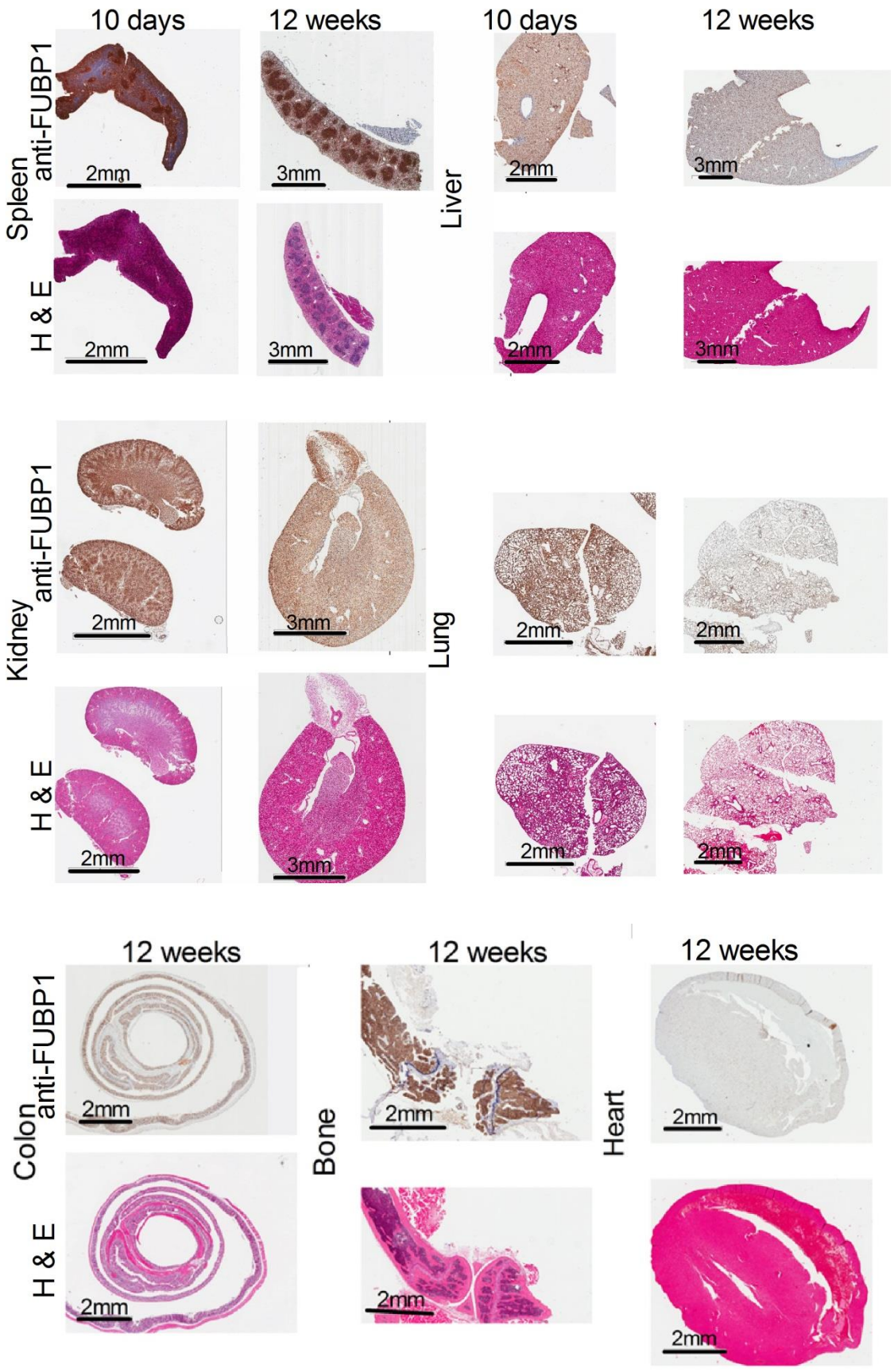

Figure 30: Immunhistochemichal staining for FUBP1 and H&E in organs of young (10 days old) and adult (12 weeks) mice. The analysis of the kidney, spleen, liver and lung of a young *versus* adult mouse showed

that most of the cells showed a nuclear staining for FUBP1- Some regions in the spleen of the young mice were negative for FUBP1, while in the adult mice, every cell type in the spleen was positively stained. The analysis of colon, bone and heart showed that most of the cells are positive for FUBP1, while the red blood cells, which showed no nucleus in the H&E staining, are also negative for FUBP1.

4.3.3 Proliferation and apoptosis analysis in the *Fubp1* GT mouse model

The analysis of WT mice showed no significant differences in FUBP1 expression levels in histochemical analysis, immunoblotting and on mRNA levels, but in general, I could detect high expression levels of FUBP1 during embryonic development until adulthood in almost every kind of tissue and organ. FUBP1 is described to act as an anti-apoptotic protein and supports proliferation. Especially during embryogenesis, a high proliferation rate, very little apoptosis and fast migration of cells is necessary (Stuckey et al. 2011). In order to exclude that the *Fubp1* GT mice are dyeing due to the inhibition of proliferation or a big wave of apoptosis, I investigated the homozygous *Fubp1* GT embryos at day E9.5 and E13.5 and compared them to their WT siblings (Figure 31 and Figure 32).

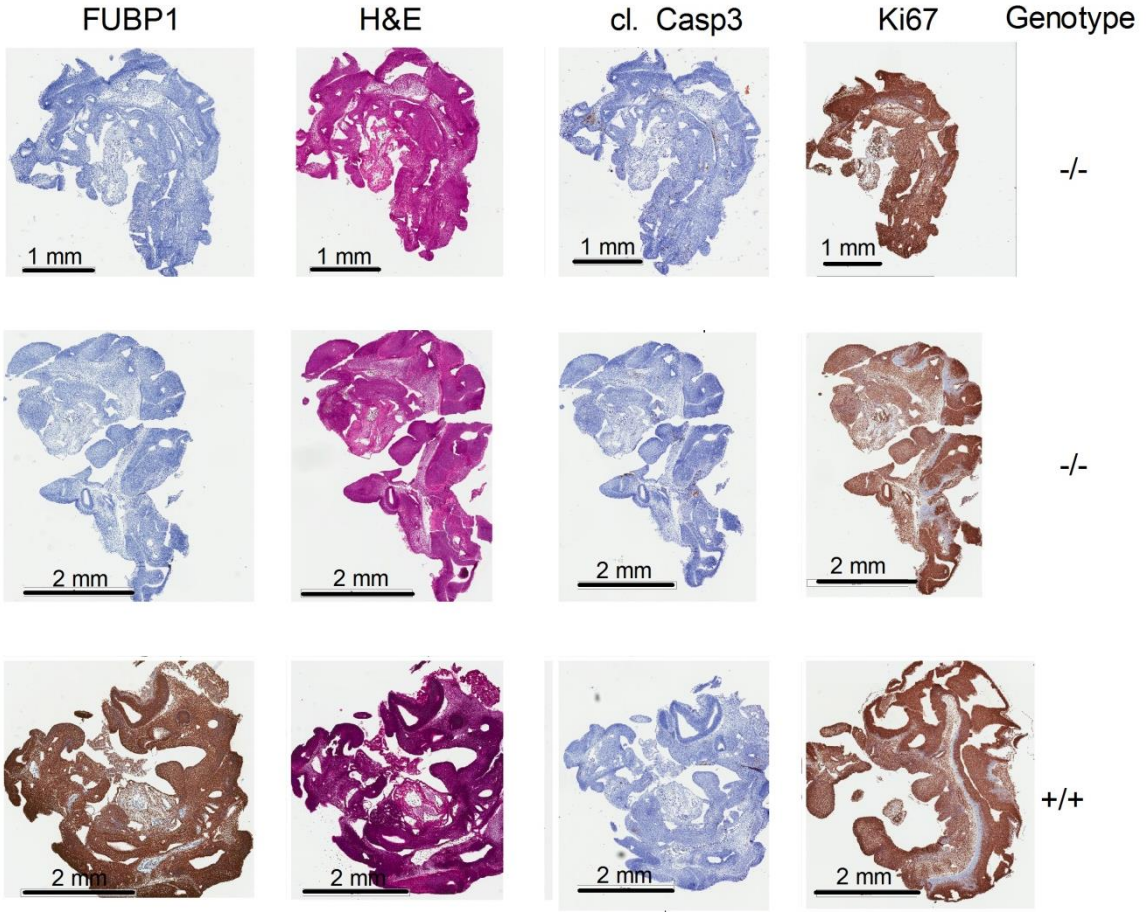

Figure 31: Analysis of homozygous *Fubp1* GT embryos at day E9.5 compared to their WT siblings. Stainings from left to right: anti-FUBP1 (ab181111), H & E, cleaved Caspase3 and Ki67. The staining for FUBP1 confirmed the complete absence of the protein. The folding of the homozygous embryos was not

yet completed compared to the WT sibling. The apoptosis marker cleaved Casp3 indicated no significant increase of apoptotic cells, and the proliferation marker Ki67 showed no difference.

Interestingly, I could not detect a difference in the expression of the proliferation marker Ki67 or in the amount of apoptotic cells although FUBP1 was completely absent. I could observe that the homozygous mice were smaller and the folding of the somites was not yet completed at day 9.5 (Figure 31).

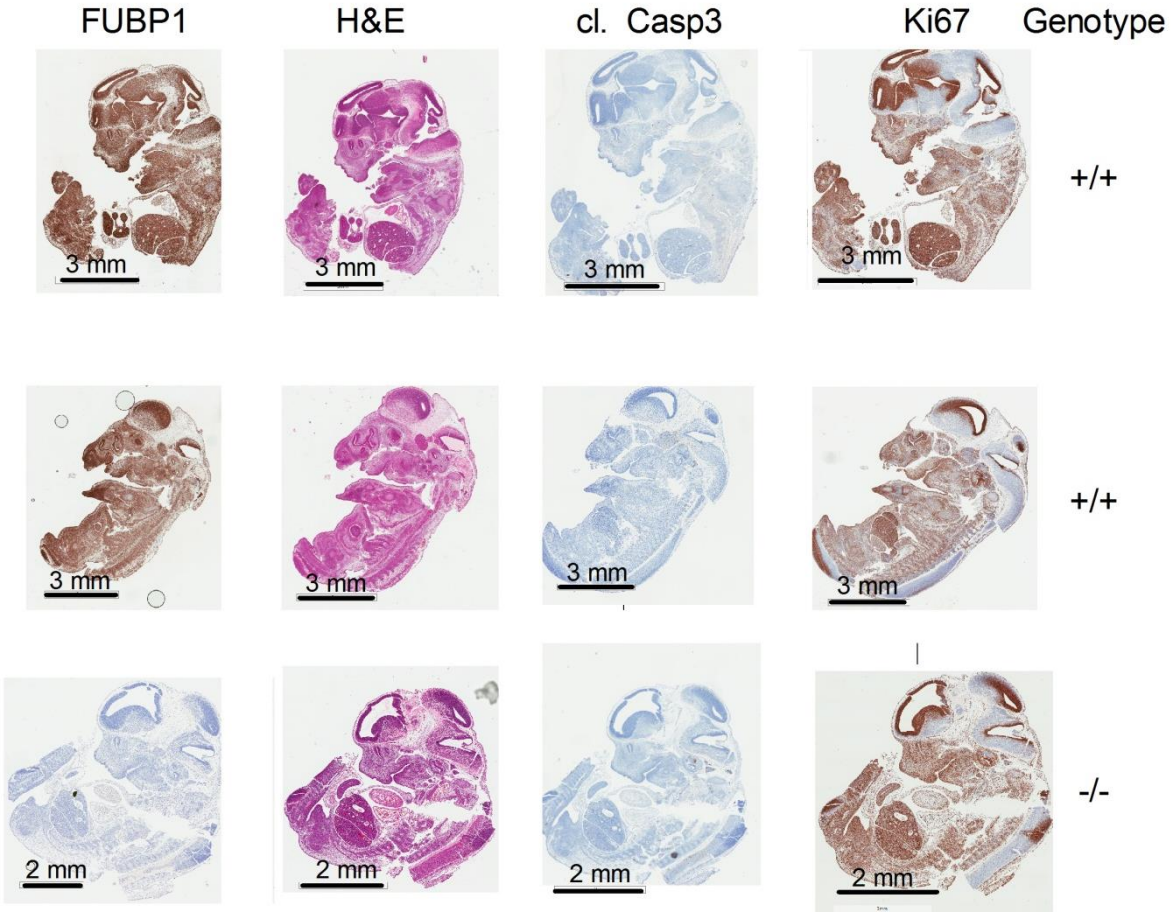

Figure 32: Analysis of homozygous *Fubp1* GT mice compared to their WT siblings at day E13.5. Stainings from left to right: anti-FUBP1 (ab181111), H & E, cleaved Caspase3 and Ki67. The staining for FUBP1 confirmed the complete absence of the protein in the homozygous GT embryo. Neither in the WT animals nor in the homozygous *Fubp1* GT mouse a difference in proliferation or in the amount of apoptotic cells became visible.

The analysis of the embryos at day E13.5 for proliferation showed that for all the animals (WT and homozygous *Fubp1* GT mice) a high proliferation rate, especially in the brain and the liver was detected. No difference between WT and FUBP1-deficient embryos became apparent. I could observe some single cells in the animals which showed a positive signal for the apoptosis marker cleaved Caspase 3, but again no difference between the genotypes could be detected.

5 Discussion

The transcriptional regulator FUBP1 was first described to be involved in the upregulation of the proto-oncogene *c-myc* (Duncan et al. 1994) by binding to the single stranded FUSE element. Later on, it was mainly shown to be overexpressed in a number of solid tumors such as HCC (Malz et al., 2009; Rabenhorst et al., 2009), breast cancer (Xu, Yan, and Shao 2010), bladder and prostate cancer (Weber et al. 2008). Recently, the physiological role of FUBP1 was described in two publications using two different mouse models (knockout and gene trap). Both groups could show that upon the depletion of FUBP1 no mice were born and the homozygous embryos are dying in utero between days E10.5 to E19.5 (Rabenhorst et al. 2015; Zhou et al. 2016). It was shown that FUBP1 plays a crucial role in the hematopoiesis of these mice, and upon the missing of this transcriptional regulator, there was a significantly reduced number of HSCs. Additionally, these FUBP1 lacking HSCs are functionally impaired as they are losing their full ability to recover the blood lineage in transplantation experiments compared to normal HSCs.

We wanted to elucidate further roles of FUBP1 in healthy embryonic stem cells. Therefore, the analysis of ESCs and their differentiation ability was the main aim of this project. Additionally, the histological analysis of early WT as well as homozygous *Fubp1* GT mice should support our ESC culture results.

5.1 Characterization and optimization of the ESC culture system and differentiation protocols

5.1.1 ESC cultivation, differentiation and analysis of stem cell marker, differentiation marker and FUBP1 expression

The analysis of the two well described stem cell marker Oct4 and Nanog (Boyer et al. 2005; Loh et al. 2006; Wang et al. 2012) showed a prominent expression of both markers and the absence or very low expression of markers that we used as differentiation markers for the three germ layers (Figure 11). During differentiation of the ESCs into EBS the stem cell marker were already at day 5 of differentiation rapidly decreased. In parallel, the differentiation markers were increased. The mesoderm marker *Brachyury* showed a 500-fold increase at day 5 of EB formation and decreased back to zero at day 10. A similar pattern was monitored for the endoderm marker *Sox17* with a 150-fold increase at day 5 and a decrease to a lower level at day 7 to 10. For the ectoderm marker *Nestin* we observed a 4-fold increase at

day 7. These results are comparable to other studies, where these markers were used as germ layer differentiation markers (Faial et al. 2015; Mansergh et al. 2009; Qu et al. 2008).

After we could confirm that the ESC line used for this study is able to differentiate into the three germ layers with the corresponding change of marker expression, we were analyzing the FUBP1 expression level in these cells and during EB formation. We observed a significant expression of FUBP1 on protein level in western blot and cytochemical analysis as well as a relative high mRNA expression level compared to *Gapdh*. Moreover, we could not observe a change during the formation of EBs and the differentiation of the three germ layers. Additionally, we analyzed the direct target gene of FUBP1, *p21* and could observe an upregulation of *p21* during EB differentiation. Although it is known that FUBP1 is repressing *p21* in HCC cells (Rabenhorst et al., 2009), in normal growing cells *p21* is expressed at a very low level to allow cell cycle progression. Upon DNA damage or stress, *p21* is upregulated through a p53-dependent and independent regulatory network (Jung, Qian, and Chen 2010). The change of *p21* in the differentiated EBs can be explained by a shift towards the G1 phase due to the upregulation of *p53* (Jain et al. 2012), but there is no inverse correlation between *Fubp1* and *p21* expression in the normal ESCs.

5.1.2 Optimization of the OP9 co-culture differentiation assay

The OP9 stroma cell line was originally generated from a mouse strain with a homozygous deletion of the osteopetrosis *(op)* gene, in which a reduced number of macrophages and osteoclasts was observed (Yoshida et al. 1990). Later, the OP9 stroma cells were applied them for a co-culture system to generate hematopoietic progenitor cells (Nishikawa et al. 1998) or for the generation of erythroid cells (Nakano, Kodama, and Honjo 1996).

I wanted to use this assay for the ESC experiments and characterization, and therefore tried to find the optimal conditions for our purpose. The use of different ESC numbers in the OP9 co-culture showed that I could reach a similar percentage of Flk-1^+ and Flk-1^+/VE-Cad^+ cells in our experiment with 10,000 ESCs, while higher numbers showed less differentiation efficacy as shown in Figure 14. I did not sort the Flk-1^+ cells at this point of differentiation, but tested different dilutions to re-plate the cells onto freshly prepared OP9 cells. After 7 days, I analyzed the different conditions for the two previously mentioned markers and additionally CD45. In general, I could see a differentiation towards hematopoietic progenitors in all samples to a comparable extent as described in (Nishikawa et al. 1998). However, I observed the generation of up to 6% $CD46^+$ cells in the sample with a 1:200 dilution of 10,000 cells as

the starting cell number (Figure 14b). Therefore, we decided to perform the OP9 experiments with this set-up.

Additionally, I tested different supplementations to enhance the differentiation of ESCs in this assay towards the erythroid directions. We analyzed the ESCs after re-plating on OP9 cells using medium without supplements, with SCF and with SCF and EPO. The addition of SCF and EPO to the medium led to the generation of 40% $CD71^+$ cells, which represent the early erythroid progenitor compartment (Koulnis et al. 2011; Chao et al,. 2015), and 5% of late erythroblasts. I could only observe a low amount of 1% of reticulocytes using this assay. However, more than 95% of the reticulocytes showed also a negative staining for the CD45 surface marker which means that these cells were mature red blood cells.

5.2 Generation and characterization of *Fubp1* KO ESC clones

To elucidate the role of FUBP1 in ESCs and during differentiation I applied the CRISPR/Cas9 technology to generate *Fubp1* KO ESC clones and non-target control clones.

5.2.1 Generation of *Fubp1* KO clones using the CRISPR/Cas9 technology

The CRISPR/Cas9 technology became more and more famous during the last few years and with that available for every research institute. The huge number of applications ranges from gene repair, deletion, mutation, replacement to activating a silent gene again (Patrick, Eric, and Zhang 2014). I used this technology to introduce an unspecific frame-shift mutation into the first or second exon of the *Fubp1* locus, with the aim of a functional FUBP1 knockout.

Finally, I could generate six *Fubp1* KO clones using the guideRNA#1 and #3 and additionally generated 6 non-target control clones. We tested the ESC cells by Western Blot and in cell-spin stainings with anti-FUBP1 antibody and could confirm the total absence of FUBP1 in the KO clones. In contrast, the NTC clones showed high FUBP1 expression (Figure 18 and Figure 19). For the further analysis of these ESC clones, I used 3-6 *Fubp1* KO clones and at least 3 NTC clones, dependent on the individual experiment.

5.2.2 The deletion of Fubp1 does not interfere with ESC growth and stemness

We successfully generated *Fubp1* KO clones, and could not detect a difference in the apoptotic sensitivity or cell cycle distribution of these cells. The analysis of the cell cycle inhibitor *p21* and direct target gene of FUBP1 did also not reveal significant differences in gene expression. However, the analysis of the FUBP1 target gene *c-myc* displayed a

significantly upregulation in the *Fubp1* KO clones compared to the NTC clones. Although FUBP1 was described to enhance *c-myc* mRNA level (Duncan et al., 1994), the promoter region of *c-myc* contains several *cis*-regulatory elements and is context dependently regulated by many factors (Meyer and Penn 2008). The analysis of the stem cell and differentiation marker in the *Fubp1* KO clones showed a significant upregulation of the *Oct4* mRNA level, but no change in the expression of the other genes. Therefore, I conclude that there is no spontaneous differentiation of the ESCs upon FUBP1 depletion, but I can observe an upregulation of two genes on mRNA level, which are both described to be important for stem cells and are used to induce pluripotent stem cell from mouse fibroblasts (Blum et al. 2008).

5.2.3 Deletion of FUBP1 in ESCs leads to a delay in mesoderm differentiation during EB formation

After I confirmed that the *Fubp1* KO ESCs did not undergo a differentiation because of the absence of FUBP1, I differentiated the ESCS in medium without LIF, where they formed EBs which contained cells from the three germ layers. The first analysis showed the rapid decrease of the stem cell marker *Oct4* and *Nanog* and an increase of the three germ layer maker *Brachyury*, *Nestin* and *Sox17*. Although the loss of stem cell marker expression showed a similar kinetic in NTC clones and *Fubp1* KO clones, for the mesoderm marker *Brachyury* I could observe a significantly reduced mRNA expression level in the *Fubp1* KO clones at day 3 of EB differentiation (Figure 21). However, ectoderm and endoderm marker expression was not altered in the absence of FUBP1. *Brachyury* is a very early mesoderm marker, and during EB differentiation the expression of this protein peaks between day 3 and 4 (Evans et al. 2012; Willey et al. 2006). Moreover, the analysis of a higher number of mesoderm markers, Brachyury target genes, as well as ectoderm and endoderm markers supported and confirmed that the *Fubp1* KO ESC clones fail to differentiate into mesoderm cells in a similar extend as the NTC clones (Figure 22a and b). In more detail, there was a significant reduction in the expression of the mesoderm marker *Brachyury*, *Flk-1*, *SnaiI* and the Brachyury target gene *Foxa2* at day 3 of EB formation. Interestingly at day 5 only *Snai2* is significantly reduced in the *Fubp1* KO clones, but the markers mentioned above are equalizing their expression level in the *Fubp1* KO clones to the NTC clones (Figure 22b). The addition of 3 genes (*FgfR1*, *Bmp4* and *Wnt3a*) to the panel, which are described to be important for a very specific mesoderm cell type, migrating in different directions in the primitive streak of the early embryogenesis (Winnier, Blessing, and Labosky 1995; Deng et al., 1994; Yoshikawa et al., 1997) showed similar mRNA expression patterns. While I could not detect *Wnt3a* during

EB formation, *FgfR1* was significantly reduced at day 3 of EB differentiation and *Bmp4* showed a reduced expression level from day 3 to 5 on (Figure 22a and b).

Additionally, I set up another differentiation experiment to perform flow cytometry analysis for mesoderm cell. I used the already described markers Brachyury and Flk-1 and analyzed the differentiated EBs at day 3, 4 and 5 of differentiation. 3-5 % of cells were Brachyury$^+$ at day 3 and 4 of EB formation in the NTC controls, while less than 2% of *Fubp1* KO clones were positively stained. However, at day 5 of differentiation, NTC clones and Fubp1 KO clones reached an equal percentage of 15% Brachyury$^+$ cells (Figure 23a). The second mesoderm marker Flk-1 was expressed in NTC clones and Fubp1 KO clones to a very low amount at day 3. However, at day 4 of EB differentiation, more than 25% of the control cells were Flk-1$^+$, while the amount of Flk-1$^+$ cells in the FUBP1 deleted clones was reduced to only 15%. This reduction of Flk-1$^+$ cells was significant at day 5 of EB differentiation and confirms the decreased capability for mesoderm differentiation in the *Fubp1* KO clones (Figure 23b).

As shown in Figure 33, I hypothesize that upon FUBP1 depletion the accurate enhancement of mesoderm marker expression cannot be implemented at the beginning of EB differentiation, while over time the required expression level can be reached through other mechanisms. This implicates a delayed and insufficient mesoderm cell differentiation, but does not affect the ectoderm and endoderm lineages in the EB differentiation method.

However, the analysis of the *Fubp1* mRNA level in Flk-1$^+$ *versus* Flk-1$^-$ cells showed no significant difference, so that I can at least exclude a higher amount of *Fubp1* in Flk-1$^+$ cells. Another idea was that FUBP3 could perhaps partly take over the role of FUBP1, because of their high similarity of 80.9 % of the DNA binding domain (Davis-Smyth et al. 1996) and the initial binding of FUBP3 to the *FUSE* element, which is replaced by FUBP1 (Chung et al. 2006). Interestingly, I could observe a downregulation of *Fubp3* mRNA levels during EB differentiation, but no difference between the NTC clones and the *Fubp1* KO clones (Figure 25). It would be of interest for future studies to investigate a possible role of FUBP3 during differentiation of ESCs to EBs.

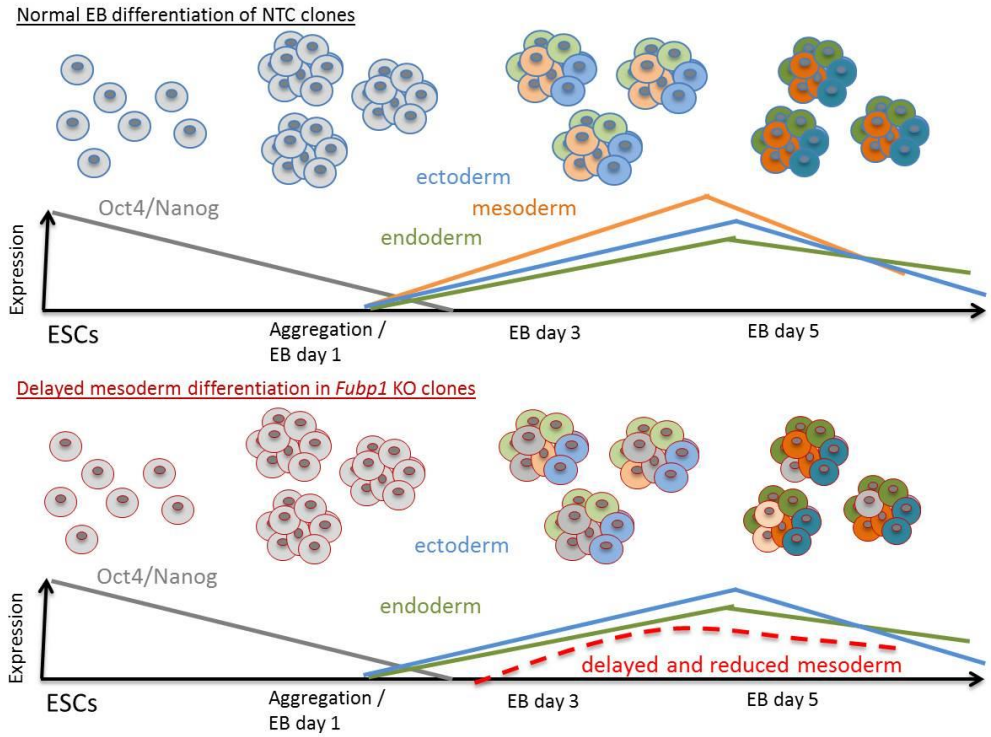

Figure 33: Model of delayed mesoderm differentiation upon FUBP1 depletion. A normal ESC has the ability to form EBs in the absence of LIF and to differentiate into the three germ layers by upregulating the respective genes. In *Fubp1* KO ESC clones, a part of this rapid upregulation of genes that are important for mesoderm differentiation is not working, and a delayed mesoderm marker expression is observed which results in a delay of the generation of mesoderm cells.

Of particular importance is the fact that the hematopoietic cells originate from the mesoderm germ layer (Mikkola 2006). Since we and others could describe an important role of FUBP1 for the self-renewal of fetal and adult hematopoietic stem cells (Rabenhorst et al. 2015; Zhou et al. 2016), it was of high interest to analyze the expression of genes such as *Runx1*, *Gata1* and *Tal*, that are important for the hematopoietic differentiation in the absence of FUBP1 in ESCs (Kuvardina et al. 2015; Tijssen et al. 2011). *Runx1* and *Tal1* mRNA levels were increased from day 5 to day 10 of EB differentiation, while *Gata1* was almost not detectable. However, there was a tendency that *Tal1* expression level was reduced in the *Fubp1* KO clones at day 7 of EB differentiation, but there was no change on the other days or for the expression level of *Runx1* (Figure 26).

5.2.4 The absence of FUBP1 in ESCs does not affect the ability to differentiate into hematopoietic cells using the OP9 co-culture assay

Finally, we wanted to apply a particular differentiation method to specifically differentiate the ESCs into hematopoietic cells. After testing and optimizing the OP9 co-culture assay (Chapter 4.1.3), I analyzed the *Fubp1* KO ESCs for their ability to differentiate into the hematopoietic

lineages. After 5 days of differentiation on the OP9 stroma cells, I stained the cells for the proximal lateral mesoderm marker Flk-1 and combined Flk-1 and VE-Cadherin to analyze the amount of early hemangioblasts. For both cell types, mesoderm cells and hemangioblasts, I observed a significantly reduced number of positive cells in the *Fubp1* KO clones (Figure 27a). This data again supports my assumption that these cells are not able to differentiate into the mesoderm direction in an appropriate way. Although I could observe this significant reduction at day 5, after re-plating 10,000 cells onto freshly prepared OP9 stroma cells, we stained for CD45 expression and could not detect a difference between NTC clones and *Fubp1* KO clones at day 12 of differentiation (Figure 27b). On the one hand, I determined a delayed expression of mesoderm marker during EB differentiation and also in the OP9 assay, on the other hand this effect is compensated over the time, so that I could not see a difference at a later state.

However, I tried to force the ESCs into the erythroid lineage using the OP9 assay, because we could detect a diminished number of mature erythroid cells in the *Fubp1* GT mouse at day 15.5 (Rabenhorst et al., 2015 Supplements S1c). With the addition of the cytokines EPO and SCF to the differentiation medium at day 5 of ESC OP9 co-culture, I could generate a number of erythroid cells at different stages of maturation. I was able to see a slight but not significant reduction of late erythroblasts ($Cd71^{+}/Ter119^{+}$) in the *Fubp1* KO cells, while the other stages of erythroid maturation showed no differences (Figure 28).

Furthermore, it is known that a lot of other lineages than the hematopoietic, such as vascular and mesenchymal lineages, are derived from the mesoderm (Moon et al. 2011). I cannot exclude that these lineages are more affected by this delayed mesoderm differentiation of the *Fubp1* KO cells. Moreover, the absence or reduced expression of mesoderm marker, such as Brachyury or SnaiI does not necessarily lead to the total lack of mesoderm cells during embryogenesis. Herrmann at al, 1991 detected Brachyury in the primitive streak, where mesoderm cells appeared during embryogenesis and could also show the abnormal development of mouse embryos lacking Brachyury. However, these mouse embryos are able to generate mesoderm cells to a limited degree, so that they develop at least until day E10.5 (Herrmann 1991; Scheludko et al. 1998). The phenotype of *SnaiI*$^{-/-}$ mutants is more dramatic and lead to a very early death of the fetus. Here the abnormalities are already very dramatic during gastrulation and early mesoderm formation (Ethan A Carver et al. 2001). The delayed and reduced upregulation of a combination of these mesoderm markers can be an early event

of deregulated cell differentiation which lead to the reduced number of HSCs and also to underdeveloped tissue as it was described before (Rabenhorst et al. 2015; Zhou et al. 2016).

The C-terminal binding proteins CtBP1 and CtBP2 are examples for the importance of time-specific activation of mesoderm genes. These proteins are described to interact with the transcriptional repressor *kruppel* and *knirps* and their importance during early development. The study of (Tarleton and Lemischka 2010) showed a delay of ESC differentiation resulting in a reduced blast formation upon CtBP2 knockdown.

5.3 FUBP1 during the development of mice and the analysis of the *Fubp1* GT mouse strain

5.3.1 FUBP1 is strongly expressed during embryogenesis and in almost every kind of tissue in adult mice

I performed time-matings to analyze the FUBP1 expression during the early development of embryogenesis. A strong staining in almost all the cells of the embryo was visible except for some cells in the liver and the heart at day E9.5. Following up the FUBP1 expression at day E13.5, I could not detect changes in the expression pattern. The heart showed also a strong positive staining, while there were only few cells which were negative for FUBP1 in the liver. The analysis of organs in young and adult mice showed an expression of FUBP1 to a similar extent. Moreover, the liver in adult mice was completely positive for FUBP1. *Fubp1* GT embryos show no reduced proliferation capacity or increased apoptosis.

FUBP1 is described to act as an anti-apoptotic and pro-proliferative protein, especially when overexpressed in solid tumors (Malz et al., 2009; Rabenhorst et al., 2009), but also in normal cells such as hematopoietic stem cells (Rabenhorst et al. 2015). I wanted to find out whether one of these functions could be the reason for the lethality of the *Fubp1* GT embryos. Therefore, I prepared E9.5 and E13.5 embryos from the *Fubp1* GT mouse model and analyzed them for cleaved Caspase 3 as a marker for apoptosis (Cullen and Martin 2009), and for Ki-67, a well described proliferation marker used for prognostic diagnosis of cancer patients (Ermiah et al. 2012). Interestingly, we could not detect a high proportion of apoptotic cells or a reduced proliferation in the *Fubp1* KO embryos compared to WT siblings (Figure 31 and Figure 32). These results may be explained by the fact that FUBP1 is described as a transcriptional regulator to orchestrate a huge network of genes, which differ upon cell type and the stage of differentiation (Zhang and Chen 2012). Interesting finding when analyzing

the FUBP1-deficient embryos was the incomplete folding of the E9.5 embryos, adding another hint for the underdeveloped stage of the embryos.

5.4 *Fubp1* KO ESC clones provide evidence for a broader phenotype in the *Fubp1* GT mice

Although, I could not confirm the hematopoietic phenotype of the *Fubp1* GT mouse model using the OP9 co-culture system, I obtained data that showed a delay of mesoderm differentiation in ESCs. Comparing the hematopoietic differentiation and production of blood cells during embryogenesis and the differentiation of ESCs towards the hematopoietic direction in cell culture, a number of parameters are very different. One of the most important facts to keep in mind is that the development of the hematopoietic system during embryogenesis takes place at different stages of embryogenesis in different parts of the developing embryo as shown in Figure 34. Using an *ex vivo* system to model this process is almost impossible, however, the differentiation of ESCs or iPSCs into hematopoietic cells using a co-culture system or extracellular matrix is possible but does not reflect the *in vivo* complexity as it occurs during embryogenesis (Mikkola 2006).

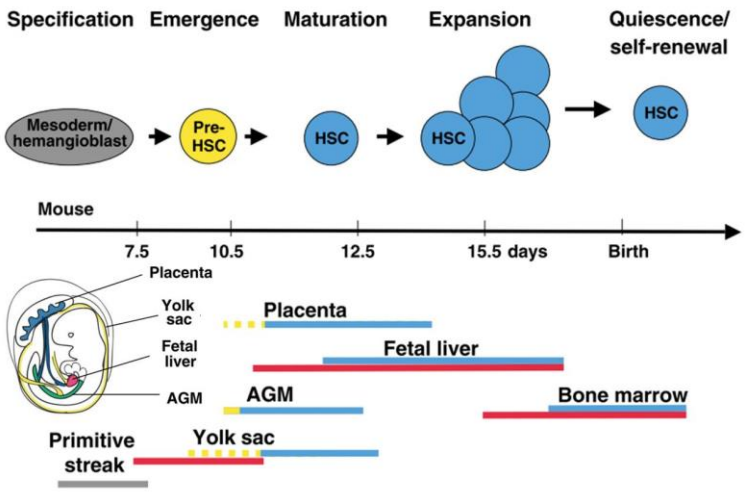

Figure 34: The development of the hematopietic system during mouse embryogenesis is a complex mechanism that occurs at different time points and in different regions of the embryo. It starts at the very early stage of the primitive streak with the generation of mesoderm/hemangioblasts. Following the early generation of pre-HSCs and erythroid cells in the yolk sac, cells then migrate to the AGM (aorta-gonad-mesonephros) and placenta. Between day E10.5 and 15.5 the HSCs and HPCs are migrating into the liver, where a huge expansion of cells takes place. Shortly before birth, HSCs migrate to their niche in the bone marrow of the developing organism. (yellow: pre-HSCs, blue: HSCs, red: red blood cells) adapted from (Mikkola 2006)

Mesoderm cells are representing one of the three germ layers, and they develop into the hematopoietic, vascular and mesenchyme lineage. With the analysis of genes that are

deregulated during mesoderm differentiation in the *Fubp1* KO ESC clones, I hypothesize that these genes could also be downregulated in the *Fubp1* GT mouse model and could affect a broader range of tissue or cells that originally arise from the mesoderm. FgfR1 and Bmp4, for example, are important for cardiac mesoderm and hepatic induction (Duncan 2003; Jung et al. 1999). It is unclear where the direct connection between FUBP1 and the analyzed genes is, but if the molecular phenotype of the *Fubp1* KO clones during EB formation is reflecting the molecular mechanism during embryogenesis, it is necessary to follow up other lineages of mesoderm differentiation to understand the complex role of FUBP1 during embryogenesis, especially because embryonic development is a dynamic process that combines morphogenic movements with cell signaling to control patterning and differentiation of all cell types (Li, Baibakov, and Dean 2008; Hamatani et al. 2004).

6 Literature

Avigan, Mark I., Bruce Strober, and David Levens. 1990. "A Far Upstream Element Stimulates c-Myc Expression in Undifferentiated Leukemia Cells." *Journal of Biological Chemistry* 265(30):18538–45.

van den Berg, Debbie L. C. et al. 2010. "An Oct4-Centered Protein Interaction Network in Embryonic Stem Cells." *Cell Stem Cell* 6(4):369–81. Retrieved (http://linkinghub.elsevier.com/retrieve/pii/S1934590910000913).

Blum, M. et al. 2008. "References and Notes 1." 322(September):1468–72.

Borthwick, Jane M. et al. 2003. "Determination of the Transcript pro ® Le of Human Endometrium." *Molecular Human Reproduction* 9(1):19–33. Retrieved (http://molehr.oxfordjournals.org/content/9/1/19.long).

Boyer, Laurie et al. 2005. "Core Transcriptional Regulatory Circuitry in Human Embryonic Stem Cells." *Cell* 122(6):947–56. Retrieved (citeulike-article-id:350303 http://dx.doi.org/10.1016/j.cell.2005.08.020).

Bradley, J. Andrew, Eleanor M. Bolton, and Roger a Pedersen. 2002. "Stem Cell Medicine Encounters the Immune System." *Nature reviews. Immunology* 2(11):859–71.

Carotta, Sebastian et al. 2012. "Directed Differentiation and Mass Cultivation of Pure Erythroid Progenitors from Mouse Embryonic Stem Cells Directed Differentiation and Mass Cultivation of Pure Erythroid Progenitors from Mouse Embryonic Stem Cells." 104(6):1873–80.

Carson, D. D. 2002. "Changes in Gene Expression during the Early to Mid-Luteal (Receptive Phase) Transition in Human Endometrium Detected by High-Density Microarray Screening." *Molecular Human Reproduction* 8(9):871–79. Retrieved (http://molehr.oxfordjournals.org/content/8/9/871.short).

Carver, E. A., R. Jiang, Y. Lan, K. F. Oram, and T. Gridley. 2001. "The Mouse Snail Gene Encodes a Key Regulator of the Epithelial-Mesenchymal Transition." *Molecular and Cellular Biology* 21(23):8184–88. Retrieved October 18, 2015 (http://mcb.asm.org/content/21/23/8184.full).

Carver, Ethan A., Rulang Jiang, Yu Lan, Kathleen F. Oram, and Thomas Gridley. 2001. "The Mouse Snail Gene Encodes a Key Regulator of the Epithelial-Mesenchymal Transition." *Mol Cell Biol* 21(23):8184–88.

Chao, Ruihua, Xueping Gong, Libo Wang, Pengxiang Wang, and Yuan Wang. 2015. "CD71high Population Represents Primitive Erythroblasts Derived from Mouse Embryonic Stem Cells." *Stem Cell Research* 14(1):3038. Retrieved (http://dx.doi.org/10.1016/j.scr.2014.11.002).

Chung, Hye-Jung H. J. et al. 2006. "FBPs Are Calibrated Molecular Tools To Adjust Gene Expression." *Molecular and Cellular Biology* 26(17):6584–97. Retrieved (http://mcb.asm.org/cgi/doi/10.1128/MCB.00754-06\nhttp://www.pubmedcentral.nih.gov/articlerender.fcgi?artid=1592819&tool=pmcentrez&rendertype=abstract).

Cullen, S. P. and S. J. Martin. 2009. "Caspase Activation Pathways: Some Recent Progress." *Cell Death and Differentiation* 16(7):935–38. Retrieved (http://www.nature.com/doifinder/10.1038/cdd.2009.59).

Davis-Smyth, Terri, Robert C. Duncan, Tian Zheng, Gregory Michelotti, and David Levens. 1996. "The Far Upstream Element-Binding Proteins Comprise an Ancient Family of Single-Strand DNA-Binding Transactivators." *Journal of Biological Chemistry* 271(49):31679–87.

Deng, C. X. et al. 1994. "Murine FGFR-1 Is Required for Early Postimplantation Growth and Axial Organization." *Genes and Development* 8(24):3045–57.

Douglas, Nataki C. et al. 2014. "VEGFR-1 Blockade Disrupts Peri-Implantation Decidual Angiogenesis and Macrophage Recruitment." *Vascular cell* 6(1):16. Retrieved (http://www.pubmedcentral.nih.gov/articlerender.fcgi?artid=4122670&tool=pmcentrez&rendertype=abstract).

Duncan, R. et al. 1996. "A Unique Transctivation Sequence Motif Is Found in the Carboxyl-Terminal Domain of the Single-Strand-Binding Protein FBP." *Molecular and Cellular Biology* 16(5):2274–82.

Duncan, Robert et al. 1994. "A Sequence-Specific, Single-Strand Binding Protein Activates the Far Upstream Element of c-Myc and Defines a New DNA-Binding Motif." *Genes and Development* 8(4):465–80.

Duncan, Stephen A. 2003. "Mechanisms Controlling Early Development of the Liver." *Mechanisms of Development* 120(1):19–33.

Engert, S. et al. 2013. "Wnt/ -Catenin Signalling Regulates Sox17 Expression and Is Essential for Organizer and Endoderm Formation in the Mouse." *Development* 140(15):3128–38. Retrieved (http://dev.biologists.org/cgi/doi/10.1242/dev.088765).

Ermiah, Eramah et al. 2012. "Prognostic Value of Proliferation Markers: Immunohistochemical Ki-67 Expression and Cytometric S-Phase Fraction of Women with Breast Cancer in Libya." *Journal of Cancer* 3(1):421–31.

Evans, Amanda L. et al. 2012. "Genomic Targets of Brachyury (T) in Differentiating Mouse Embryonic Stem Cells." *PloS one* 7(3):e33346. Retrieved (http://journals.plos.org/plosone/article?id=10.1371/journal.pone.0033346).

Faial, Tiago et al. 2015. “Brachyury and SMAD Signalling Collaboratively Orchestrate Distinct Mesoderm and Endoderm Gene Regulatory Networks in Differentiating Human Embryonic Stem Cells.” *Development* 142(12):2121–35. Retrieved (http://www.pubmedcentral.nih.gov/articlerender.fcgi?artid=4483767&tool=pmcentrez&rendertype=abstract).

Fauzi, Iliana, Nicki Panoskaltsis, and Athanasios Mantalaris. 2012. “Enhanced Hematopoietic Differentiation Toward Erythrocytes from Murine Embryonic Stem Cells with HepG2-Conditioned Medium.” *Stem Cells and Development* 21(17):120816074616001.

Fraser, Stuart T., Joan Isern, and Margaret H. Baron. 2007. “Maturation and Enucleation of Primitive Erythroblasts during Mouse Embryogenesis Is Accompanied by Changes in Cell-Surface Antigen Expression.” *Blood* 109(1):343–52.

Garbutt, C. L., M. H. Johnson, and M. a George. 1987. “When and How Does Cell Division Order Influence Cell Allocation to the Inner Cell Mass of the Mouse Blastocyst?” *Development (Cambridge, England)* 100(2):325–32. Retrieved (http://www.ncbi.nlm.nih.gov/pubmed/3652974).

Gerlach, Katharina. 2015. “Characterization of FUSE -Binding Protein 1 as a Hematopoietic Stem Cell Self-Renewal Factor.” *PhD Thesis* 2015.

Gherzi, Roberto, Ching Yi Chen, Michele Trabucchi, Andres Ramos, and Paola Briata. 2010. “The Role of KSRP in mRNA Decay and microRNA Precursor Maturation.” *Wiley Interdisciplinary Reviews: RNA* 1(2):230–39.

Graf, Urs, Elisa a. Casanova, and Paolo Cinelli. 2011. “The Role of the Leukemia Inhibitory Factor (LIF) - Pathway in Derivation and Maintenance of Murine Pluripotent Stem Cells.” *Genes* 2(1):280–97.

Hamatani, Toshio et al. 2004. “Global Gene Expression Analysis Identifies Molecular Pathways Distinguishing Blastocyst Dormancy and Activation.” *Proceedings of the National Academy of Sciences of the United States of America* 101(28):10326–31. Retrieved (http://www.pnas.org/content/101/28/10326.long#T1).

Han, Seok Ko, Who Kim Seong, Sathya R. Sriram, Valina L. Dawson, and Ted M. Dawson. 2006. “Identification of Far Upstream Element-Binding Protein-1 as an Authentic Parkin Substrate.” *Journal of Biological Chemistry* 281(24):16193–96.

Hanna, Lynn a., Ruth K. Foreman, Illya a. Tarasenko, Daniel S. Kessler, and Patricia a. Labosky. 2002. “Requirement for Foxd3 in Maintaining Pluripotent Cells of the Early Mouse Embryo.” *Genes and Development* 16(20):2650–61.

Herrmann, B. G. 1991. “Expression Pattern of the Brachyury Gene in Whole-Mount TWis/TWis Mutant Embryos.” *Development (Cambridge, England)* 113(3):913–17.

Hooper, M., K. Hardy, a Handyside, S. Hunter, and M. Monk. 1987. “HPRT-Deficient (Lesch-Nyhan) Mouse Embryos Derived from Germline Colonization by Cultured Cells.” *Nature* 326(6110):292–95.

Hsiao, Hsin Hao et al. 2010. “Quantitative Characterization of the Interactions among c-Myc Transcriptional Regulators FUSE, FBP, and FIR.” *Biochemistry* 49(22):4620–34.

Huang, Guanyi, Hexin Yan, Shoudong Ye, Chang Tong, and Qi Long Ying. 2014. “STAT3 Phosphorylation at Tyrosine 705 and Serine 727 Differentially Regulates Mouse Esc Fates.” *Stem Cells* 32(5):1149–60.

Huang, Guanyi, Shoudong Ye, Xingliang Zhou, Dahai Liu, and Qi Long Ying. 2015. “Molecular Basis of Embryonic Stem Cell Self-Renewal: From Signaling Pathways to Pluripotency Network.” *Cellular and Molecular Life Sciences* 72(9):1741–57.

Ivanova, Natalia et al. 2006. “Dissecting Self-Renewal in Stem Cells with RNA Interference.” *Nature* 442(7102):533–38. Retrieved (http://www.nature.com/doifinder/10.1038/nature04915).

Jain, Abhinav K. et al. 2012. “P53 Regulates Cell Cycle and Micrornas to Promote Differentiation of Human Embryonic Stem Cells.” *PLoS Biology* 10(2).

Jang, M. et al. 2009. “Far Upstream Element-Binding Protein-1, a Novel Caspase Substrate, Acts as a Cross-Talker between Apoptosis and the c-Myc Oncogene.” *Oncogene* 28(12):1529–36. Retrieved (http://www.ncbi.nlm.nih.gov/pubmed/19219071).

Jung, J. et al. 1999. “Initiation of Mammalian Liver Development from Endoderm by Fibroblast Growth Factors.” *Science (New York, N.Y.)* 284(5422):1998–2003. Retrieved (http://www.ncbi.nlm.nih.gov/pubmed/10373120).

Jung, Yong Sam, Yingjuan Qian, and Xinbin Chen. 2010. “Examination of the Expanding Pathways for the Regulation of p21 Expression and Activity.” *Cellular Signalling* 22(7):1003–12.

Kaebisch, Constanze, Dorothee Schipper, Patrick Babczyk, and Edda Tobiasch. 2015. “The Role of Purinergic Receptors in Stem Cell Differentiation.” *Computational and Structural Biotechnology Journal* 13:75–84. Retrieved (http://dx.doi.org/10.1016/j.csbj.2014.11.003).

Kao, L. C. 2002. “Global Gene Profiling in Human Endometrium during the Window of Implantation.” *Endocrinology* 143(6):2119–38. Retrieved (http://endo.endojournals.org/cgi/doi/10.1210/en.143.6.2119).

Keller, Gordon. 2005. “Embryonic Stem Cell Differentiation : Emergence of a New Era in Biology and Medicine.” 1129–55.

Kim, Min Jung et al. 2003. “Downregulation of FUSE-Binding Protein and c-Myc by tRNA Synthetase Cofactor p38 Is Required for Lung

Cell Differentiation." *Nature genetics* 34(3):330–36. Retrieved (http://www.ncbi.nlm.nih.gov/pubmed/12819782).

Koike, Mikiko, Shujiro Sakaki, Yoshifumi Amano, and Hiroshi Kurosawa. 2007. "Characterization of Embryoid Bodies of Mouse Embryonic Stem Cells Formed under Various Culture Conditions and Estimation of Differentiation Status of Such Bodies." *Journal of bioscience and bioengineering* 104(4):294–99. Retrieved (http://www.ncbi.nlm.nih.gov/pubmed/18023802).

Koulnis, Miroslav et al. 2011. "Identification and Analysis of Mouse Erythroid Progenitors Using the CD71/TER119 Flow-Cytometric Assay." *Journal of visualized experiments : JoVE* i(54):6–11.

Kraus, Yulia, Andy Aman, Ulrich Technau, and Grigory Genikhovich. 2016. "Pre-Bilaterian Origin of the Blastoporal Axial Organizer." *Nature Communications* 7(May):11694. Retrieved (http://www.nature.com/doifinder/10.1038/ncomms11694).

Kuehn, M. R., a Bradley, E. J. Robertson, and M. J. Evans. 1987. "A Potential Animal Model for Lesch-Nyhan Syndrome through Introduction of HPRT Mutations into Mice." *Nature* 326:295–98.

Kurosawa, Hiroshi. 2007. "Methods for Inducing Embryoid Body Formation: In Vitro Differentiation System of Embryonic Stem Cells." *Journal of Bioscience and Bioengineering* 103(5):389–98. Retrieved (http://linkinghub.elsevier.com/retrieve/pii/S1389172307700786).

Kuvardina, Olga N. et al. 2015. "RUNX1 Represses the Erythroid Gene Expression Program during Megakaryocytic Differentiation." *Blood* 125(23):3570–79.

Latham, Keith E., James I. Garrels, Cecile Chang, and Davor Solter. 1991. "Quantitative Analysis of Protein Synthesis in Mouse Embryos . I . Extensive Reprogramming at the One- and Two-Cell Stages." 932:921–32.

Li, Lei, Boris Baibakov, and Jurrien Dean. 2008. "A Subcortical Maternal Complex Essential for Preimplantation Mouse Embryogenesis." *Developmental Cell* 15(3):416–25.

Lin, Tongxiang et al. 2005. "p53 Induces Differentiation of Mouse Embryonic Stem Cells by Suppressing Nanog Expression." *Nature Cell Biology* 7(2):165–71. Retrieved (http://www.nature.com/doifinder/10.1038/ncb1211).

Liu, Juhong et al. 2006. "The FUSE/FBP/FIR/TFIIH System Is a Molecular Machine Programming a Pulse of c-Myc Expression." *The EMBO journal* 25(10):2119–30. Retrieved (http://www.pubmedcentral.nih.gov/articlerender.fcgi?artid=1462968&tool=pmcentrez&rendertype=abstract\nhttp://www.ncbi.nlm.nih.gov/pubmed/16628215).

Liu, Juhong et al. 2011. "JTV1 Co-Activates FBP to Induce USP29 Transcription and Stabilize p53 in Response to Oxidative Stress." *The EMBO journal* 30(5):846–58. Retrieved (http://www.pubmedcentral.nih.gov/articlerender.fcgi?artid=3049210&tool=pmcentrez&rendertype=abstract).

Loh, Yuin-Han et al. 2006. "The Oct4 and Nanog Transcription Network Regulates Pluripotency in Mouse Embryonic Stem Cells." *Nature Genetics* 38(4):431–40. Retrieved (http://www.nature.com/doifinder/10.1038/ng1760).

Lopes, Flavia L., Jo??lle A. Desmarais, and Bruce D. Murphy. 2004. "Embryonic Diapause and Its Regulation." *Reproduction* 128(6):669–78.

Malz, Mona et al. 2009. "Overexpression of Far Upstream Element Binding Proteins: A Mechanism Regulating Proliferation and Migration in Liver Cancer Cells." *Hepatology* 50(4):1130–39.

Mansergh, Fiona C. et al. 2009. "Gene Expression Profiles during Early Differentiation of Mouse Embryonic Stem Cells." *BMC developmental biology* 9:5. Retrieved (http://www.pubmedcentral.nih.gov/articlerender.fcgi?artid=2656490&tool=pmcentrez&rendertype=abstract).

Martello, Graziano and Austin Smith. 2014. "The Nature of Embryonic Stem Cells." *Annual Review of Cell and Developmental Biology* 30(1):647–78.

Meyer, Natalie and Linda Z. Penn. 2008. "Reflecting on 25 Years with MYC." *Nature reviews. Cancer* 8(12):976–90.

Mikkola, H. K. A. 2006. "The Journey of Developing Hematopoietic Stem Cells." *Development* 133(19):3733–44. Retrieved (http://www.ncbi.nlm.nih.gov/pubmed/16968814).

Mirkin, S. et al. 2005. "In Search of Candidate Genes Critically Expressed in the Human Endometrium during the Window of Implantation." *Human Reproduction* 20(8):2104–17.

Mitsui, Kaoru et al. 2003. "The Homeoprotein Nanog Is Required for Maintenance of Pluripotency in Mouse Epiblast and ES Cells." *Cell* 113(5):631–42. Retrieved (http://www.sciencedirect.com/science/article/pii/S0092867403003933).

Montes de Oca Luna, R., D. S. Wagner, and G. Lozano. 1995. "Rescue of Early Embryonic Lethality in mdm2-Deficient Mice by Deletion of p53." *Nature* 378(6553):203–6.

Moon, Sung Hwan et al. 2011. "Differentiation of hESCs into Mesodermal Subtypes: Vascular-, Hematopoietic- and Mesenchymal-Lineage Cells." *International Journal of Stem Cells* 4(1):24–34.

Motosugi, Nami, Tobias Bauer, Zbigniew Polanski, Davor Solter, and Takashi Hiiragi. 2005. “Polarity of the Mouse Embryo Is Established at Blastocyst and Is Not Prepatterned.” *Genes and Development* 19(9):1081–92.

Nakano, T., H. Kodama, and T. Honjo. 1994. “Generation of Lymphohematopoietic Cells from Embryonic Stem Cells in Culture.” *Science (New York, N.Y.)* 265(5175):1098–1101.

Nakano, T., H. Kodama, and T. Honjo. 1996. “In Vitro Development of Primitive and Definitive Erythrocytes from Different Precursors.” *Science (New York, N.Y.)* 272(5262):722–24.

Nichols, Jennifer et al. 1998. “Formation of Pluripotent Stem Cells in the Mammalian Embryo Dependes on the POU Transcription Factor Oct4.” *Cell* 95:379–91.

Nishikawa, S. I., S. Nishikawa, M. Hirashima, N. Matsuyoshi, and H. Kodama. 1998. “Progressive Lineage Analysis by Cell Sorting and Culture Identifies FLK1+VE-Cadherin+ Cells at a Diverging Point of Endothelial and Hemopoietic Lineages.” *Development (Cambridge, England)* 125(9):1747–57.

Niwa, H., T. Burdon, I. Chambers, and a Smith. 1998. “Self-Renewal of Pluripotent Embryonic Stem Cells Is Mediated via Activation of STAT3.” *Genes & development* 12(13):2048–60. Retrieved (http://www.pubmedcentral.nih.gov/articlerender.fcgi?artid=316954&tool=pmcentrez&rendertype=abstract).

Okamoto, K. et al. 1990. “A Novel Octamer Binding Transcription Factor Is Differentially Expressed in Mouse Embryonic Cells.” *Cell* 60(3):461–72.

Paria, Bibhash C. et al. 1998. “Coordination of Differential Effects of Primary Estrogen and Catecholestrogen on Two Distinct Targets Mediates Embryo Implantation in the Mouse.” *Endocrinology* 139(12):5235–46.

Patrick, Hsu D., Lander S. Eric, and Feng Zhang. 2014. “Development and Applications of CRISPR-Cas9 for Genome Engineering Patrick.” *Cell* 157(6):1262–78.

Poh, Yeh-Chuin et al. 2014. “Generation of Organized Germ Layers from a Single Mouse Embryonic Stem Cell.” *Nature communications* 5(May):4000. Retrieved (http://www.pubmedcentral.nih.gov/articlerender.fcgi?artid=4050279&tool=pmcentrez&rendertype=abstract).

Qu, Xue Bin, Jie Pan, Cong Zhang, and Shu Yang Huang. 2008. “Sox17 Facilitates the Differentiation of Mouse Embryonic Stem Cells into Primitive and Definitive Endoderm in Vitro.” *Development Growth and Differentiation* 50(7):585–93.

Rabenhorst, Uta, Rasa Beinoraviciute-Kellner, Marie Luise Brezniceanu, et al. 2009. “Overexpression of the Far Upstream Element Binding Protein 1 in Hepatocellular Carcinoma Is Required for Tumor Growth.” *Hepatology* 50(4):1121–29.

Rabenhorst, Uta, Rasa Beinoraviciute-Kellner, Marie-Luise Brezniceanu, et al. 2009. “Overexpression of the Far Upstream Element Binding Protein 1 in Hepatocellular Carcinoma Is Required for Tumor Growth.” *Hepatology (Baltimore, Md.)* 50(4):1121–29. Retrieved (http://eutils.ncbi.nlm.nih.gov/entrez/eutils/elink.fcgi?dbfrom=pubmed&id=19637194&retmode=ref&cmd=prlinks\npapers2://publication/doi/10.1002/hep.23098).

Rabenhorst, Uta et al. 2015. “Single-Stranded DNA-Binding Transcriptional Regulator FUBP1 Is Essential for Fetal and Adult Hematopoietic Stem Cell Self-Renewal.” *Cell reports* 11(12):1847–55. Retrieved (http://www.ncbi.nlm.nih.gov/pubmed/26095368).

Riesewijk, Anne et al. 2003. “Gene Expression Profiling of Human Endometrial Receptivity on Days LH+2 versus LH+7 by Microarray Technology.” *Mol. Hum. Reprod.* 9(5):253–64. Retrieved (http://molehr.oxfordjournals.org/cgi/content/abstract/9/5/253).

Sakaki-Yumoto, Masayo et al. 2006. “The Murine Homolog of SALL4, a Causative Gene in Okihiro Syndrome, Is Essential for Embryonic Stem Cell Proliferation, and Cooperates with Sall1 in Anorectal, Heart, Brain and Kidney Development.” *Development (Cambridge, England)* 133(15):3005–13.

Sanjana, Neville E., Ophir Shalem, and Feng Zhang. 2014. “Improved Vectors and Genome-Wide Libraries for CRISPR Screening.” *Nature Methods* 11(8):783–84. Retrieved (http://www.nature.com/doifinder/10.1038/nmeth.3047).

Scheludko, Alexei D. et al. 1998. “© 19 90 Nature Publishing Group.” *Journal of Colloid and Interface Science* 245(1):118–43. Retrieved (http://www.ncbi.nlm.nih.gov/pubmed/16290341\nhttp://link.springer.com/10.1007/BF01177222\nhttp://linkinghub.elsevier.com/retrieve/pii/0021979780905019\nhttp://scitation.aip.org/content/aip/journal/pof2/10/9/10.1063/1.869740\nhttp://www.sciencedirect.com/scien).

Schöler, H. R., R. Balling, a K. Hatzopoulos, N. Suzuki, and P. Gruss. 1989. “Octamer Binding Proteins Confer Transcriptional Activity in Early Mouse Embryogenesis.” *The EMBO journal* 8(9):2551–57.

Schrank, B. et al. 1997. “Inactivation of the Survival Motor Neuron Gene, a Candidate Gene for Human Spinal Muscular Atrophy, Leads to Massive Cell Death in Early Mouse Embryos.” *Proceedings of the National Academy of Sciences of the United States of America* 94(18):9920–25. Retrieved (http://www.pubmedcentral.nih.gov/articlerender.fcgi?artid=23295&tool=pmcentrez&rendertype=abstract).

Sem??nov, Mikhail V. et al. 2001. “Head Inducer Dickkopf-1 Is a Ligand for Wnt Coreceptor LRP6.” *Current Biology* 11(12):951–61.

Smith, A. G. and M. L. Hooper. 1987. “Buffalo Rat Liver Cells Produce a Diffusible Activity Which Inhibits the Differentiation of Murine

Embryonal Carcinoma and Embryonic Stem Cells." *Dev Biol* 121(1):1–9. Retrieved (http://www.ncbi.nlm.nih.gov/entrez/query.fcgi?cmd=Retrieve&db=PubMed&dopt=Citation&list_uids=3569655).

Smith, J. L., K. M. Gesteland, and G. C. Schoenwolf. 1994. "Prospective Fate Map of the Mouse Primitive Streak at 7.5 Days of Gestation." *Developmental dynamics : an official publication of the American Association of Anatomists* 201(3):279–89. Retrieved (http://www.ncbi.nlm.nih.gov/pubmed/7881130).

Soria, B. 2001. "In-Vitro Differentiation of Pancreatic Beta-Cells." *Differentiation; research in biological diversity* 68(4-5):205–19. Retrieved (http://dx.doi.org/10.1046/j.1432-0436.2001.680408.x).

Stuckey, Daniel W. et al. 2011. "Coordination of Cell Proliferation and Anterior-Posterior Axis Establishment in the Mouse Embryo." *Development (Cambridge, England)* 138:1521–30.

Surani, M. Azim H. and Sheila C. Barton. 1984. "Spatial Distribution of Blastomeres Is Dependent on Cell Division Order and Interactions in Mouse Morulae." *Developmental Biology* 102(2):335–43.

Tai, Chih-I., Eric N. Schulze, and Qi-Long Ying. 2014. "Stat3 Signaling Regulates Embryonic Stem Cell Fate in a Dose-Dependent Manner." *Biology open* 3(10):958–65. Retrieved (http://www.pubmedcentral.nih.gov/articlerender.fcgi?artid=4197444&tool=pmcentrez&rendertype=abstract).

Talkhabi, Mahmood, Nasser Aghdami, and Hossein Baharvand. 2015. "Human Cardiomyocyte Generation from Pluripotent Stem Cells: A State-of-Art." *Life Sciences* 145:98–113. Retrieved (http://linkinghub.elsevier.com/retrieve/pii/S0024320515301144).

Tamm, Christoffer, Sara Pijuan Galitó, and Cecilia Annerén. 2013. "A Comparative Study of Protocols for Mouse Embryonic Stem Cell Culturing." *PLoS ONE* 8(12):e81156. Retrieved (http://dx.plos.org/10.1371/journal.pone.0081156).

Tang, Ke, Xiang Yu, Yousheng Shu, Chunmei Yue, and Naihe Jing. 2015. "Stem Cell Reports Symptoms Associated with Alzheimer ' S Disease in Mouse Models." *Stem Cell Reports* 5(5):776–90. Retrieved (http://dx.doi.org/10.1016/j.stemcr.2015.09.010).

Tarleton, Heather P. and Ihor R. Lemischka. 2010. "Delayed Differentiation in Embryonic Stem Cells and Mesodermal Progenitors in the Absence of CtBP2." *Mechanisms of Development* 127(1-2):107–19. Retrieved (http://dx.doi.org/10.1016/j.mod.2009.10.002).

Tijssen, Marloes R. et al. 2011. "Genome-Wide Analysis of Simultaneous GATA1/2, RUNX1, FLI1, and SCL Binding in Megakaryocytes Identifies Hematopoietic Regulators." *Developmental Cell* 20(5):597–609.

Wang, H. and S. K. Dey. 2006. "Roadmap to Embryo Implantation: Clues from Mouse Models." *Nat Rev Genet* 7(3):185–99. Retrieved (http://www.ncbi.nlm.nih.gov/pubmed/16485018).

Wang, Zheng, Efrat Oron, Brynna Nelson, Spiro Razis, and Natalia Ivanova. 2012. "Distinct Lineage Specification Roles for NANOG, OCT4, and SOX2 in Human Embryonic Stem Cells." *Cell Stem Cell* 10(4):440–54. Retrieved (http://dx.doi.org/10.1016/j.stem.2012.02.016).

Weber, Achim et al. 2008. "The FUSE Binding Proteins FBP1 and FBP3 Are Potential c-Myc Regulators in Renal, but Not in Prostate and Bladder Cancer." *BMC cancer* 8:369. Retrieved (http://eutils.ncbi.nlm.nih.gov/entrez/eutils/elink.fcgi?dbfrom=pubmed&id=19087307&retmode=ref&cmd=prlinks\npapers2://publication/doi/10.1186/1471-2407-8-369).

Willey, Stephen et al. 2006. "Acceleration of Mesoderm Development and Expansion of Hematopoietic Progenitors in Differentiating ES Cells by the Mouse Mix-like Homeodomain Transcription Factor." *Blood* 107(8):3122–30.

Williams, Barbara Y., Susan L. Hamilton, and Hemanta K. Sarkar. 2000. "The Survival Motor Neuron Protein Interacts with the Transactivator FUSE Binding Protein from Human Fetal Brain." *FEBS Letters* 470(2):207–10.

Wilson, Valerie and Rosa S. P. Beddington. 1996. "Cell Fate and Morphogenetic Movement in the Late Mouse Primitive Streak." *Mechanisms of Development* 55(1):79–89.

Winnier G, Blessing M, Labosky P, Hogan B. 1995. "Bone Mor Hogenetic Protein-4 Is Reqmrea for Mesoderm Formation and Patterning in the Mouse." *Genes & Development* 2105–16.

Wray, Jason, Tuzer Kalkan, and Austin G. Smith. 2010. "The Ground State of Pluripotency." *Biochemical Society transactions* 38(4):1027–32. Retrieved (http://www.biochemsoctrans.org/content/38/4/1027.abstract).

Xu, Si-Guang, Pei-Jun Yan, and Zhi-Ming Shao. 2010. "Differential Proteomic Analysis of a Highly Metastatic Variant of Human Breast Cancer Cells Using Two-Dimensional Differential Gel Electrophoresis." *Journal of cancer research and clinical oncology* 136(10):1545–56. Retrieved (http://www.ncbi.nlm.nih.gov/pubmed/20155427).

Ye, Xiaoqin et al. 2005. "LPA3-Mediated Lysophosphatidic Acid Signalling in Embryo Implantation and Spacing." *Nature* 435(May):104–8.

Yoshida, H. et al. 1990. "The Murine Mutation Osteopetrosis Is in the Coding Region of the Macrophage Colony Stimulating Factor Gene." *Nature* 345(6274):442–44. Retrieved (http://www.ncbi.nlm.nih.gov/pubmed/2188141).

Yoshikawa, Y., T. Fujimori, a P. McMahon, and S. Takada. 1997. "Evidence That Absence of Wnt-3a Signaling Promotes Neuralization

instead of Paraxial Mesoderm Development in the Mouse." *Developmental biology* 183(2):234–42.

Young, Richard A. 2011. "Control of the Embryonic Stem Cell State." *Cell* 144(6):940–54. Retrieved (http://linkinghub.elsevier.com/retrieve/pii/S0092867411000717).

Zhang, J. and Q. M. Chen. 2012. "Far Upstream Element Binding Protein 1: A Commander of Transcription, Translation and beyond." *Oncogene* 32(24):2907–16. Retrieved (http://dx.doi.org/10.1038/onc.2012.350).

Zheng, Jie et al. 2008. "Differential Effects of GATA-1 on Proliferation and Differentiation of Erythroid Lineage Cells Differential Effects of GATA-1 on Proliferation and Differentiation of Erythroid Lineage Cells." *Library* 107(2):520–27.

Zhou, Weixin et al. 2016. "Far Upstream Element Binding Protein Plays a Crucial Role in Embryonic Development, Hematopoiesis, and Stabilizing MYC Expression Levels." *The American Journal of Pathology* (January). Retrieved (http://linkinghub.elsevier.com/retrieve/pii/S0002944015006562).

Zubaidah, Ramdzan M. et al. 2008. "2-D DIGE Profiling of Hepatocellular Carcinoma Tissues Identified Isoforms of Far Upstream Binding Protein (FUBP) as Novel Candidates in Liver Carcinogenesis." *Proteomics* 8(23-24):5086–96.

7 List of Abbreviations

°C	degree Celsius
µg	microgram
µl	microliter
µm	micrometer
µM	micromolar
A	ampere
aa	amino acid(s)
ARS	cytoplasmic multi-aminoacyl-tRNA synthetase
α-MEM	alpha modified essential medium
BIK	Bcl-2-interacting killer
bp	base pairs
BSA	bovine serum albumin
Cas	CRSIPR associated
cm	centimeter
CMV	Cytomegalovirus
c-myc	c-myc myelocytomatosis viral oncogene homolog
CO_2	carbon dioxide
CRISPR	Clustered Regularly Interspaced Short Palindromic Repeats
C-terminal	carboxy-terminal
DMSO	dimethylsulfoxide
DNA	deoxyribonucleic acid
DNase	deoxyribonuclease
dNTP	deoxynucleoside triphosphate
DPBS	Dulbecco's phosphate buffered saline
dsDNA	double stranded DNA
DTT	dithiothreitol
EB	embryoid body
E. coli	*Escherichia coli*
ECL	enhanced chemiluminescence
EDTA	ethylenediaminetetraacetic acid
ESC	embryonic stem cell
EtOH	ethanol
FACS	fluorescence activated cell sorting
FBP1,2 and 3	FUSE binding protein 1, 2 and 3
FBS	fetal bovine serum
FIR	FBP interacting repressor
fw	forward
FUSE	far upstream element
GMEM	Glasgow minimal essential medium
GT	gne trap
h	hour(s)
H_2O	water
HBV	hepatitis B virus
HCC	hepatocellular carcinoma
HCl	hydrochloric acid
HCV	hepatitis C virus
HER2	human epidermal growth factor receptor 2
hnRNP K	human heterogeneous nuclear ribonucleoprotein K
HRP	horseradish peroxidase
kb	kilobase(s)
KCl	potassium chloride
kDa	kilodalton
KH	K homology
KH_2PO_4	potassium dihydrogenphosphate
KO	knockout
KOAc	potassium acetate
LB	Luria-Bertani medium
m	minute(s)
M	molar
mA	milliampere
$MgCl_2$	magnesium chloride
$MgSO_4$	magnesium sulfate
min	minute(s)
ml	milliliter

mm	millimeter
mM	millimolar
mRNA	messenger RNA
Na_2HPO_4	disodiumhydrogenphosphate
NaCl	sodium chloride
NaOAc	sodium acetate
NaOH	sodium hydroxide
NCBI	national center for biotechnology information
ng	nanogram
nm	nanometer
nM	nanomolar
NTC	non-target control
NOXA	noxa (for damage), Bcl-2 homology 3 (BH3) only protein
N-terminal	amino-terminal
PAGE	polyacrylamide gel electrophoresis
PBS	phosphate buffered saline
PBS-T	PBS supplemented with Tween-20
PCR	polymerase chain reaction
PEI	polyethyleneimine
Pen	penicillin
PMSF	phenylmethylsulfonylfluoride
rev	reverse
RNA	ribonucleic acid
RNase	ribonuclease
rpm	rounds per minute
s	second(s)
SDS	sodium dodecyl sulfate
SMN	survival motor neuron protein
ssDNA	single stranded DNA
Strep	streptomycin
TA	transactivation domain
TBE buffer	Tris-borate-EDTA buffer
TBS	Tris buffered saline
TBS-T	TBS supplemented with Tween-20
TEMED	tetramethylethylenediamine
TFIIH	transcription factor II H
TGF-α/β	transforming growth factor-α/β
TNF-α	tumor necrosis factor-α
Tris	2-Amino-2-hydroxymethyl-propane-1,3-diol
TRE	tetracycline response element
u	unit(s)
USP	ubiquitin specific protease
UV	ultraviolet
V	volt
v/v	volume/volume
w/v	weight/volume
WT	wild type